# Evaluating the impacts of disturbance scale, management history, and stochastic effects on succession by remote sensing and field surveys

（リモートセンシングおよび野外調査による撹乱規模、管理履歴、確率事象が遷移に与える影響の評価）

Lea Végh

A dissertation submitted

to the

Graduate School of Environmental Science

Hokkaido University

for the Doctor of Philosophy degree in Environmental Science

2021

# Table of contents

# List of tables

# List of figures

## Summary

Human and natural activities lead to continuous change of plant communities, called succession, which is the focus of interest after disturbances. If the vegetation cover and any legacy effect are completely removed from an area, for example, by a volcanic eruption or mining activities, the process of vegetation development is called primary succession. Primary succession often takes decades, but active management practices, like plantations, hasten the development of vegetation cover. The long-term effects of management practices are unclear, due to the uncertainty surrounding successional processes, and because stochastic effects cause divergent trajectories.

The aim of this research was to detect long-term trajectories after primary succession, and examine the effects of scale, management history, and stochastic effects after volcanic eruptions. For this purpose, three eruptions sites of Mount Usu, an active volcano in northern Japan, were studied by combining remote sensing and field surveys. The three eruptions sites studied were Yosomi (1910 eruption), the summit (1977-78), and Konpira (2000). The first two chapters used remote sensing to observe landscape scale processes and to address the shortcomings of traditional field survey methods. However, remote sensing is unable to detect the community species composition and abiotic factors, which are the focus of previous research on Mount Usu. Therefore, to examine species composition and environmental factors, and to maintain comparability with previous studies, Chapters 3 and 4 are based on traditional field surveys.

Chapter 1 focused on vegetation patch dynamics at the summit and at Konpira, and used remote sensing to quantify patch development by developing a novel approach, called imagery chronosequence. The scale of eruptions was larger at the summit than at Konpira, and the large disturbance and harsh environment slowed patch development at the summit, where the patches remained sparsely vegetated, especially on steep slopes. At the smaller Konpira site patch growth was quick and not restricted by slope steepness, and in contrast to the summit, almost the whole area became revegetated by the end of the study.

In Chapter 2, plant community diversities were evaluated by using remotely-sensed (spectral) diversities, examining the effect of image resolution and spectral plot size (extent) on the spectral diversities. Two different field layer diversities, canopy and total diversities at the Yosomi and summit, were estimated by the spectral indicators, testing multiple combinations of field indices and spectral diversities. Spectral indicators developed from the low resolution image (approximately 3 m) and from the same spectral plot size as the field plot (narrow extent) correlated strongly with field indices, especially if calculated from the first principal component axis. The canopy and total diversities were evaluated similarly, with evenness and true diversity indices being estimated best.

Chapter 3 compared forest types either developed by succession or from plantations at Yosomi and the summit. Species composition, plant richness, and diversity were measured by field surveys during 2015–2019. The canopy was more diverse, but the herb layer was less diverse at Yosomi than at the summit. Richness and diversity were higher in natural forests

than in plantations, but variance was lower. The species composition remained distinct in the plantations, often preventing the immigration of native species, indicating that management history had larger impact than stochastic effects on successional trajectories.

Species diversity is affected by abiotic factors, such as soil nutrients, temperature, and light competition. The impact of abiotic factors on forest development was examined in Chapter 4 via analysing soil nutrients, seedbank, temperature and light intensity of the forests. The soil conditions did not vary greatly among the sampling locations, apart from a plantation where *Alnus* spp. were established. *Alnus* spp. are good nitrogen-fixers, and the plantation had increased levels of soil nitrogen compared to the other forests. Plantations had also higher seed density, diversity, and percentage similarity at the summit than natural forests. Temperature did not differ between the forest types, but the summit forests had higher light intensity. Thus, nitrogen-fixing species and light conditions separated forests and had a larger effect than soil chemistry and temperature on vegetation composition and succession.

In conclusion, the imagery chronosequence and spectral diversities evaluated successional developments well on large scales and in various forests across Mount Usu. The remote sensing was complemented by field surveys, which established the diversity relationships of canopy and herb layers and also detected edaphic and light conditions. Active management strategies, such as the plantation of woody species, had larger impact than stochastic processes, and often resulted in decreased diversity compared to naturally recovered forests. However, if plantations would be carried out following a mosaicked spatial pattern instead of planting contiguous areas, they may enhance patch dynamics and promote recovery after large scale disturbances. As successional processes are comparable between distant geographic locations, the combination of remote and field observations can examine vegetation and patch dynamics after various disturbances on landscape scale, focusing field surveys on areas where successional developments deviate from expectations.

# General introduction

Severe disturbances destroy vegetation cover and subsequent successional developments take decades to restore the communities and ecosystems (Prach and Walker 2020). Succession can lead to undesirable communities; therefore, to restore high quality habitats, interventions may be needed (Perrow and Davy 2002). Restoration practices can be divided into passive and active management, depending on the level of involvement to accelerate revegetation. Passive restoration intervenes minimally or not at all in natural processes, while active restoration includes a range of practices (e.g., seeding, planting, mowing) that hasten revegetation, but the resultant community is often far from the former vegetation (Mansourian, Vallauri, and Dudley 2005). Clarifying successional processes after natural disturbances is important to understand revegetation dynamics and to help identify suitable management practices to decrease the risk of adverse events such as landslides and biological invasion (Gilbert and Anderson 1998; Prach and Hobbs 2008; Young, Petersen, and Clary 2005). This dissertation examined the successional outcomes on Mount Usu, an active volcano with regular eruptions in Japan (Katsui, Yokoyama, and Murozumi 1981), with the aim to compare the impacts of scale, management practices, and stochastic effects on different eruption sites.

Mount Usu is part of the few volcanoes of the world which are well-studied from a successional point of view. The 1977-78 eruption site received much attention (Haruki and Tsuyuzaki 2001; Tsuyuzaki 1987, 2019) and recently the 2000 eruption site has also been studied (Obase et al. 2008; Otaki, Takeuchi, and Tsuyuzaki 2016). However, the older 1910 eruption site is not well researched, and comparative analysis of the different eruption sites is also lacking. Observing the outcomes of primary succession after longer time-periods is important to understand the impact of management practices and stochastic effects (del Moral 2010). The present study addressed these issues.

Monitoring succession by field observations is restricted by the spatial and temporal extent of the recovery (Irl et al. 2019; Sutomo, Hobbs, and Cramer 2011). The combination of field and remote surveys diminishes the risk of overlooking spatial characteristics (White, Cornett, and Wolter 2017), and temporal developments can be examined by creating a time-series from images. Since the increased availability of high quality satellite images, many ecological studies have incorporated remote observations into their study design (Meiners et al. 2015; Turner et al. 2003; Wang and Gamon 2019).

In Chapter 1, I used aerial and satellite images to understand vegetation development and patch dynamics after the 1977-78 and 2000 eruptions of Mount Usu. The eruptions occurred at different locations and spatial scales at the mountain, and because revegetation is affected by the type, intensity, and scale of the disturbance (Prach and Walker 2020), the two sites were suitable to examine vegetation patch developments. Changes in vegetation cover has been analysed by following pixel-by-pixel alterations in a wide geographic range (De Rose et al. 2011; De Schutter et al. 2015; Lawrence and Ripple 2000), but the single pixel based approach does not take into consideration the impact of vegetation patches. Vegetation patches form habitats protecting the plants from the harsh environment and often facilitate the survival of later successional species (Tirado, Pugnaire, and Eriksson 2005). Hence, vegetation patches are important for determining vegetation development patterns. By creating an imagery chronosequence from aerial and satellite images, Chapter 1 analysed the location, size, and vegetation density of early successional vegetation patches to understand their impact in relation to the scale of disturbance.

Chapter 2 turns from remote sensing of patch dynamics to remote sensing of plant diversities at the 1910 and 1977-78 eruption sites of Mount Usu. Remotely sensed diversity indicators, also called spectral diversities, measure the spectral heterogeneity of the surface. According to the spectral variation hypothesis, spectral heterogeneity positively correlates with surface heterogeneity, and greater surface heterogeneity increases species diversity (Palmer et al. 2002). Spectral diversities can map large areas, assisting the selection of suitable areas for research (Kerr and Ostrovsky 2003; Peng et al. 2012). Because spectral diversities are site-specific, studies are needed to develop a common set of tools to measure diversity (Skidmore et al. 2015; Warren et al. 2014). Chapter 2 compared field diversity indices with spectral diversity indicators calculated from four combinations of image resolutions and spectral plot areas and aimed to identify the requirements for calculating effective spectral diversity indicators to estimate field diversity indices.

Although remote sensing provides promising new research opportunities, local effects and abiotic conditions are hard to detect by it. Therefore, field surveys are required to validate and support remote analysis (Feilhauer et al. 2014). In addition, as previous studies were carried out by field surveys on Mount Usu, continuity and comparability of past observations with present ones could not have been granted without examining diversity and species composition in situ. Thus, Chapter 3 and 4 applied traditional monitoring methods to facilitate the validation and incorporation of remote surveys.

Chapter 3 compared the diversities and species compositions of forests either developed by natural succession or originated by human interventions at the 1910 and 1977-78 eruption sites based on field surveys between 2015 and 2019. A common approach is to use space for time substitution (chronosequence) when studying succession: research sites are ordered by their lag since the disturbance, assuming identical developmental trends (Cutler, Belyea, and Dugmore 2008; Irl et al. 2019). This assumption is questioned recently (Prach and Walker 2020), because even geographically close areas experience different management practices and stochastic events. By comparing the characteristics of the forests at the eruption sites, Chapter 3 aimed to understand the effects of human interventions and stochastic events at an early and a mature successional stage to assist future management practices.

While Chapter 3 engaged in the aboveground characteristics of the research plots, Chapter 4 examined the underground characteristics: the soil chemical composition, seedbank, and further two abiotic factors, the light intensity and temperature. Nutrient limitation plays a major role in the early stages of succession (Bishop et al. 2010; Hulshof and Spasojevic 2020), but facilitating species can improve the soil chemical composition, especially the nitrogen content of the soil, thus enhancing succession (Kamijo et al. 2002; Titus 2009). Additionally, the rate of succession is accelerated by the exposure of the old topsoil and its seedbank (Tsuyuzaki 1995; Tsuyuzaki and Haruki 1996a), although standing species often control the emergence of seedlings (Kardol et al. 2007; van der Putten et al. 2013). Extreme temperatures and light competition also affect the establishment and survival of seedlings from the seedbank (Brooker and Callaghan 1998; Uesaka and Tsuyuzaki 2005). Chapter 4 aimed to examine the differences in the soil chemistry, seedbank, and microclimate of the forests to determine their influence on the observed species diversity.

Mount Usu is part of the Shikotsu-Toya National Park (NP) and the Toya-Usu UNESCO Global Geopark. It is a popular tourist destination not only because of its natural beauty, but also because of its proximity to the hot spring resort town Toyako. Managing the forests on the mountain has to be done by balancing the needs of nature protection and humans who are connected to the NP, either by living nearby or visiting it (Sakurai 2019). The research presented here aims to help managing primary succession when needed, to ensure that the vegetation is restored for the dual benefit of the ecosystem and people.

**Mount Usu**

Mount Usu is a basalt-andesite stratovolcano in Hokkaido Island, northern Japan (42°32'N, 140°50'E, 733 m elevation, Photo 1), belonging to the Nasu Volcanic Group (Oba 1966). After an active pre-historic period, it was dormant until 1663; since then, it had erupted every 30-50 years in different locations across the mountain (Katsui et al. 1981, Figure 1). The eruptions usually destroyed the plants in their immediate vicinity, but the surrounding vegetation survived despite tephra accumulation (Tsuyuzaki 1987; Obase et al. 2008). The mountain belongs to a temperate zone, with an average annual precipitation of 891 mm and annual mean temperature of 8°C during 1976-2018 (Date Meteorological Station at 5 km from Usu; JMA 2019). The climax vegetation is deciduous oak or mixed broad-leaved forests in the lowlands of this region, including Mount Usu (Okitsu 2003).

Because Toyako Town is in constant risk of getting damaged from the eruptions, artificial revegetation, building of erosion control dams, and other protection countermeasures were established on and around the mountain over time. In addition, trails and tourism-related facilities are established, especially at the 1944-45 eruptions site and the 2000 eruption site. The 1944-45 eruptions site is surrounded with non-native vegetation and is one of the local touristic attractions. Therefore, successional processes could not be followed there and the area was excluded from the research.

Three eruption sites were examined in this study: Mount Yosomi, which was denuded by the 1910 eruption; the summit, destroyed by the 1977-78 eruptions; and Konpira, which suffered from the 2000 eruptions (Table 1, Figure 1). As a result of the different eruptions and management activities, a mosaic of plant communities, including forests, developed at various successional stages on Mount Usu. The forest types studied in Chapter 2–4 were identified by satellite and aerial images from 1972 to 2015 (Table 2).

At Yosomi (1910 eruption), three forest types were examined: a broadleaf forest (mainly *Populus suaveolens* and *Acer pictum* spp., nomenclature follows Iwatsuki 1993), an *Abies* spp. plantation from 1971 (Forest Agency of Japan, pers. comm.), and an old *Abies* plantation from 1952, which were invaded by broadleaved species (*Abies sachalinensis* and *Alnus hirsuta*). These three forest types are called Broadleaf, Picea (with roman letters), and Mixed forest (Photo 2).

At the summit, four forest types were studied: Closed-broadleaf forest (*Populus suaveolens* and *Acer pictum* spp.), Open-broadleaf forest (*Populus suaveolens* and *Salix* spp.),

a broadleaf plantation of *Sorbus commixta, Alnus* spp., and *Betula platyphylla* forest (Sorbus-Alnus forest), and a *Picea glehnii* plantation from 1992 (Picea forest, Photo 3). The Closed- and Open-broadleaf forests were separated by their location and by the different light intensity levels in them; the Open-broadleaf forest had higher light intensity. The Sorbus-Alnus forest is not listed as an official plantation in the forest registry, but the signs of erosion dams and trees growing in rows on top of the dams indicate human planting.

The forests did not change much during the study period, but some plots were affected by a typhoon in 2016. Several trees fell in the Mixed and Sorbus-Alnus forests, and because of the damage, four plots in the Mixed forest could not be monitored from 2017.

Photo 1 Mount Usu viewed from the north and its location in Hokkaido (subset map). The highest elevation is a peak called O-Usu (733 m). In the foreground are Lake Toya and Toyako town.

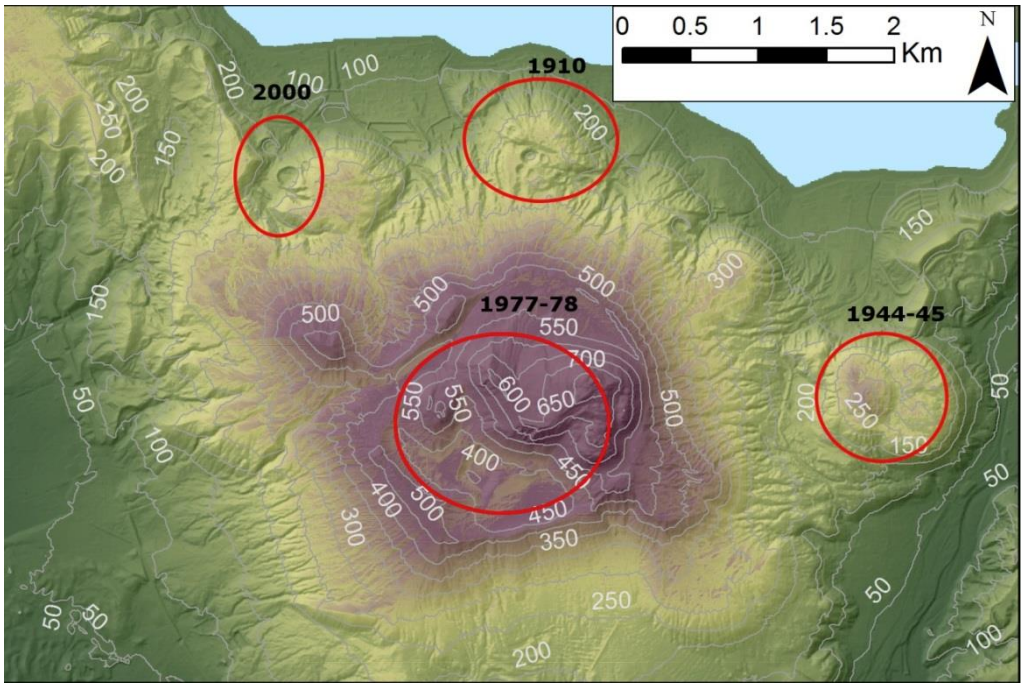


Figure 1 Locations of the last four major eruptions on Mount Usu. See also Table 1.

Table 1 List of eruptions and their location name used during the study.

| Eruption year | Location name | Sections involved |
|---|---|---|
| 2000 | Konpira | Chapter 1 |
| 1977-78 | Summit | Chapters 1–4 |
| 1910 | Yosomi | Chapters 2–4 |

Table 2 List of aerial and satellite images used to identify the boundaries of eruptions and forest types.

| | Source | | Bands | Resolution (m) | Date |
|---|---|---|---|---|---|
| | Satellite | Aerial | | | |
| USGS* | LandSat 1 | | G, R, NIR-1, NIR-2 | 60 | 29 Aug 1972 |
| GSI** | | Plane | B, G, R | | 24 Sep 1976 |
| USGS | LandSat 2 | | G, R, NIR-1, NIR-2 | 60 | 19 Sept 1980 |
| | LandSat 5 | | B, G, R, NIR(3), Thermal | 30 | 10 Aug 1985 |
| | LandSat 5 | | B, G, R, NIR(3), Thermal | 30 | 08 Aug 1990 |
| | LandSat 5 | | B, G, R, NIR(3), Thermal | 30 | 23 Sept 1995 |
| GSI | | Plane | Panchromatic | | 18 Jul 1995 |
| USGS | LandSat 5 | | B, G, R, NIR(3), Thermal | 30 | 24 Aug 1996 |
| GSI | | Plane | B, G, R | | 14 Aug 2000 |
| DigitalGlobe | QuickBird | | B, G, R, NIR | 2.4 | 08 Sep 2006 |
| | IKONOS-2 | | B, G, R, NIR | 3.2 | 01 Aug 2014 |
| GSI | | Plane | B, G, R | | 21 Jun 2015 |

*United States Geological Survey

**Geospatial Information Authority of Japan


Photo 2 Forest types at Yosomi, recovered after the 1910 eruptions. (a) Broadleaf forest, (b) Abies forest, (c) Mixed forest. The photos were taken between June–August 2015.

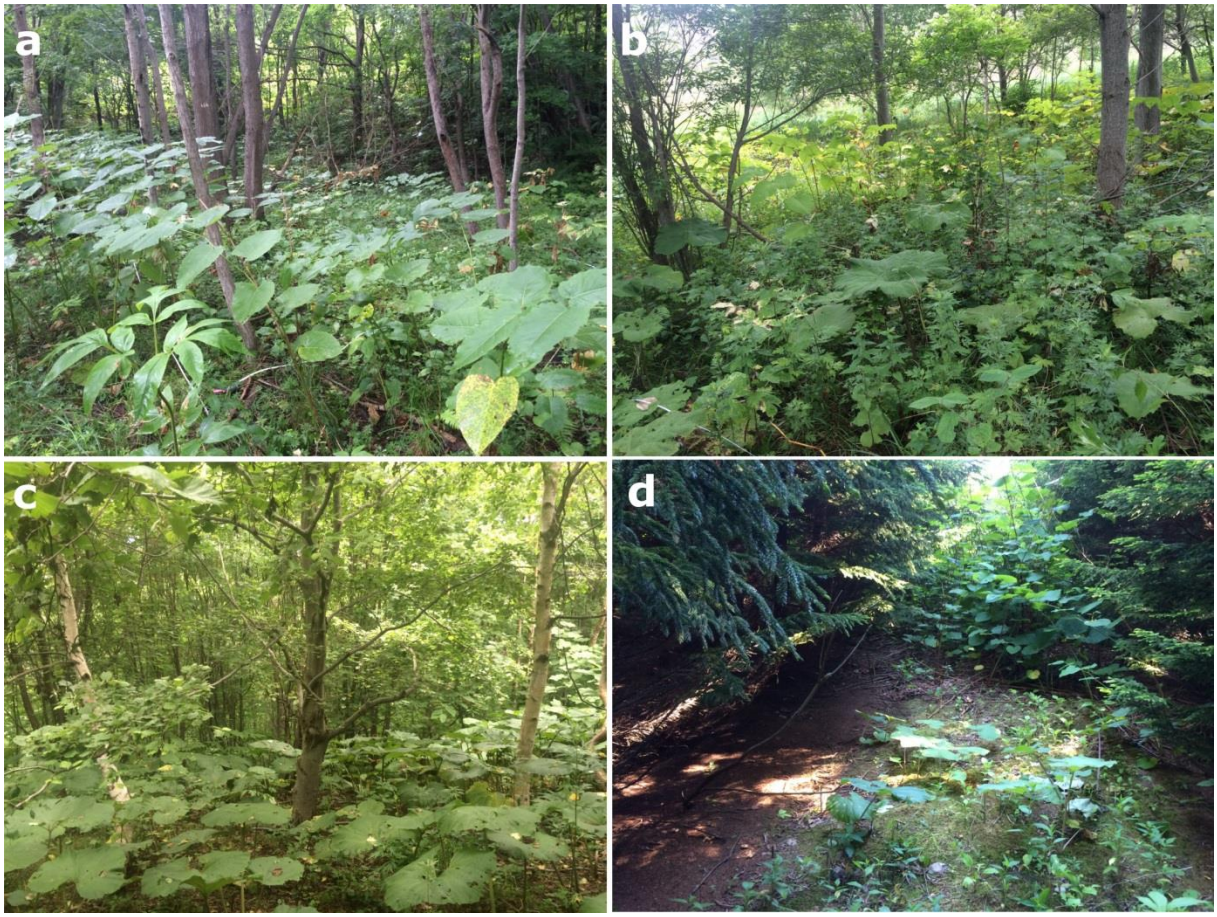


Photo 3 Forest types at the summit, recovered after the 1977-78 eruptions. (a) Closed-broadleaf forest, (b) Open-broadleaf forest, (c) Sorbus-Alnus forest, (d) Picea forest. The photos were taken between July–August 2015.

# Chapter 1 Comparison of vegetation patch dynamics after the eruptions of the volcano Mount Usu in 1977-78 and 2000, detected by imagery chronosequence


## Abstract

Vegetation patch dynamics were analysed to detect vegetation development patterns after eruptions at two sites (summit destroyed in 1977-78, and a foothill, Konpira destroyed in 2000) on the volcano Mount Usu, in northern Japan. Aerial photos and satellite images taken in 2000, 2006, and 2014 were used to develop an imagery chronosequence of vegetation patch dynamics. Vegetation patches were identified by the Normalized Difference Vegetation Index (NDVI) for satellite images, and by the Normalized Green-Red Difference Index (NGRDI) for aerial photos. The vegetation patch types were categorized based on whether the patches overlapped (touching) or not (isolated) with the future vegetation patches and whether their area increased (growing) or decreased (shrinking). Afterwards, patch dynamics were compared between the two sites through changes in patch types, dense vegetation, and patch growth with slope degree, elevation, and time. Isolated patches were established more at the summit and showed high mortality, while at Konpira most isolated patches survived until 2006 and merged into touching patches by 2014. Moreover, the vegetation density of patches was higher at Konpira than at the summit. Patch growth was associated with patch types at both sites. However, the time was more important for the patch dynamics at the summit, and the vegetation density affected the dynamics more at Konpira. Therefore, the two sites had different vegetation patch dynamics, which were related to the characteristics of topography and eruptions. In conclusion, the imagery chronosequence proposed in this study monitored patch dynamics well, and patches developed faster at Konpira.

## 1.1 Introduction

Succession is studied through the chronosequence approach, though caution should be taken with interpretation, because of the exclusion of stochastic and unpredictable processes, and the assumption of homogenous successional sere (Buma et al. 2019; Johnson and Miyanishi 2008). Therefore, long-term monitoring of permanent plots is crucial to detect spatio-temporal vegetation changes to compensate the weakness of the chronosequence approach (Fischer et al. 2019). However, long-term field monitoring is constrained by time consumption and inaccessibility, particularly on volcanoes. In addition, vegetation patch dynamics should be investigated on a large scale, such as at landscape level, when large areas are disturbed (Prach and Walker 2020).

Harsh environments formed by catastrophic disturbances restrict plant colonization and establishment (Chapin and Bliss 1989). Vegetation patches, defined as clusters of plants (Pickett and White 1985), alleviate the harsh environments, particularly in the early stages of succession, although the role of vegetation patches in revegetation are unclear (Prach and Walker 2020). The impact of vegetation patches on plants in and around the patches is positive (facilitation) or negative (inhibition), and is dependent on the size and growth rate of the patch-forming plants (Brooker et al. 2008). Therefore, clarifying vegetation patch dynamics is key to predicting the trajectory of succession.

Remote sensing is capable to investigate vegetation patch dynamics at landscape level (White et al. 2017). For example, time-series satellite images from the first 15 years after the 1980 catastrophic eruption on Mount St. Helens, USA, detected that disturbance intensity affects the pattern and pace of revegetation (Lawrence and Ripple 2000). So far, remote analyses have mostly been conducted at pixel level (De Rose et al. 2011; De Schutter et al. 2015).

When such time-series analysis of remotely sensed data is applied to investigate vegetation patch dynamics, the dynamics may be clarified in more detail at landscape level. However, there are some obstacles when creating time-series analysis: high resolution images are often not available from the same sensor for long periods and there are inaccuracies when overlaying images which hinder pixel level comparisons. To reduce these disadvantages, I investigated vegetation patch dynamics by images obtained from different platforms and focused on clusters of pixels. Here, this approach is called imagery chronosequence. The combination of images from various sensors, i.e., aerial and satellite images, provides high

resolution, long-term coverage. Using clustered pixels reduces the inaccuracies of images and also improves the analysis of vegetation patches. A vegetation patch includes multiple plants, and changes in the size and vegetation density can be followed at cluster level but not at single pixel level.

Vegetation density within patches, which is often evaluated by vegetation indices (VIs), increases during the early to middle stages of succession, then decline again with aging, if the environments are unsuitable (Cipriotti and Aguiar 2015). This indicates that vegetation density is diverse even for the same patch size and is related to vegetation patch dynamics. In addition, the numbers of newly established and persevering patches are affected by geological factors, represented by elevation and slope degree (Tsuyuzaki 1995; Walker and del Moral 2003). Therefore, vegetation patch dynamics were analysed by variations in the number, size, and vegetation density of patches in relation to elevation and slope degree on each patch.

The first aim of this study was to examine the applicability of imagery chronosequence using different sources of images; and the second one was to evaluate vegetation patch dynamics. Vegetation patches were defined as surrounded by bare ground and their vegetation could be sparse, dense, or a mix of sparse and dense vegetation. Patch dynamics were examined by the growth and changes in vegetation density of the patches, with two abiotic factors: elevation and slope degree, both of which were plausible to determine vegetation patch dynamics. To confirm these, two eruption sites on Mount Usu, northern Japan, were used.

## 1.2 Methods

### 1.2.1 Study area

The last two eruptions of Mount Usu occurred at different sites, at the summit in 1977-78 and at a foothill called Konpira in 2000. The major volcanic ejecta were volcanic ash and pumice at the two sites (Obase et al. 2008; Tsuyuzaki 1989a). The eruptions denuded both areas, although the eruption scale was smaller at Konpira (Table 1.1). The summit is 340 m higher in elevation than Konpira, and was covered with seeded pastures and broad-leaved forests dominated by pioneer trees prior to the eruptions (Tsuyuzaki 1987). Natural revegetation occurred mostly by vegetative reproduction of large perennial forbs soon after the eruptions (Tsuyuzaki 1989a), which were then replaced by broadleaved forests. Konpira was covered mostly with broad-leaved forests and plantations of needle-leaved trees before the eruptions

(Obase et al. 2008), and the revegetation has been promoted mostly by pioneer forbs and trees until now.

### 1.2.2 Analysis of aerial and satellite images

Image analysis was carried out by ArcGIS (ver. 10.2, ESRI) in WGS 1984 UTM zone 54N projection system. The satellite images were acquired on 8 September 2006 (QuickBird, resolution 2.4 m) and 1 August 2014 (IKONOS, resolution 3.2 m), while the aerial photographs were taken on 14 August 2000 (obtained from the Geospatial Information Authority of Japan). The satellite images were ortho-rectified by the Digital Elevation Model provided by the Geospatial Information Authority of Japan (accuracy within 0.7 m, resolution 6.2 m). After the ortho-rectification, a small misalignment remained between the images and was manually corrected by georeferencing the IKONOS image to the Quickbird image using zero order polynomial transformation (i.e., shifting the image). Afterwards, the digital numbers of the satellite images were converted to top of atmospheric reflectance (Krause 2003; Taylor 2009). Because the aerial photographs lacked spatial reference, the photographs were georeferenced to the Quickbird image using geographical features (spline transformation). Finally, the Quickbird and aerial images were resampled to 3.2 m pixel resolution.

The blue, green, red, and near-infrared (NIR) bands of the satellite images were used for calculating the Normalized Difference Vegetation Index (NDVI) = (NIR - red)/(NIR + red) (Rouse et al., 1974), and the blue, green, and red bands of the aerial images were used to calculate the Normalized Green-Red Difference Index (NGRDI) = (green - red)/(green + red) (Gitelson et al. 2002), depending on the wavelength range of the sensors; NDVI was used for satellite images and NGRDI for aerial photo images. I chose these indices because NDVI was shown to classify vegetation cover well fifteen years after the eruptions on Mount St. Helens (Lawrence and Ripple 1998), and because NGRDI is a good alternative to NDVI if NIR is not present (Rasmussen et al. 2016). However, to test the similarity of NDVI and NGRDI, both VIs were calculated from satellite images, and the Pearson's correlation coefficient of pixel values was examined.

Supervised maximum likelihood classification (37 training areas) on the VI images categorized land cover into no vegetation cover (bare ground and water surface), sparse, and dense vegetation cover. Sparse and dense vegetation cover was separated roughly by VIs, i.e., dense vegetation cover showed higher VI than sparse cover (Table 1.2). Vegetation patches

were separated by bare ground from each other, and the vegetation of the patches could be completely sparse, completely dense, or a mix of sparse and dense vegetation. Additionally, the field observations in 2014–15 confirmed that the sparse and dense vegetation cover consisted largely of short (mostly herbs and shrubs) and tall plants (mostly trees), respectively. However, further improvement was required as shown below. To eliminate misclassified pixels, the classified images were generalised by dissolving areas less than 3 pixels in size. Thus, the completed maps detected the locations and sizes of patches larger than 20 $m^2$ that was covered by two pixels or more. The accuracy of patch classification was assessed by Kappa coefficients on randomly-selected points on the maps. In total, 100 and 200 points were selected at Konpira and the summit, respectively, in each image acquisition year, 2000, 2006, and 2014. The Kappa coefficients were obtained by the confusion matrices of the relationships between classification by VIs and visual validation (Cohen 1960). Areas altered by erosion control works by the Forest Agency of Japan, such as artificial seeding, plantation and embankment, were removed from the completed maps.

### 1.2.3 Measurements of patch characteristics

The study was divided into two observation periods: the first observation period was from 2000 to 2006 and the second was from 2006 to 2014. Finer temporal resolution could not be achieved due to the lack of images meeting the criteria for the study, but as vegetation recovery takes decades after volcanic eruptions, the length of census periods were suitable to observe patch dynamics. The vegetation patches were classified into two types, “touching” and “isolated” to investigate different dynamics between persisting and transient patches (Figure 1.1). Touching patches were defined as patches present throughout the observation periods, whereas isolated patches were present only at the first or final census during each period. When patches merged or split, the patches were handled as a patch group (touching), and the patch size was calculated as the sum of the area of the individual patches.

Assuming patch shape to be circular, the annual growth was expressed by the change of radius: (radius of the final observation year – radius of the first year) / (years between the two observations). The radius was zero in the first or final observation year for isolated patches, as these patches either appeared or disappeared during the periods. Positive and negative annual growths indicated that the patches were “shrinking” and “growing”, respectively. Therefore, there were four categories of patch growth types: isolated and touching patches by shrinking and growing patches. The patch mortality during each period

was calculated by (the number of isolated patches disappeared by the end of period) / (the total number of patches). When analysing annual growth, patches whose growth was artificially restricted to zero (8 patches at the summit and 20 patches at Konpira) were excluded from the analyses.

To consider the effect of initial patch size on patch dynamics, proportional change of area (rate of change) for touching patches was calculated as the geometric mean of the area at the start and end of the period. The vegetation density of the patches (%) was calculated as: (area of sparse vegetation cover) / (area of total cover) by 100. For touching patches, the vegetation density was averaged between the first and final year of the period. Slope degree and elevation on each patch was calculated from the digital elevation model using weighted mean within the patch, and was averaged for touching patches between the first and final year of the observation periods.

### 1.2.4 Statistical analyses

Generalized linear models (GLMs) were used to investigate the changes in vegetation patches, because of the non-normal distribution (Shapiro-Wilk normality test, $P \leq 0.01$). The numbers of growing and shrinking patches were compared by GLMs with binominal distribution and logit link (Bates et al. 2015). The explanatory variables were eruption sites, patch types, and observation periods. Since the interactions between the explanatory variables were not significant, the interactions were not included in the analyses. Differences in slope degree, elevation, patch size and vegetation density on touching and isolated patches were compared between the two sites by Wilcoxon signed rank test and Kruskal-Wallis test, as these tests work without specifying the distribution. The ratio of newly vegetated areas to the total eruption areas showed normal distribution (Shapiro-Wilk normality test, $P = 0.45$) and was analysed with linear model (LM) using eruptions sites as explanatory variables.

Because patches often increase their vegetation densities without changes in their sizes, vegetation density and patch growth were analysed separately. For investigating the factors affecting vegetation density of the patches, GLMs were used with logistic binomial regression on the respective eruption sites. When analysing the two sites together, the site was coded as a categorical variable. The explanatory variables were observation period, patch type, slope degree, and elevation. Fittest model to explain vegetation density of the patches was obtained by backward procedure. The initial model contained all the variables. Then, less significant

variables were removed until the model became stable, indicated by the F-values of analysis of variance. Significance level was adjusted to $P < 0.01$ to reduce Type I error.

The annual growth of patches was transformed to absolute values and analysed by GLMs with Gamma distribution and log link. Including vegetation density as explanatory variable distorted the analysis at the summit, because 96% of the patches had sparse vegetation. Therefore, the explanatory variables at the summit were observation period, patch type, slope, and elevation. At Konpira, vegetation density was included among the variables. The interactions between the explanatory variables were also examined. The rate of change of touching patches was examined using the same variables and GLMs. The spatial-autocorrelation of patch growth on the final model was examined by Moran's *I* with the coordinates of the patches. Statistical analyses were carried out using R software (ver. 3.5.1, R Core Team, 2018).

## 1.3 Results

### 1.3.1 The accuracy of vegetation indices and classification

The Pearson's correlation coefficients (*r*) between NDVI and NGRDI of the same satellite images were higher than 0.85 in both 2006 and 2014 at the summit ($P < 0.001$, Table 1.3). Open water surfaces at Konpira were evaluated differently by the VIs, but removed from the analysis, *r* was 0.60 in 2006 and 0.90 in 2014, respectively ($P < 0.001$, Figure 1.2). Therefore, the vegetation patches identified by NDVI and NGRDI were comparable.
The NGRDI-based patch distribution map of 2000 and the NDVI-based maps of 2006 and 2014 had high classification accuracy (Table 1.4). The Kappa coefficients were 0.95, 0.98, and 0.99 for the 2000, 2006 and 2014 images, respectively. In addition, field observations of a subset of the sites (46 points at the summit and 17 points at Konpira) supported that misclassification was low. Hence, the location and vegetation density of patches were detected with high accuracy.

### 1.3.2 Comparison of eruption sites

The study area at the summit was 291 ha while that at Konpira encompassed 38 ha (Table 1.1). The slope degree of the sites averaged 25° with a maximum of 85° at the summit and 26° with a maximum of 88° at Konpira. Therefore, the slope degrees did not differ greatly between the two sites.

The numbers of growing and shrinking patches differed between the sites, patch types and observation periods (Table 1.5). The maximum patch densities at the summit were 2.32/ha and 1.61/ha during 2000–2006 and 2006–2014, respectively. The densities at Konpira were 2.96/ha and 1.04/ha. The ratio of shrinking patches to the total was higher at the summit than at Konpira (GLM, $P < 0.001$, $z = 5.9$), but increased at both sites during the second period ($P < 0.001$, $z = 5.7$). The increased ratio of shrinking patches was due to the low number of growing isolated patches in the second period. Touching patches had a higher ratio of growing patches than isolated patches during the surveyed periods ($P = 0.01$, $z = -2.5$). Although the isolated patches outnumbered touching patches in both periods, the ratios of isolated patches decreased from the first to the second periods. The increased ratio of touching patches with the decrease in patch density at both sites indicated that a number of isolated patches in the first period merged by the end of second period, especially at Konpira.

Slope degrees where the patches established were not different between the two sites (Table 1.5), but the elevation of patches was higher at the summit than at Konpira. Isolated patches established at lower elevation than the touching patches at the summit (Wilcoxon rank sum test, $P < 0.001$). The sizes of touching patches were comparable at the two sites, and were larger than isolated patches. In contrast, the isolated patches were smaller at the summit than at Konpira, although the statistical significance was low ($P = 0.02$). The touching patches developed more dense vegetation than the isolated patches at the two sites. However, the vegetation density of isolated patches at Konpira did not differ from that of the touching patches at the summit. While the difference between the mean of sparse cover ratios of isolated and touching patches was 7% at the summit, the mean was approximately 50% at Konpira.

Patch establishment had already proceeded on the edges of the crater at the summit in 2000 after the 1977-78 eruptions (Figure 1.3a). Afterwards, the patch establishment progressed to the centre of the crater, but the ratio of newly vegetated area was only 17% in the first and 3% in the second period (Figure 1.3b-d). Likewise, the patch establishment started on the edges of the crater at Konpira (Figure 1.3e-f). Since the eruption at Konpira occurred in 2000, the initial stage of patch establishment was clearly detected from 2000 to 2014 (Figure 1.3e-h), and more areas became newly vegetated in the first and second periods with 40% and 37%, respectively, than at the summit (LM, $P = 0.05$, $t = -4.1$). At Konpira, 83% of the area was covered with vegetation by 2014; while vegetation covered 57% of the summit leaving the central area largely bare. In addition, the patch mortality at the summit

was over 30% in both periods, while the mortality at Konpira was low, under 10%, during these periods. These results indicated that most isolated patches in the first period persisted and became touching patches in the second period at Konpira.

### 1.3.3 Effects of topography on patch vegetation density

GLM with logistic regression showed that at the summit, both elevation and slope degree negatively affected the vegetation density when the opposing factor was excluded ($P < 0.05$). As slope degree did not differ between isolated and touching patches (Table 1.5), the slope degree was retained in the model and elevation was discarded. The touching patches were significantly denser than isolated patches ($P < 0.001$, $z = -4.8$, df = 955). Both isolated and touching patches became sparsely vegetated as the slope degree increased at the summit, although the significance was low ($P = 0.03$, $z = 2.2$, df = 955, Figure 1.4a). The negative effect of slope was weak in the isolated patches, as their vegetation cover was sparse even on gentle slopes. These results indicated that steep slopes did not decrease patch establishment, but negatively affected the development of dense vegetation cover.

At Konpira, only the patch type influenced vegetation density. The touching patches had denser vegetation than the isolated patches ($P < 0.001$, $z = -4.7$, Figure 1.4b), but period, elevation, slope degree, and patch size did not affect the vegetation density of the patches.

### 1.3.4 Annual growth of patches

Slope degree, patch size, and elevation did not affect the annual growth at the summit, but the patch type and observation period did (Table 1.6). The touching patches displayed faster positive or negative growth than the isolated patches ($P < 0.001$, $t = 4.2$, df = 946), while all patches showed slower size change during the second period ($P < 0.001$, $t = -4.2$). The decrease of annual growth was more pronounced for the touching patches than for the isolated patches in the second period ($P < 0.001$, $t = -8.0$).

The elevation and patch size did not influence annual growth at Konpira, but in contrast to the summit, observation period and slope degree also did not affect growth. The annual growth of patches was determined by the patch type and vegetation density; the touching patches changed their area faster than the isolated patches (Table 1.6, $P = 0.006$, $t = 2.8$, df = 100), and the dense patches, not depending on their type, grew faster than the sparse patches ($P < 0.001$, $t = -3.9$).

The annual growth was slower at the summit than at Konpira (GLM, $P < 0.001$, $t = -8.2$, df= 1048). The difference was mainly due to the large variation of patch growth at Konpira (Figure 1.5), where a few touching patches grew fast due to multiple patches merging together. The residuals of the patch growth models did not show spatial auto-correlation at the summit and at Konpira ($I = –0.003$, $P = 0.68$ and $I = 0.003$, $P = 0.41$, respectively).

Of the touching patches, the growing patches showed larger rate of change than the shrinking patches at the summit (GLM, $P < 0.001$, $t = 11.4$, df = 179). All patches decreased their rate of change during the second period ($P = 0.003$, $t = -3.0$). At Konpira, both slope degree and elevation had significant effects on proportional change. Steeper slopes showed an accelerated rate of change ($P = 0.003$, $t = 9.4$, df = 3), while higher elevation slowed the rate of change ($P < 0.001$, $t = -26.7$). Likewise to the summit, the growing patches increased their size quickly ($P < 0.001$, $t = 18.5$), and the rate of change of patches slowed during the second period ($P < 0.001$, $t = -26.0$).

## 1.4 Discussion

### 1.4.1 Applicability of imagery chronosequence

The imagery chronosequence used in this study was accurate based on the high Kappa coefficients. This technique can be applied to various time-series analysis, although further improvement is desirable to objectively compare with field surveys, e.g., calibration with ground VI measurements. So far, pixel-based analysis has been popular for analysing vegetation (De Rose et al. 2011; Lawrence and Ripple 2000), partly due to the widespread availability of course resolution imagery. However, vegetation patches cannot be extracted from course resolution images. Since revegetation is often promoted by vegetation patches after large disturbances (Prach and Walker 2020), investigating vegetation patch dynamics on a large scale is important. The obstacle to examining patch dynamics is that good quality images captured over longer time periods are difficult to obtain (Loarie, Joppa, and Pimm 2008). The imagery chronosequence introduced here removed this obstacle and succeeded in detecting vegetation patches.

However, this approach is limited if high resolution observations are required. Because the focus is on clusters of pixels, the resolution of the analysis decreases. Investing in more image pre-processing steps and validation efforts will resolve this issue.

### 1.4.2 The effects of environments on vegetation patch dynamics

During the 15 years from 2000 to 2014, vegetation cover increased both at the summit and Konpira, progressing from the edges towards the centre of the craters. Both sites were surrounded by undamaged forests, and the vegetation recovery started from these refugia, a pattern also observed on Mount St. Helens (Lawrence and Ripple 2000). However, isolated patches farther from the edge did not persist at the summit, so the central area still retained bare lands, whereas isolated patches persisted at Konpira and the plant cover extended.

This suggested that the proximity of plant sources induced fast immigration of plants in the early successional stages (Fuller and del Moral 2003; Makoto and Wilson 2016) and large disturbance scale slowed revegetation. Moreover, annual growth of the patches was slower and vegetation density of the patches was lower at the summit than at Konpira. Vegetation patches provide stable environments, protection from erosion and strong winds at high elevation (Marler and del Moral 2011; del Moral, Saura, and Emenegger 2010), although vegetation cover increases slowly with increasing elevation on Mount St. Helens (del Moral 2007). These implied that the patches at the summit experienced more stress and grew more slowly.

The elevation difference was approximately 340 m between the two sites. Because the elevation differed greatly between the summit and Konpira, the elevation and its related factors should be more severe at the summit. Small elevation differences were related to the vegetation development patterns at the summit of Mount Usu (Tsuyuzaki, 2019), and high elevation slowed down succession on Mount Ontake, central Japan, because of the short growing season and low species diversity (Nakashizuka et al. 1993). Other factors, such as soil properties, species compositions and stochastic events also affect patch dynamics as well (del Moral et al. 2010; Wilmshurst and McGlone 1996; Zobel and Antos 2017). However, soil properties did not differ greatly between the two sites, and the species composition was comparable (Otaki et al. 2016; Tsuyuzaki 2019). Therefore, the stresses caused by the elevation and its related environmental factors seemed to determine slow patch dynamics at the summit.

The vegetation density of patches was reduced on steep slopes at the summit. However, steep slopes sometimes provide suitable environments for revegetation on Mount St. Helens in USA and Mt. Pinatubo in Philippines, because the ground surfaces at steep slopes become stable soon after the eruptions due to soil erosion (De Rose et al. 2011; del Moral,

Titus, and Cook 1995). In comparison, the ground surface instability persists for many years on Mount Usu due to the properties of the volcanic ejecta (Tsuyuzaki 2009). At Konpira, the slope degree did not affect the vegetation density of the patches, and all patches became densely vegetated as time passed. The responses of plants to slope degrees, which were different between the two sites, suggested that the slope degree hid the prime factors, such as ground surface stability.

#### 1.4.3 Vegetation patch growth

The touching patches grew faster than the isolated patches, especially at Konpira. The fast growth of touching patches in the early stages is explained partly by vegetative reproduction, because the common species were derived from vegetative reproduction soon after the eruptions at the two sites on Mount Usu (Obase et al. 2008; Tsuyuzaki 1989a). Likewise on Mount St. Helens, vegetative reproduction quickly increases the cover when tephra is thin or removed (del Moral and Eckert 2005; Wilmshurst and McGlone 1996).

Between the two periods, the touching patches growth decreased faster than the isolated patches at the summit. Vegetation recovery rate decreases with the number of years increasing after eruptions, e.g., on Mount St. Helens (del Moral and Magnússon 2014), due often to an increase in inter- and intra-specific competition within patches (Endo et al. 2008). However, the vegetation patches act as seed traps and facilitate the seedling establishment (Tirado et al. 2005). Therefore, patches act as facilitators, even though competition is present (Cipriotti and Aguiar 2015). The denser vegetation of touching patches suggested that the facilitation promoted increased density of plants instead of increased growth (Berdugo et al. 2019).

The patch dynamics at Konpira resulted in faster revegetation, by developing touching patches with low mortality. The isolation of vegetation patches delays succession on Mount St. Helens and Iceland's Surtsey (del Moral and Magnússon 2014), and the proximity of plant sources and patch connectivity had positive effects on the patch growth and vegetation density at Konpira. As patches at Konpira persisted more, the number of years that passed following the eruptions was less influential on patch development.

## 1.5 Conclusion

The imagery chronosequence presented here clarified the vegetation patch dynamics. These findings have never been obtained on a large scale by remotely sensed data. The revegetation

was slower at the summit, likely due to the large distance to seed sources that induced slow patch growth and low patch survival. The touching patches developed denser vegetation than the isolated patches at the two sites, and the vegetation density of the patches positively correlated with the patch growth. Steep slopes showed more sparsely-vegetated patches at the summit, and showed less effect on the patches at Konpira. The imagery chronosequence can also detect stochastic events, which affect long-term vegetation patch dynamics at landscape level (del Moral et al. 2010; Wilmshurst and McGlone 1996; Zobel and Antos 2017). In conclusion, the imagery chronosequence is applicable to clarify revegetation investigated by vegetation patch dynamics, and further improvements can develop its potential.

**Tables and Figures**

Table 1.1 Characteristics of the two eruption sites. The ranges of elevation and slope degree are shown with means in parentheses. Artificial areas were excluded from the study area for given year.

| Study site | | Summit | Konpira |
|---|---|---|---|
| Eruption year | | 1977–78 | 2000 |
| Study area (ha) | | 291.43 | 37.91 |
| Altitude (m) | | 400-732 (528) | 111-271 (188) |
| Slope (°) | | 0-85 (25) | 0-88 (26) |
| Artificial areas (ha) | 2000 | 47.56 | 7.19 |
| | 2006 | 48.07 | 7.19 |
| | 2014 | 48.01 | 7.30 |

Table 1.2 Mean and standard deviation of the NGRDI (2000) and NDVI values of the training samples used for supervised classification.

| Study area\Year | 2000 (Aerial) | 2006 (QuickBird) | 2014 (IKONOS) |
|---|---|---|---|
| No vegetation | 0.00 (0.02) | 0.13 (0.09) | 0.15 (0.08) |
| Sparse vegetation | 0.02 (0.04) | 0.44 (0.08) | 0.43 (0.07) |
| Dense vegetation | 0.09 (0.06) | 0.67 (0.06) | 0.61 (0.04) |

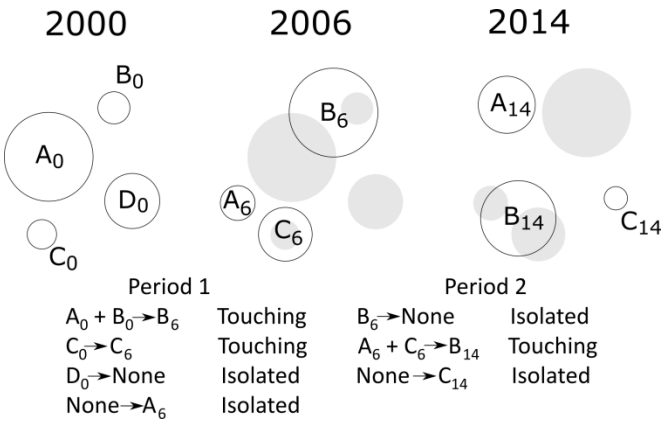


Figure 1.1 Patch classification based on persistency of the patches. Empty circles show patches present in the given year, while filled circles show the location of patches from the previous observation year (not present anymore). The respective patches are marked alphabetically with the subscript showing the year in which the patch is observed. Period 1 and 2 refers to 2000–2006 and to 2006–2014, respectively. As an example, patch $B_6$ is identified as touching patch during the first period, developing from the patch group $A_0$ and

$B_0$. However, in the second period $B_6$ is identified as an isolated patch. Although patch history is unknown within a period, e.g., patch $B_0$ might disappear and only patch $A_0$ develops into patch $B_6$, the biotic legacy of patch $B_0$ is likely to influence patch $B_6$ and therefore should be included in the patch group and defined as touching patch.

Table 1.3 Pearson's correlation coefficients between the NDVI values and NGRDI values of satellite images. $P < 0.001$ in all cases.

| Study area\Year | 2006 (QuickBird) | 2014 (IKONOS) |
|---|---|---|
| Summit | 0.85 | 0.97 |
| Konpira | 0.39[a] | 0.72[b] |

[a]The low value is due to construction work in 2006. Human artefacts and open water surfaces are evaluated differently by the indices. After the exclusion of open water surfaces, the coefficient becomes 0.60.
[b]The low value is due to open water surfaces. After the exclusion of open water surfaces, the coefficient becomes 0.90.

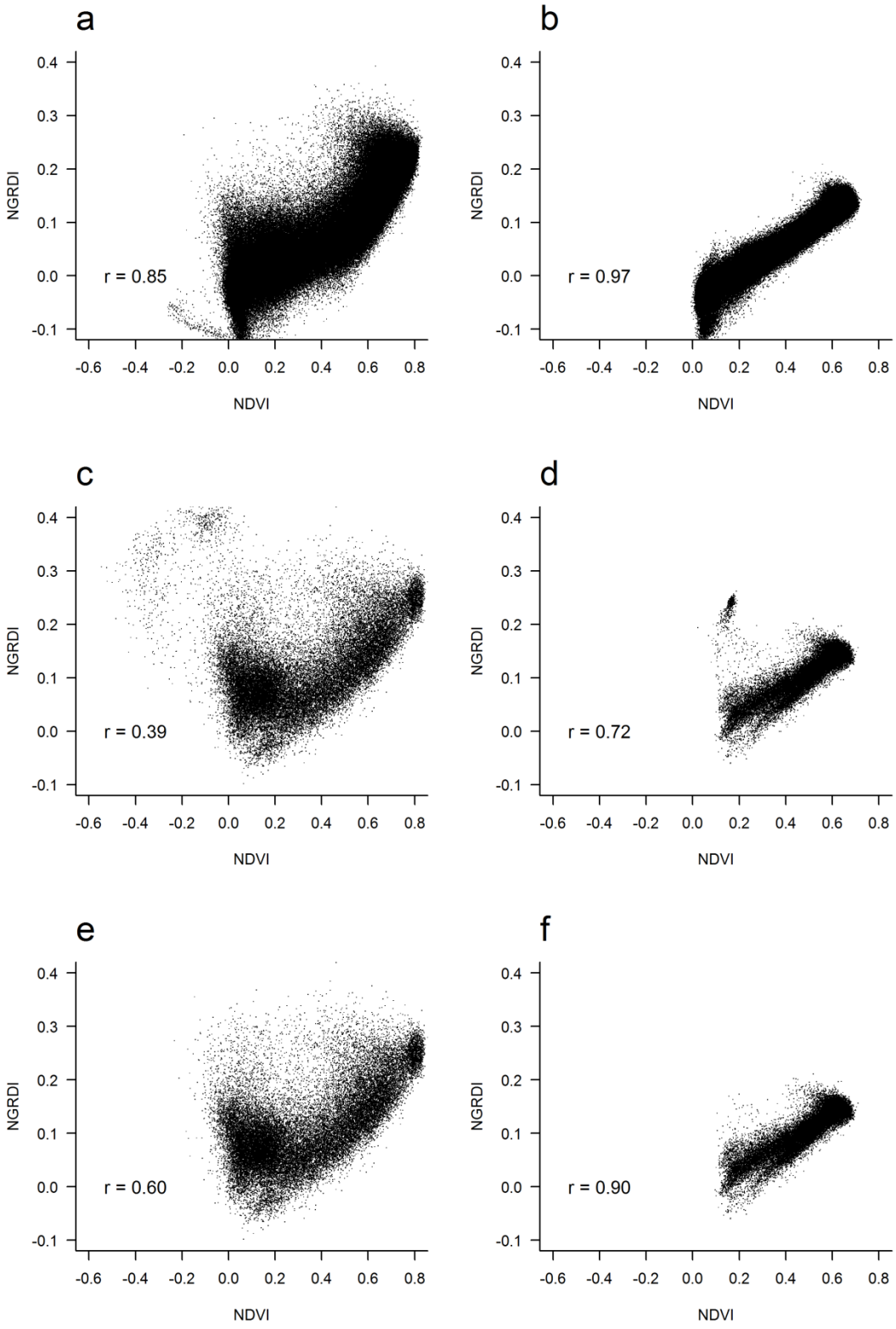


Figure 1.2 Scatterplots between NDVI and NGRDI values of the satellite images at the summit (a: 2006, b: 2014) and at Konpira (c,e: 2006, d,f: 2014) with Pearson's correlation coefficients. Water surfaces are excluded from Konpira at (e) and (f). $P < 0.001$ in all cases.

Table 1.4 The accuracy of vegetation cover classification examined by Kappa coefficients. Confusion matrices show the relationships between the results obtained by index-based classification and visual validation. In every image acquisition year 300 randomly-selected points (100 points for Konpira and 200 for the summit) are used. NGRDI and NDVI are abbreviations of Normalized Green-Red Difference Index and Normalized Difference Vegetation Index.

| 2000 (Aerial) | Index based (NGRDI) | | |
|---|---|---|---|
| Visual validation | No vegetation | Sparse vegetation | Dense vegetation |
| No vegetation | 228 | 2 | 0 |
| Sparse vegetation | 0 | 22 | 2 |
| Dense vegetation | 0 | 2 | 44 |

Kappa = 0.95

| 2006 (Quickbird) | Index based (NDVI) | | |
|---|---|---|---|
| Visual validation | No vegetation | Sparse vegetation | Dense vegetation |
| No vegetation | 160 | 1 | 0 |
| Sparse vegetation | 0 | 72 | 0 |
| Dense vegetation | 0 | 2 | 65 |

Kappa = 0.98

| 2014 (IKONOS) | Index based (NDVI) | | |
|---|---|---|---|
| Visual validation | No vegetation | Sparse vegetation | Dense vegetation |
| No vegetation | 114 | 0 | 0 |
| Sparse vegetation | 0 | 84 | 0 |
| Dense vegetation | 0 | 2 | 100 |

Kappa = 0.99

Table 1.5 Patch characteristics compared between the patch types and eruption sites. The growing and shrinking patches appear and disappear during the periods in the case of isolated patches, while touching patches are present all along the periods, only their size change. The examined characteristics are: patch number, patch size, slope degree of patches, elevation and sparse cover percentage. Patch number is shown for all patch type, and mean of isolated or touching patches is shown with standard error in parentheses. Mean values are compared by Wilcoxon rank sum test. Different letters on the upper-right of mean values indicate significant differences ($P < 0.001$ unless marked by *, where $P < 0.05$).

| | | Summit | | | | Konpira | | | |
|---|---|---|---|---|---|---|---|---|---|
| Location | | Isolated | | Touching | | Isolated | | Touching | |
| Development | | Growing | Shrinking | Growing | Shrinking | Growing | Shrinking | Growing | Shrinking |
| Patch number | Period 1 (2000–2006) | 303 | 169 | 75 | 19 | 79 | 3 | 8 | 1 |
| | Period 2 (2006–2014) | 144 | 152 | 51 | 45 | 17 | 3 | 11 | 1 |
| Slope (°) | | 25.5[a] | (0.4) | 26.5[a] | (0.8) | 22.9[a] | (1.2) | 22.1[a] | (2.4) |
| Elevation (m) | | 542.4[b] | (3.1) | 569.5[a] | (5.9) | 187.9[c] | (3.9) | 197.6[c] | (12.1) |
| Patch size ($m^2$) | | 57.5[c] | (1.3) | 12,855.5[a] | (6,497.9) | 337.6[b]* | (148.0) | 12,258.2[a] | (8,179.7) |
| Patch sparse cover (%) | | 99.7[a] | (0.1) | 92.1[b] | (1.6) | 91.1[b] | (2.3) | 41.9[c] | (4.9) |

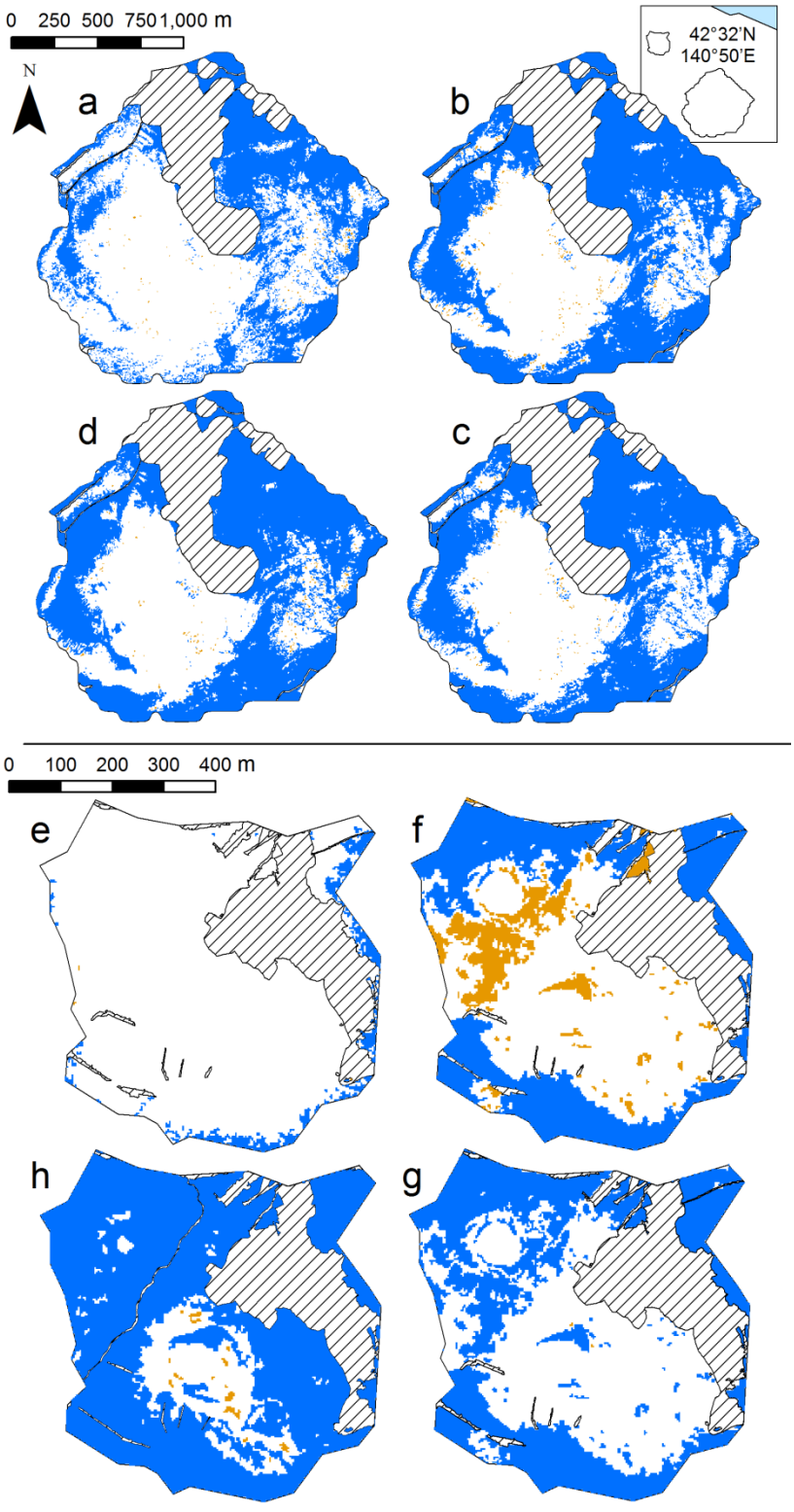


Figure 1.3 Vegetation patch establishment at the summit (a-d) and Konpira (e-h). The inset map shows the location of the summit (large area) and Konpira (small area) to each other. Alphabetical letters (a, b) and (e, f) mark 2000 and 2006, and show patch growth in the first period. Letters (c, d) and (g, h) mark 2006 and 2014 (from right to left), and show patch growth during the second period. Orange colour shows isolated patches and blue colour shows touching patches. The hatched areas are artificially influenced and excluded from the

analysis, while white colour marks bare ground. Note that the scales are different between the summit and Konpira.

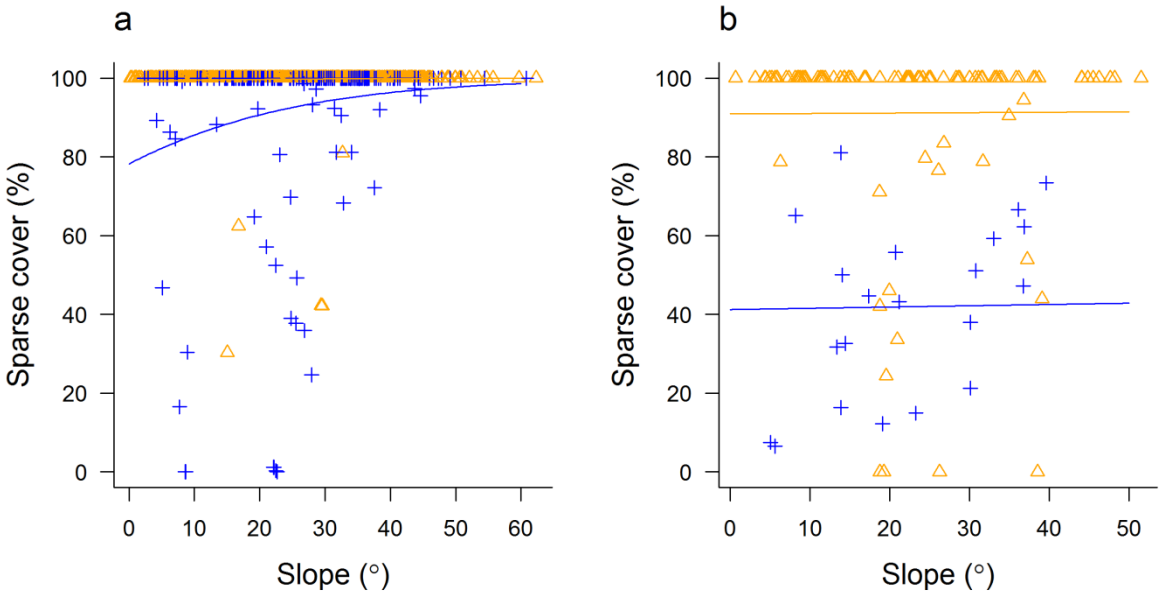


Figure 1.4 Effects of slope degree on vegetation density at the summit (a) and Konpira (b). Touching patches are marked by cross (+), while isolated patches are marked by (Δ). The response curves are generated by binomial GLM, with blue corresponding to touching and orange to isolated patches.

Table 1.6 Factors influencing the annual growth of vegetation patches. Only the significant effects are shown in the table (GLM, Gamma distribution with log link, ***: $P < 0.001$, **: $P < 0.01$).

| Summit | Estimate | Std. Error | *t* value | |
|---|---|---|---|---|
| (Intercept) | -0.38 | 0.04 | -10.24 | *** |
| Second period | -0.25 | 0.06 | -4.19 | *** |
| Patch type – Touching | 0.39 | 0.09 | 4.17 | *** |
| Interaction | -1.08 | 0.14 | -7.96 | *** |
| Null deviance: 472.55 on 949 degrees of freedom | | | | |
| Residual deviance: 385.61 on 946 degrees of freedom | | | | |

| Konpira | Estimate | Std. Error | *t* value | |
|---|---|---|---|---|
| (Intercept) | 1.69 | 0.45 | 3.76 | *** |
| Patch type – Touching | 1.14 | 0.41 | 2.77 | ** |
| Sparse % | -0.02 | 0.00 | -3.90 | *** |
| Null deviance: 107.804 on 102 degrees of freedom | | | | |
| Residual deviance: 63.55 on 100 degrees of freedom | | | | |

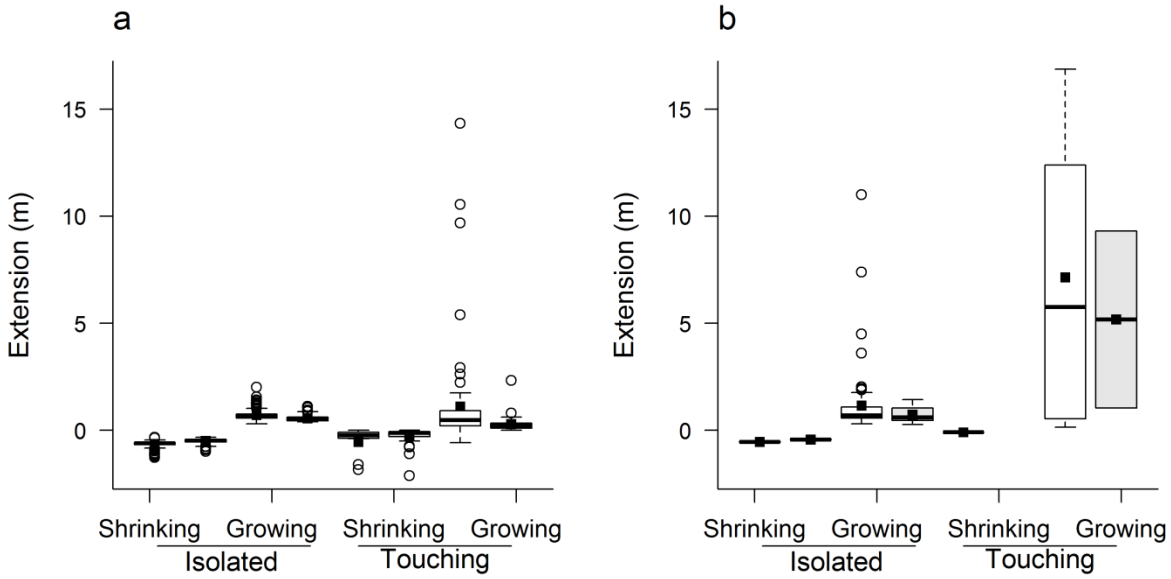


Figure 1.5 Annual growth (and shrinkage) of vegetation patches in relation to patch types and observation period at the summit (a) and at Konpira (b). Empty boxes mark the first period (2000–2006) and grey boxes mark the second period (2006–2014). The boxplots follow standard notation and the filled squares mark the means.

# Chapter 2 Using remote sensing to detect forest diversities – comparing different image resolutions and spectral plot extents


## Abstract

Detecting field diversities via remote sensing is becoming important to monitor vegetation dynamics at large scale. The characteristics of the remotely sensed image, depending on the study organism and habitat, affect the efficiency of measuring α-and β-diversities. Therefore, we examined the impact of image resolutions and spectral plot extents on the accuracy of estimating forest α-diversities and compositional variances on the active volcano Mount Usu, northern Japan. Low (3.2 m) and high (0.8 m) resolution IKONOS multispectral images were used to create spectral indicators from pixels covering the field plots (narrow extent) and from pixels including neighbouring area (wide extent). Six forest field diversity indices were obtained for canopy and for canopy-herb layer (total diversity): species richness (*S*), Shannon (*H*'), evenness (*J*'), Gini-Simpson (*D*), and true diversity of order 1 ($N_1$ = exp*H*') and order 2 ($N_2 = 1/D$). Changes in species composition were assessed by dissimilarity matrices. The spectral diversity indicators were calculated from the combination of image resolutions and spectral plot extents, and then compared with field diversities. The low resolution–narrow extent based spectral indicators showed the highest correlations with canopy and total diversities. The best spectral indicators were derived from the scores of the first axis of principal component analysis and from the near infrared band, reaching high correlations with both canopy and total field diversity indices. Of the six field diversities, *J*' showed the highest correlations with single spectral indicators and $N_{1,2}$ showed the highest correlations with pairs of spectral indicators. The correlations between spectral and field dissimilarities were lower than the correlations between α-diversities and spectral indicators, and were unaffected by the resolution and extent. In conclusion, the best spectral indicators were obtained from the low resolution–narrow extent combination, and the indicators estimated canopy and total field diversity indices of temperate forests equally.

## 2.1 Introduction

Monitoring diversity by field surveys (field diversity) is important to conserve vegetation and to identify biodiversity hotspots. α-diversity (community or plot diversity) is typically measured by establishing plots, but field surveys are time-consuming and often limited to a small number of samples. If plot diversity and compositional variations were estimated prior to the field surveys, monitoring could be better focused on the area of interest. Remote sensing shows potential to assess field diversities on large scales after validation, and is increasingly studied to complement field surveys.

Remotely sensed images have been applied for mapping habitats and species via evaluating spectral diversity measures (Wang and Gamon 2019): high resolution image analysis can accurately recognize species (Clark, Roberts, and Clark 2005; Underwood, Ustin, and DiPietro 2003) or estimate functional diversity (Huemmrich et al. 2013; Zomer, Trabucco, and Ustin 2009). Diversity is estimated by measuring the spectral heterogeneity of pixels; greater heterogeneity assumes greater heterogeneity within an area (Palmer et al., 2002). This is called the spectral variation hypothesis (SVH), which predicts that heterogeneous surfaces lead to increased richness, so increased spectral heterogeneity reflects increased diversity.

Most spectral diversity indicators are derived from single bands (Hall et al. 2012), vegetation indices (Gould 2000; Levin et al. 2007), or integrating multiple bands by principal component analysis (PCA, Stickler and Southworth 2008). Common indicators are expressed by the mean, standard deviation (SD), or the coefficient of variation (CV) of the pixel values overlaying the field plots (Wang, Gamon, Cavender-Bares, et al. 2018). The accuracy of remotely sensed diversities varies due to the large range of landscapes and plant life forms. To increase the accuracy of diversity predictions, a present challenge is to identify the source image requirements (Paganini et al. 2016) and a common set of habitat specific spectral diversity indicators (Skidmore et al. 2015). Therefore, the efficiency of spectral diversities should be tested on a wide range of environments using different source images to identify suitable community-specific indicators. Spectral indicators follow not only α-diversities, but also species compositional variations among plots (Feilhauer et al. 2013; Laliberté, Schweiger, and Legendre 2020). The methods used to detect changes in species composition range from ordination approaches by dissimilarity matrices (Cayuela et al. 2006) to applying Rao's Q (Botta-Dukát 2005; Rocchini et al. 2018).

Image characteristics vary with the sensor, and images need to be selected to suit the species being studied. If the resolution of the image is too fine compared to the species, the spectral diversities will be sensitive to within-target variance and overestimate spatial heterogeneity, while coarse resolution images will be insensitive to among-target variance and will underestimate heterogeneity (Rocchini et al. 2010; Woodcock and Strahler 1987). Several other factors influence the correlation between spectral and field diversities. Topographical factors, such as elevation, increase the correlation coefficients (Dogan and Dogan 2006; Feilhauer and Schmidtlein 2009), especially when the study species is small (Camathias et al. 2013). The spectral plot area covered by the pixels (hereafter, extent, Figure 2.1), from which the diversities are calculated also affects the relationship between field and spectral diversities; the inclusion of pixels surrounding the plot increases the accuracy of field diversity estimation (Parviainen, Luoto, and Heikkinen 2009). However, few studies examined the effects of including neighbouring pixels on spectral indicators, so their impact on evaluating field indices is unclear. Estimating total forest diversity (herb layer incorporated) has been also rarely examined, even though total diversity may be estimated with equal or higher accuracy than canopy diversity (Hakkenberg et al. 2018).

To confirm the effects of image resolution and different spectral plot extents on estimating field diversities, and to examine whether incorporating herb layer diversity in forest diversity increases the accuracy of the estimation, I created four different set of spectral diversity indicators from an IKONOS image covering temperate forests on Mount Usu, Japan. Because the estimation accuracy also depends on the field diversity indices used to survey plots (Schmidtlein and Fassnacht 2017), I calculated six field indices for canopy layer only and for total diversity. My aim was to clarify the effects of resolution and spectral plot extent on the spectral diversities when estimating canopy and total diversities measured in the field.

## 2.2 Methods

### 2.2.1 Image processing and plot selection

The study site, Mount Usu (42°32’N, 140°50’E), is an active volcano in the temperate region of northern Japan. Mount Usu erupted in every 20-30 years at different locations in the past century. Because the eruptions occurred at different locations, there are various forest types and transplantations differing in age on the mountain. As a result, the area is suitable to examine the performance of spectral diversity indicators in diverse forest types.

The IKONOS satellite image was taken on 1 August 2014 (wavelengths of bands: Blue 0.45–0.53 μm, Green 0.52–0.61 μm, Red 0.64–0.72 μm, Near-infrared (NIR) 0.76–0.86 μm, off-nadir: 19.27°), and was orthorectified using the Digital Elevation Model provided by the Geospatial Information Authority of Japan (accuracy within 0.7 m, resolution 6.2 m). After the orthorectification, the image was aligned to reference coordinates measured by portable GPS (Garmin GPSMAP 60CSx, accuracy ± 3 m) using second order polynomial transformation. The digital numbers were converted to surface reflectance by the dark-object subtraction method (Chavez 1988) and IKONOS correction factors (Taylor 2009), and pan-sharpening was done using the Brovey method (Gillespie, Kahle, and Walker 1986). All image processing was done by ArcGIS (ver. 10.2, ESRI).

A total of 35 plots measuring 10 m × 10 m were selected using stratified random sampling in the areas destroyed by the 1910 and 1977-78 eruptions (Figure 2.2). Of the 35 plots, 20 plots were established in young forests (less than 40 years old, 5 plots in closed- and 5 plots in open-canopy broadleaved forests, 5 plots in a *Picea* spp. plantation and 5 plots in a semi-artificial broadleaved forest) and 15 plots were established in mature forests (5 plots in an around 100 years old broadleaved forest, 5 plots in 70 years old and 5 plots in a 50 years old *Abies* spp. plantation, Figure 3.1). The mature forest plots were located at approximately 300 meters lower elevation than the young forest plots. The plots were established and located with GPS.

### 2.2.2 Field survey and diversity indices

The field surveys in the 35 plots were conducted between 2015 and 2019, one to five years later than the satellite image was taken. Similar gaps between image acquisition and field survey did not cause problems in other studies (Levin et al. 2007; Warren et al. 2014), and field observations confirmed that the plots did not receive severe damages during this period. Canopy diversity was calculated from the number of stems on each tree species with a DBH above 3 cm (range: 3-67 cm) in 2016. In 15 plots, the survey covered 5 m × 5 m plots in 2016, and the plots were extended to 10 m × 10 m in 2019. In five of these plots, all of which were transplantations, trees fell due to a typhoon in the late summer of 2016. The fallen trees were left in the forest and were identified; therefore, the forest structure of the plots could be reconstructed to 2014 canopy conditions. Herb layer (understorey) diversity was measured in four 1 m × 1 m quadrats within the plots during 2016 (before the typhoon) by counting the number of aboveground shoots rooted inside the quadrats on each species shorter than 2 m in

height.

Species richness (*S*), Shannon's entropy (*H*'), Gini-Simpson concentration (*D*), Shannon's evenness (*J*'), true diversity of order 1 ($N_1$) and true diversity of order 2 ($N_2$) were calculated for each plot by *vegan* (Oksanen et al. 2019) and *simba* (Jurasinski and Retzer 2012) packages in R. The equations are:

$$S = \text{number of species in a given plot}, \quad (1)$$

$$H' = -\sum_{i=1}^{s} p_i \ln p_i, \quad (2)$$

$$J' = \mathrm{H}'/\log S \quad (3)$$

$$D = 1 - \sum_{i=1}^{s} p_i^2, \quad (4)$$

$$N_1 = \exp H', \quad (5)$$

$$N_2 = 1/D, \quad (6)$$

, where $p_i$ is the relative dominance of *i*th species in a given plot. These indices were chosen to include popular indices like species richness (Carlson et al. 2007; Rocchini, Ricotta, and Chiarucci 2007; Viedma et al. 2012), and the Shannon entropy (Oldeland et al. 2010; Wang, Gamon, Cavender-Bares, et al. 2018), and the relatively untested true diversities, which are argued to be better suited to describe diversity and compare studies (Jost 2006; Tuomisto 2010). Two sets of field diversities were calculated: canopy diversity and total diversity, the latter being the average of canopy and herb layer diversity. Variation in species composition between plots was evaluated by Bray-Curtis dissimilarity matrices by presence/absence (i.e., Sørensen index) and by abundance of species (Oksanen et al. 2019).

### 2.2.3 Spectral diversity indicators

To test the effects of resolution on the spectral diversity indicators, the indicators were calculated from low (3.2 m) and high resolution (0.8 m) images. The impact of neighbouring pixels on spectral diversities was examined by using two spectral plot extents (Figure 2.1); the narrow extent covered pixels corresponding to the field plots (10 m × 10 m square), while the wide extent included additional neighbouring pixels (10 m radius circle centred in the plot). For the low resolution, the number of pixels per plot ranged between 9–12 (narrow extent) and 28–32 (wide extent), and for the high resolution ranged between 144–169 (narrow extent) and 472–480 (wide extent). Within the high resolution spectral plots, in average 5% of the pixels were in shadow for narrow extent (range 1–15%) and 3% for wide extent (range 0–12%). Excluding shaded pixels did not change the correlations between single spectral indicators and field indices (Kruskal-test, $P = 0.21$), although the regressions were slightly

increased when two spectral indicators were used as explanatory variables (Kruskal-test, $P$ = 0.02). However, the best regression pairs remained the same; therefore, we retained the shaded pixels in the high resolution spectral plots to cover the same areas as the low resolution spectral plots.

The reflectance values of the four bands, Blue, Green, Red, and NIR, and the Normalized difference vegetation index (NDVI, calculated as (NIR – Red) / (NIR+ Red); Rouse et al., 1974) were recorded for every pixel at each resolution and extent combination and were imported to R software (R Core Team 2018). Using the four bands as a matrix, PCA was carried out (Rocchini et al. 2007): the first principal component (PC1) explained more than 99% of the variation in the bands and was included for calculating spectral diversities.

The first set of spectral diversities was calculated by taking the mean, range (difference between minimum and maximum values), SD, and CV of each band, NDVI, and PC1 by plot for the four combinations of resolutions and extents. In addition, the mean Euclidean distance (Distance) from the plot centre was calculated using the bands as coordinate system axis (Rocchini et al. 2007; Schmidtlein and Fassnacht 2017).

The second set of spectral diversities was calculated by counting the unique reflectance values as species and calculating the same diversity indices as from field observations: if three and six pixels out of nine had the same values, then the richness (marked by bold $\boldsymbol{S}$ to distinguish from field diversity $S$) of the spectral plot was regarded as two. NDVI and PC1 values were sorted into 40 equal sized bins and the bins were handled afterwards as unique values. In total, 63 spectral indicators were calculated for each resolution and extent combinations (Table 2.1). Pairwise differences of the 63 spectral diversities were examined by the Euclidean distance matrices.

### 2.2.4 Comparison of the field diversity indices and spectral diversity indicators

Pearson's correlation coefficient ($r$) and linear regression models (LM) were used to investigate the relationship between the field indices and spectral indicators. From the six field diversity indices and 63 spectral indicators all together 3024 correlations were calculated for α-diversity (6 × 63 × 4 × 2, for all combinations of field and spectral diversities, resolutions, extents, and field layers) and 504 dissimilarity matrices of species composition (63 × 4× 2). Correlations with a $P$-value of less than 0.05 were treated as strong correlations. Significant differences in the number of strong correlations between low and high resolutions and between narrow and wide extents were examined by $\chi^2$-test. The effects of resolution,

extent, and elevation on the correlation coefficients were examined by non-parametric Kruskal-Wallis test and pairwise Wilcoxon test.

We applied stepwise multiple regression analysis to test the predictability of field diversities by one to five spectral indicators as explanatory variables using the R package *leaps* (Miller 2020). LM was used to examine more in detail the accuracy when the number of explanatory variables was limited to two spectral indicators, testing all combination of pairs. We retained those models, where all coefficients were significant at $P < 0.05$, to identify spectral indicator pairs estimating field indices with high accuracy. The effects of elevation on field indices and spectral indicators were examined with LM, using elevation alone and paired with spectral diversities as explanatory variable. In addition, spatial auto-correlation of field and spectral diversities was tested by Moran's *I* (Moran 1950).

The significance of correlations between the dissimilarity matrices of field diversity indices and spectral diversity indicators were determined by Mantel-test with ten thousand permutations (Legendre and Legendre 2012; Mantel 1967). The dissimilarity of the seven forest types and separately the age of forests on species composition and spectral dissimilarity were measured with ANOSIM and the *P*-value was calculated by ten thousand permutations (Clarke 1993).

## 2.3 Results

### 2.3.1 The effects of resolution and extent on correlations

The number of strong correlations, where *P* was less than 0.05, was low and changed with resolution and spectral plot extent (Table 2.2). The spectral indicators derived from low resolution had a higher number of strong correlations, both with canopy and total diversities, than those derived from high resolution ($\chi^2$-test, $P < 0.001$). The number of strong correlations increased when narrow extent was used ($P < 0.001$ against canopy and $P = 0.02$ against total indices). Canopy diversities had a higher number of strong correlations than total diversities ($P < 0.001$), but their range was the same, i.e., *r* ranging 0.34 – 0.50 with canopy and 0.33 – 0.50 with total indices (in absolute values, Kruskal-Wallis test, $P = 0.87$). The highest correlations were obtained from the low resolution–narrow extent spectral indicators (Table 2.2), both in the case of canopy ($r = 0.50$, *J'* – PC1-***D***) and total diversities ($r = 0.50$, *J'* – PC1-***H'***). The other resolution–extent combinations had significantly lower correlations with canopy diversities (Figure 2.3a, $P \leq 0.03$), while with total diversities only the high

resolution–wide extent based spectral indicators had significantly higher correlations ($P$ = 0.04).

### 2.3.2 The impacts of field indices and spectral indicators

From the field diversity indices, the canopy $N_1$ and $N_2$ yielded the highest number of strong correlations with spectral indicators (18 and 16 cases), while from the total indices, $D$ had the highest number of strong correlations (15 cases). However, the number of correlations did not indicate strong relationship; field $J'$ produced the highest $r$ (Figure 2.3b), significantly outperforming other field indices (canopy: Wilcoxon test, $p < 0.001$, total: Kruskal-Wallis test, $P < 0.01$). Most field indices showed high correlation with multiple spectral indicators, but total $N_{1,2}$ and $H'$ correlated only with high resolution–wide extent Blue-$\boldsymbol{J'}$.

Across all resolutions and extents, 20 and 15 spectral indicators were correlated significantly with canopy and total diversity indices. Most spectral indicators displayed strong correlations at low resolution–narrow extent combination (Figure 2.4), and were mostly calculated from NIR, NDVI, and PC1 scores. PC1-based spectral indicators had high correlations with both canopy and total field diversities, while NIR and NDVI based indicators were correlated stronger with canopy indices. From the PC1 indicators, SD and range were best with canopy indices, while PC1 indicators calculated as $\boldsymbol{S}$, $\boldsymbol{D}$, $\boldsymbol{H'}$, $\boldsymbol{N_{1,2}}$ were correlated stronger with total $J'$ and $D$. The highest correlations for each combination were positive among the field and spectral diversities, apart from the spectral indicators PC1-CV and Blue-$\boldsymbol{J'}$, which displayed negative correlations (Figure 2.5).

### 2.3.3 Linear relationships between field indices and spectral indicators

The best predictor variables identified by stepwise regression analysis changed with resolution, extent and the maximum number of predictors, although spectral indicators based on the Blue band and NDVI were kept often in the final regression models. To keep the number of variables low, I concentrated on models with two explanatory variables (pairs of spectral indicators).

The resolution and extent did not affect the number of significant regressions when estimating total diversity indices ($\chi^2$-test, $P$ = 0.96 and $P$ = 0.28), but regression models using low resolution–narrow extent based spectral indicator pairs fitted better than models using low–wide and high–narrow based spectral indicators (Wilcoxon test, $P < 0.01$, Figure 2.6a). When predicting canopy diversities, low resolution ($\chi^2$-test, $P < 0.001$) and wide extent ($P < 0.001$)

spectral indicator pairs had higher number of significant regressions. The low resolution–wide extent combination also increased the explained variance when canopy diversity indices were estimated by spectral diversity pairs (Wilcoxon test, $P < 0.01$). Canopy $N_1$ ($P < 0.05$) and total $D$ ($P < 0.01$) displayed larger average $r$ than the other field indices (Figure 2.6b), while total $H'$ had generally lower $r$ than other field indices ($P < 0.01$). The explained variance was highest when spectral indicator pairs were derived from low resolution and narrow extent (Figure 2.7). Namely, the pair of Blue-SD and Blue-range predicted canopy $N_1$ (LM, $r = 0.64$, $P < 0.001$) and the pair of Red-***D*** and PC1-***D*** predicted total $J'$ ($r = 0.61$, $P = 0.02$). Significant regressions against canopy indices were fewer ($\chi^2$-test, $P < 0.001$), but stronger than regressions against total indices (Kruskal-Wallis test, $P < 0.001$).

### 2.3.4 Effects of elevation and spatial autocorrelation

Field indices $S$, $H'$, and $N_{1,2}$ correlated negatively with the elevation when all 35 plots were analysed together ($r = -0.37$ to $-0.52$, $P < 0.05$). However, when the higher elevation young forest and lower elevation mature forest plots were analysed separately, the elevation of plots did not affect the field diversities. Pairing elevation with spectral diversity indicators as explanatory variable in regression models improved the fit of the models in the case of two and thirteen spectral indicators when regressing against canopy and total diversities, respectively. The highest $r$ was reached when estimating canopy $N_1$ and elevation was paired with NDVI-mean ($r = 0.65$), and when estimating total $H'$ with elevation paired with Blue-***J'*** ($r = 0.64$).

The canopy and total diversity indices displayed different spatial-autocorrelation patterns. Of the canopy diversities, only $J'$ showed spatial-autocorrelation ($I = 0.12$, $P = 0.02$), while all total indices were spatially auto-correlated except for $D$. The spectral indicators showing the highest correlations with canopy diversities did not show autocorrelation when calculated from high resolution but did show when calculated from low resolution–narrow extent ($P = 0.01$). As for the best spectral indicators correlating with total diversities, only the Blue-***J'*** calculated from high–wide combination showed spatial autocorrelation ($P < 0.001$). In general, spectral indicators calculated via SD, mean, CV, and range showed autocorrelation.

### 2.3.5 Changes in species composition

The Bray-Curtis matrices by species abundance correlated better with the spectral matrices than the matrices by presence/absence, so the analyses by abundance matrices were described here. The dissimilarity matrices of species composition and spectral diversity indicators did not show as high correlations as α-diversity indices did with spectral indicators. The dissimilarity matrix of canopy species composition had more strong correlations with the spectral indicators than the total species matrix ($\chi^2$-test, $P < 0.001$) and showed the highest correlation coefficient with PC1-mean from low resolution–wide extent image (Mantel's $r = 0.36$). Correlations with the total matrix were higher compared to the canopy matrix (Kruskal-Wallis test, $P < 0.004$), but the highest correlation—reached with low–narrow Red-***J'***, $r = 0.32$—was below that of the canopy. The canopy matrix had more significant correlations with high resolution spectral matrices ($\chi^2$-test, $P = 0.01$), while the total matrix had more correlations with low resolution matrices ($P = 0.03$). Neither the combinations of resolutions and extents, nor the selection of spectral indicators when calculating the dissimilarity matrices affected the strength of the correlations however.

In spite of the relatively low correlations between field and spectral matrices, the spectral indicators distinguished between the forest types (ANOSIM, canopy composition: $r = 0.55$, total composition: $r = 0.36$) and between old and young forests in the case of canopy composition ($r = 0.52$, Figure 2.8, Table 2.3). While the strength of correlation was lower compared to the field dissimilarity matrices when estimating the age of forests, the strength of correlation was similar when distinguishing forest types.

## 2.4 Discussion

### 2.4.1 The effects of resolution and extent

The resolution and inclusion of neighbouring pixels affected the correlations and regressions between spectral and field diversities. The effects depended on the choice of field indices and whether canopy or total diversities were evaluated.

The low and high resolution images used in this study had relatively fine resolution. Other studies report high correlations with species richness using either Quickbird (resolution same as the low resolution used here) or Landsat images (30m resolution) in wetlands (Rocchini 2007) and mountain forests (Levin et al. 2007). However, examples exist where similar fine resolution images (resolution same as the high resolution used here) are found to

have too fine spatial resolution to observe canopy richness (Nagendra et al. 2010). This study demonstrated that low resolution spectral indicators showed higher Pearson's correlation coefficients with field diversity indices. This suggests that the high resolution diversities reflected within study object heterogeneity which decreased their accuracy (Wang and Gamon 2019; Woodcock and Strahler 1987).

Increasing the pixel number per plot, i.e., wide extent, did not improve the correlations if single spectral indicators were used, and had inconsistent effect when pairs of spectral indicators were used. This contrasts the observations that larger plot size increases the correlation with spectral diversities (Rocchini et al. 2010) and that productivity in the surrounding landscape improves the evaluation of species richness in boreal ecosystem (Parviainen et al. 2009). This discrepancy may be the result of two factors: first, the forests on Mount Usu are middle-latitude forests with more favourable environmental conditions, and second, species diversity correlates better with spectral diversities than species richness (Underwood et al. 2003; Wang, Gamon, Schweiger, et al. 2018), masking any improvements from wide extent spectral plots.

However, the wide extent had an advantage to calculate unique value based spectral indicators, as the low resolution–narrow extent based spectral plots often had too few pixels and displayed perfect evenness (all values were unique). Although calculating spectral indicators from as few as nine pixels is not rare (Madonsela et al. 2017; Torresani et al. 2019; Woodcock and Strahler 1987), in those cases the indicators are based on measuring variance via traditional methods (e.g., mean, SD, or CV). Spectral indicators that strongly correlated with field indices, i.e., PC1, NDVI, and NIR, did not suffer from the problem of low pixel number, so the neighbouring pixels had no positive impact on them. The present study measured field diversities from one plot shape, but plot shape influences field measurements of diversities (Korb, Covington, and Fulé 2003; Marignani, Del Vico, and Maccherini 2007). Experimenting with multiple plot shapes and corresponding spectral extents when calculating indicators may find that plot shapes influence the performance of spectral indicators.

### 2.4.2 The effects of field indices and including herb layer diversity

Spectral indicators showed the highest correlations with *J'* when single spectral indicator was used, and with $N_1$ and $N_2$ when pairs of spectral indicators were used. Although the spectral diversities were correlated differently with canopy and with total diversities (when herb layer diversity was included), high correlations were observed with both canopy and total field

indices. Recent studies on the correlation of field and spectral indices are often using *H'* or *D* (Oldeland et al. 2010; Wang, Gamon, Schweiger, et al. 2018), as these indices incorporate information about the abundance of species and were shown to correlate stronger with spectral diversities than *S*, which only measures presence-absence (Underwood et al. 2003). This study observed low correlations between spectral indicators and *S*, but found that *J'* and $N_{1,2}$ showed higher correlations with spectral indicators than *H'* and *D*, especially when estimating canopy diversities. Abundance based dissimilarity matrices also displayed higher correlations than presence-absence based matrices when estimating compositional variations of species, supporting the importance of abundance sensitive diversity measures.

The best spectral indicators correlating with field diversities were obtained from low resolution images, although high resolution–wide extent indicators estimated total diversities well. When the study organism is large, using low resolution images for calculating spectral diversities increases the accuracy (Stickler and Southworth 2008). Conversely, spectral indicators based on high resolution images can observe small size organism, such as ant colonies (Lassau et al. 2005). These suggest that high resolution images are better to estimate total forest diversity because small plants need to be detected as well. In this study, the total diversity was evaluated well both by low resolution–narrow extent and high resolution–wide extent based spectral indicators, so the total indices seemed not to show a clear preference for high resolution images.

However, the size of study organism mattered when pairing spectral indicators with elevation; several indicators estimated total diversity better when paired with elevation, while elevation scarcely improved the estimation of canopy diversities. This corresponded to Camathias et al. (2013), who found that topographical factors improved estimations more when the size of study organism was small in temperate forests in Swiss.

Combining spectral indicators estimates field diversities better than single spectral indicators in tropical dry forest (Gillespie 2005) and in central-African forest (Thenkabail et al. 2003). Improvements were also observed in this research when two spectral indicators were used to estimate field indices, especially when assessing $N_{1,2}$. True diversities are rarely used and they display low performance compared to *H'* in Borneo tropical forests (Foody and Cutler 2003). The results suggested that $N_{1,2}$ was sensitive to habitat differences when combined with remotely sensed indicators, estimating diversities in temperate forests more than in tropical forests.

### 2.4.3 Band specificity of spectral indicators and spatial autocorrelation

When correlating spectral indicators with canopy diversity indices, the best spectral indicators were derived from the PC1 and NIR. When correlating with total diversities, the best spectral indicators were derived from the PC1 and from mostly visible bands. Spectral indicators derived from NDVI displayed weak correlations, possibly because NDVI is correlated with the productivity of plant communities rather than with the landscape heterogeneity (Johansen and Tømmervik 2014). Productivity is more related to canopy diversity than to total diversity because the biomass of trees is larger than the biomass of understorey plants (Zhang, Chen, and Taylor 2016). This is consistent with the fact that NDVI-based indices estimated the canopy diversities better than the total diversities. The high performance of PC1-based indicators showed that integrating multiple bands created the most successful spectral indicator source.

Plots close to each other often display spatial autocorrelation (Legendre 1993) and distance of plots positively correlates with species turnover in grassland habitat (Hall et al. 2012). This study did not observe spatial autocorrelation in the canopy layer, but the inclusion of herb layer induced spatial autocorrelation. Understorey vegetation disperses slower than woody species (Cain, Damman, and Muir 1998), and clumping is also influenced by the density of saplings (Miller, Mladenoff, and Clayton 2002), which might explain why only total diversity displayed autocorrelation. The best spectral indicators were unaffected by spatial autocorrelation.

A limitation of the study is the use of single source image to calculate spectral diversities, as combining multiple satellite images from different dates are shown to increase the accuracy of spectral indicators (Dudley et al. 2015; Räsänen and Virtanen 2019). However, the image acquisition date was in the summer season, when the status of local vegetation was optimal for remote observation (Schmidtlein and Fassnacht 2017). In addition, the study focused only on forest habitats, so estimating only herb layer diversity was not suitable, due to the canopy largely covering the understorey herb layer.

## 2.5 Conclusion

The spectral diversity indicators based on low resolution and narrow extent had higher correlations with the field indices. Spectral diversities based on PC1 and NIR had high correlations and using two spectral indicators estimated field diversities better. In particular,

the canopy diversities were evaluated by the spectral diversities using PC1 and NIR, while the total diversities were evaluated using the PC1 and visible bands. Among the field diversities, *J'* and $N_{1,2}$ were estimated best. Although compositional changes in species were detected less than α-diversities, forest types were distinguished well. The present study confirmed that spectral indicators estimate canopy and total field diversities in various temperate forests. As canopy diversity is a good predictor of total forest diversity (Hakkenberg et al. 2018) and it is faster to survey, future studies should focus on it to evaluate forest diversities.

**Tables and Figures**

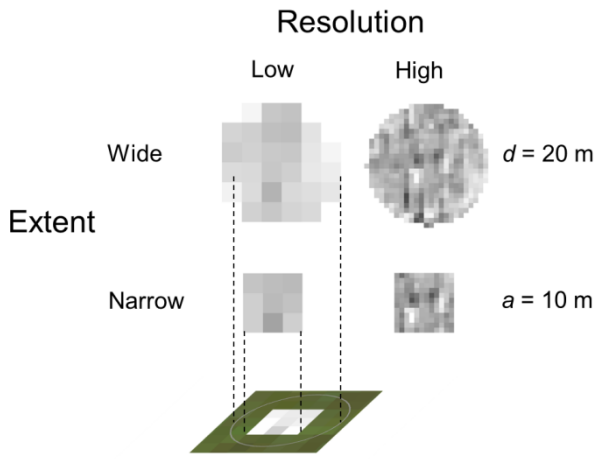


Figure 2.1 The four types of spectral plots used in the study, made by the combinations of low and high resolutions and narrow and wide extents. The field survey on forest canopy was carried out on a square plot (*a*, side = 10 m), corresponding to the low resolution–narrow extent spectral plot. The wide extent is marked by a circle (*d*, diameter = 20 m) with its centre in the middle of the plot established in the field.

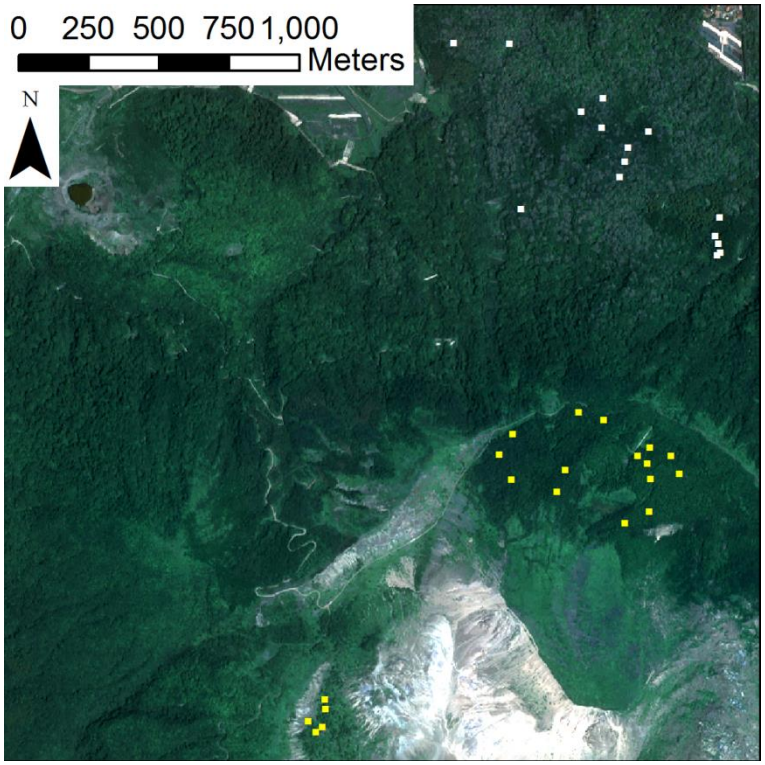


Figure 2.2 Locations of the 35 plots (10 m × 10 m) used for the study on Mount Usu, northern Japan. The white coloured plots cover mature forests, while the yellow plots are young forests, less than 110 and 40 years, respectively.

Table 2.1 Spectral diversity indicators used in the study.

| Spectral origin | | Calculation method |
|---|---|---|
| Bands | Blue<br>Green<br>Red<br>NIR | Statistical<br>Mean<br>Standard deviation (SD)<br>Range<br>Coefficient of variation (CV)<br>Mean distance from centroid (Distance) |
| Vegetation index | NDVI | Unique value based<br>***S*** |
| PCA | PC1 | ***H'***<br>***D***<br>***J'***<br>$N_1$<br>$N_2$ |

Table 2.2 The number of strong correlations and name of the best indices by resolution–extent combination between field diversity indices and spectral diversity indicators.

Number of strong correlations

| Resolution | High | | Low | | Total |
|---|---|---|---|---|---|
| Extent | Wide | Narrow | Wide | Narrow | |
| Canopy | 4 | 5 | 11 | 59 | 79 |
| Total | 3 | 1 | 5 | 21 | 30 |

Pearson's correlation coefficient

| | | | | |
|---|---|---|---|---|
| Canopy | 0.36<br>*S* – NIR-$N_2$ | - 0.36<br>$N_2$ – PC1-CV | 0.36<br>*S* – PC1-***D*** | 0.50<br>*J'* – PC1-***D*** |
| Total | - 0.44<br>*H'* – Blue-***J'*** | 0.34<br>*D* – Green-***J'*** | 0.40<br>*D* – PC1-***H'*** | 0.50<br>*J'* – PC1-***H'*** |

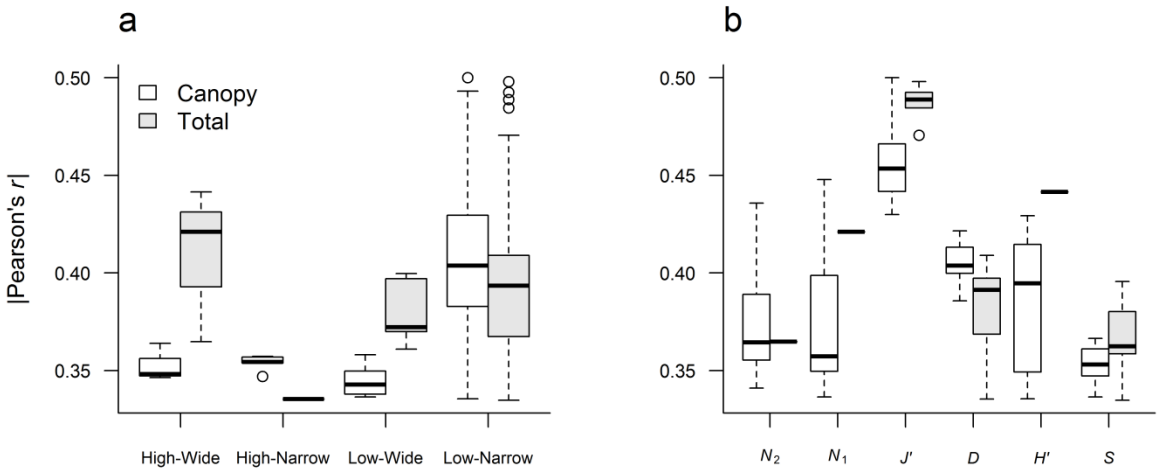


Figure 2.3 Box-whisker plots of Pearson's correlation coefficients (*r*) between spectral and field diversities depending on spectral resolution and extent (a) and on field indices used (b). Empty boxes indicate when spectral diversities are compared with canopy diversity and filled boxes when compared with total diversity. For abbreviations see text.

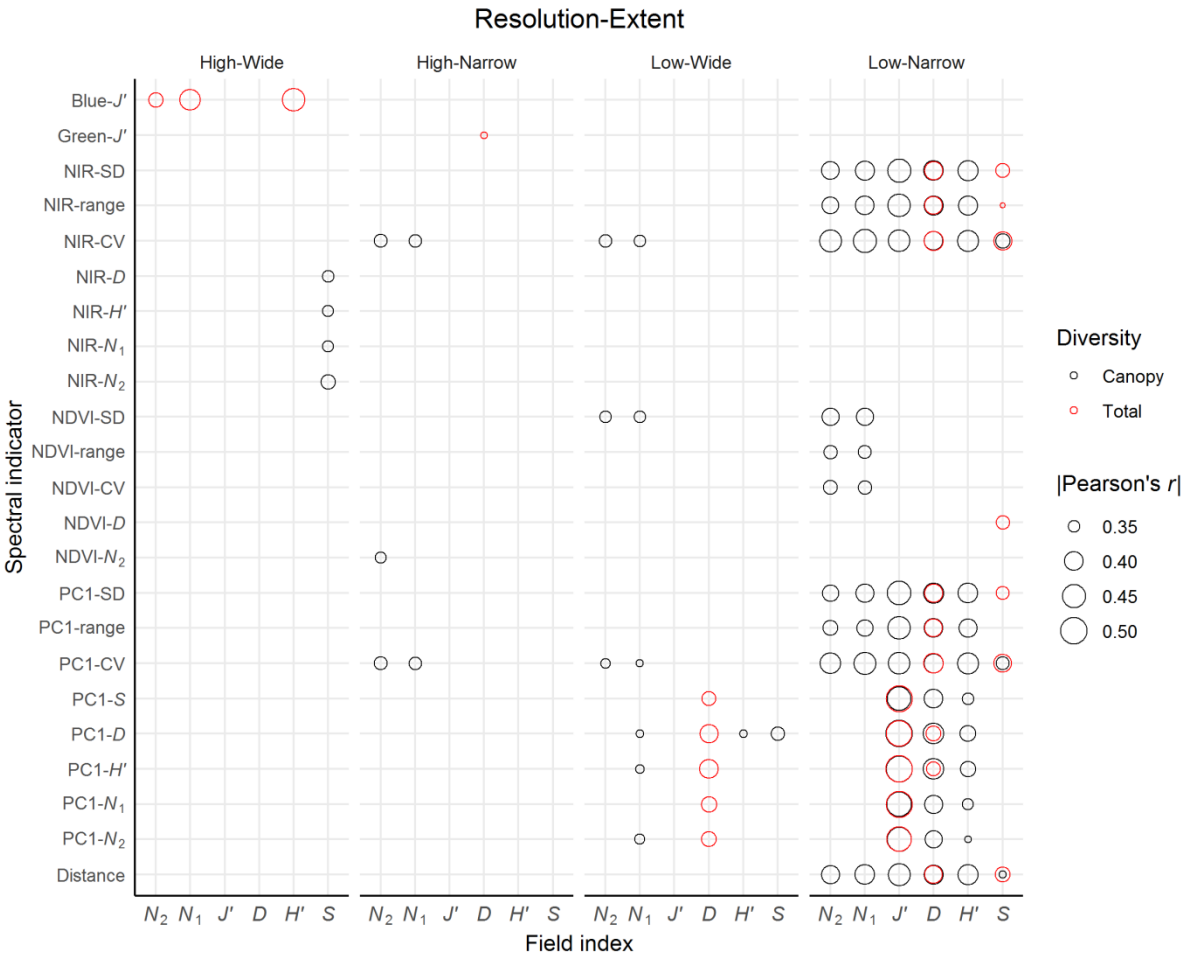


Figure 2.4 Pearson's correlation coefficients between spectral and field diversities grouped by resolution and extent combinations. Black circles mark correlations with canopy diversities and red circles with total diversities. The size of the circles increases with increasing coefficients.

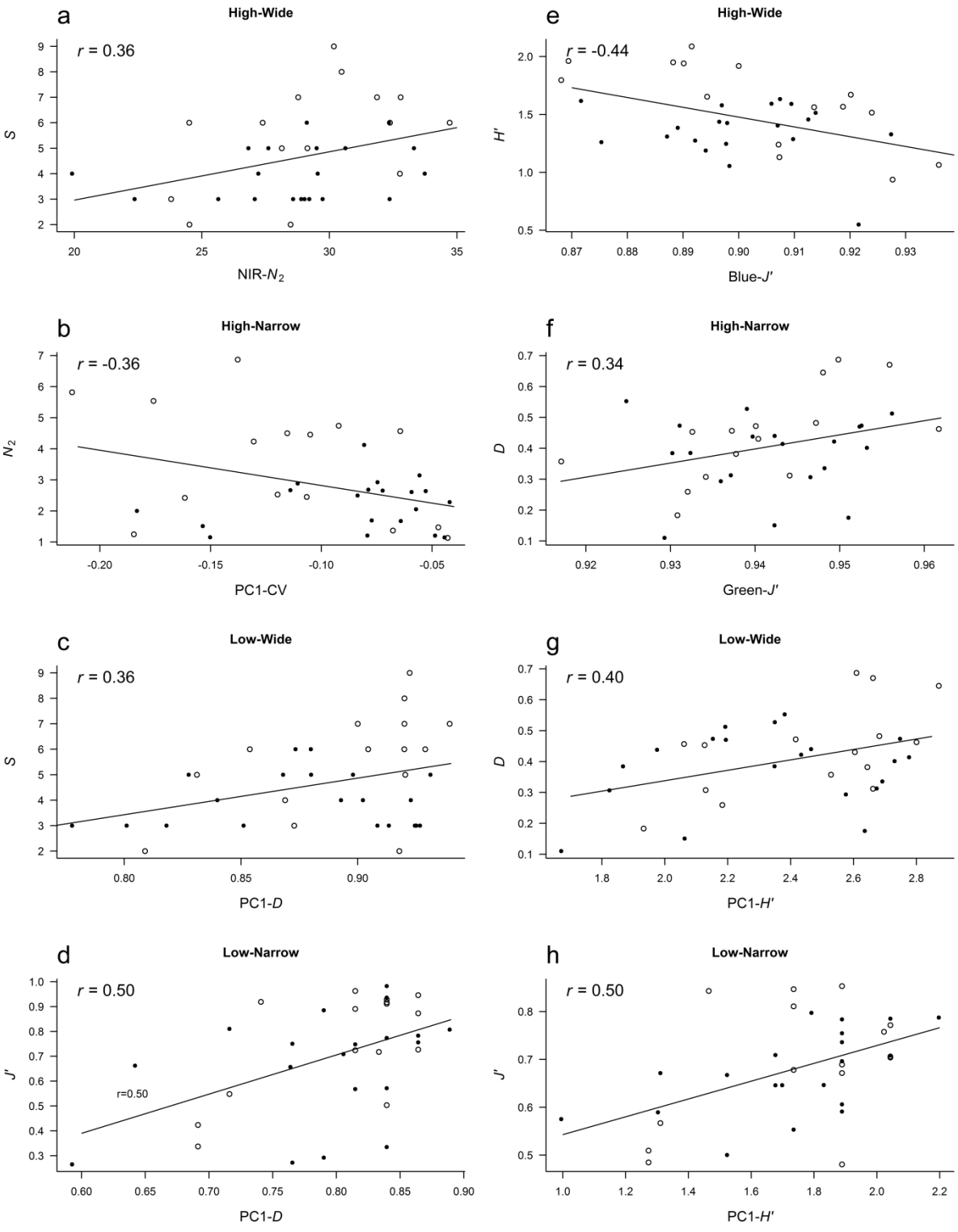


Figure 2.5 Linear regressions between the best spectral indicators and canopy (a-d) and total diversity indices (e-g), displaying Pearson's correlation coefficients. The *x* axis shows the spectral indicators and the *y* axis shows the field diversities. Filled circles indicate young forest plots while empty circles indicate mature forest plots. All regressions are significant at $P < 0.05$.

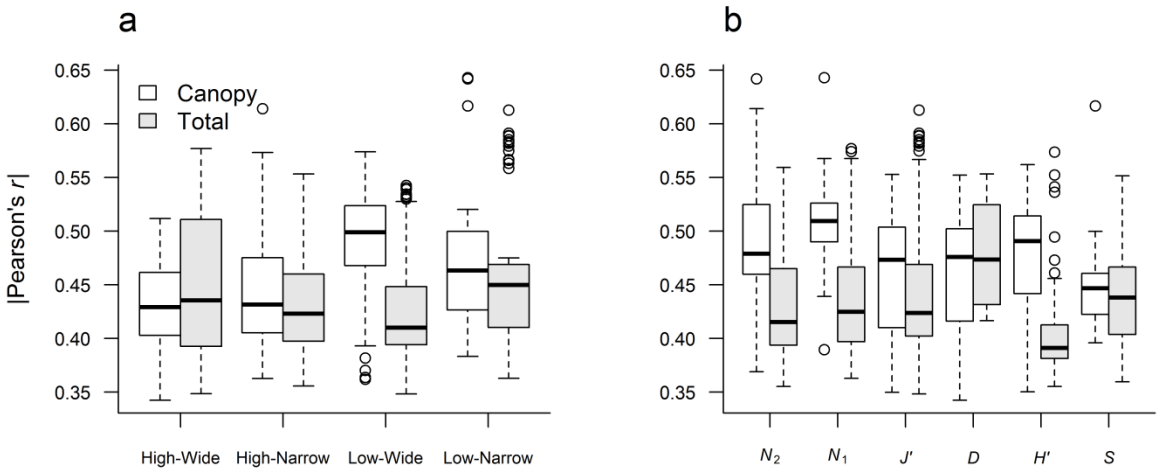


Figure 2.6 Regression between pairs of spectral indicators and field indices from the four resolution–extent combinations (a) and with different field indices (b). Empty boxes represent regression against canopy diversities and filled boxes against total diversities.

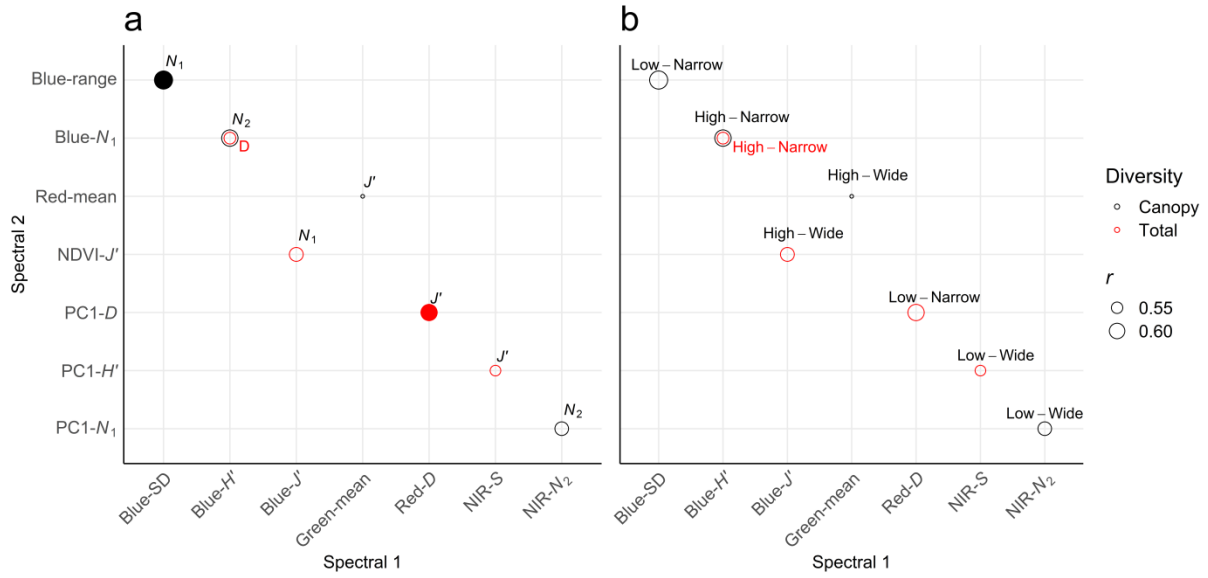


Figure 2.7 Best spectral indicator pairs to estimate field diversities (a) and the resolution–extent combination they are calculated from (b). The field diversities estimated with the highest accuracy are marked by filled circles on the left plot.

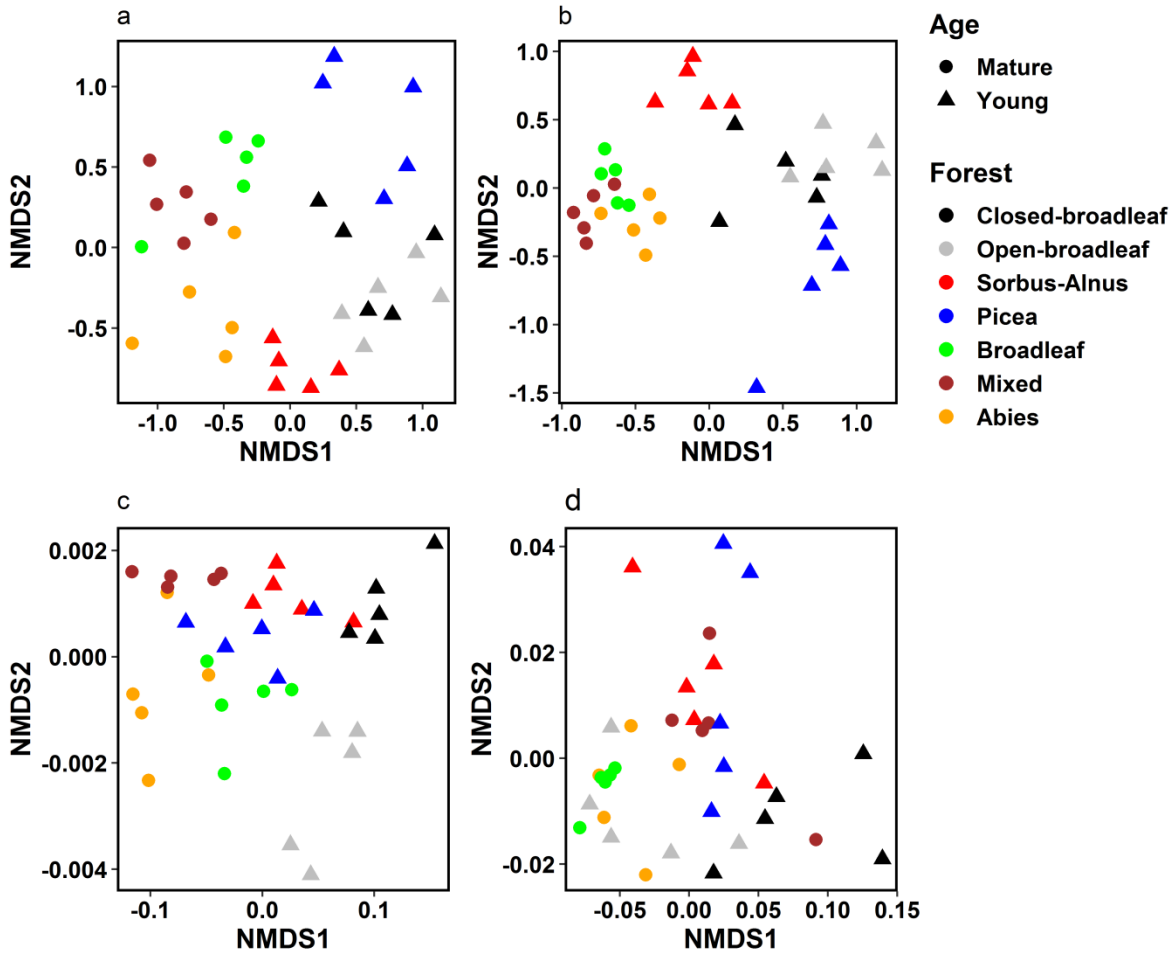


Figure 2.8 Ordination of plots with non-metric multidimensional scaling. The canopy (a) and total (b) distances were calculated with Bray-Curtis dissimilarity matrices, while for the spectral indicators (c, d) Euclidean distances were used. The spectral matrices were calculated from the two indicators with the highest Mantel's *r*: PC1-mean and NIR-mean were used to simulate canopy conditions (c) while NDVI-***J'*** and Red-***D*** were used to simulate total conditions (d). Different colours indicate different forest types and different symbols indicate the age of the forests.

Table 2.3 Distinctness of forest types and age based on the dissimilarity matrices. ANOSIM (permutation: 10 000) was used to calculate correlation and significance values. Details about calculating the dissimilarity matrices are described at Figure 2.8. $P < 0.001$ unless otherwise marked.

| *r* based on field survey | Canopy | Total |
|---|---|---|
| Age | 0.88 | 0.56 |
| Forest types | 0.53 | 0.29 |

| *r* based on spectral diversities | PC1-mean + NIR-mean | NDVI-***J'*** + Red-***D*** |
|---|---|---|
| Age | 0.55 | 0.36 |
| Forest types | 0.52 | 0.07 ($P = 0.07$) |

# Chapter 3 Species diversity 40 and 110 years after the eruptions of Mount Usu – comparing the impacts of early successional processes


## Abstract

Volcanic successional trajectories are often divergent, because of stochastic processes and management activities. Evaluating the effect of management practices and stochastic events on plant composition and diversity has been difficult because of the lack of long-term studies. This study examined the species composition and diversity in several forest types at the 1910 and 1977-78 eruption sites of Mount Usu, hereafter Yosomi and summit, to compare the impact of early successional events. Both naturally regenerated and planted forests were surveyed at the sites during 2015–2019 by observing five 10 m × 10 m plots in each forest type to measure tree diversity, and four 1 m × 1 m quadrats per plot to measure understorey (hereafter, herb layer) diversity by shoot density and cover. Species composition was analyzed by non-metric multidimensional scaling and three levels of diversity, canopy, herb layer, and total, were calculated as true diversity from order 0 (presence-absence) to 2 (weighted species). The results showed that canopy composition was more influenced by early management practices than herb layer composition. The species composition was distinct between the forest types, indicating that early restoration practices had long-term effects on species composition. The naturally regenerated forests showed the highest diversity at both eruption sites, while the plantations displayed low canopy but high herb layer diversity. Herb layer diversity was higher at the summit, but canopy diversity was higher at Yosomi. The plantations changed their species composition slowly and failed to transform into more natural forests. In addition, the plantations were more sensitive to subsequent disturbances after the eruptions, indicating that the plantations affected long-term succession and their effect was stronger than stochastic events.

## 3.1 Introduction

Early studies of plant succession promoted linear development from early stage communities toward a climax community (Clements 1916), but as disturbances alter successional processes and change the distribution and density of plants (Gleason 1926; Whittaker 1960), the convergence and divergence of succession became controversial. Although pioneer species often colonize in a deterministic manner after disturbances (Efford, Clarkson, and Bylsma 2014; Marler and del Moral 2013; Tsuyuzaki 2019), stochastic events modify successional patterns (Karadimou et al. 2018; del Moral et al. 1995). Therefore, the role of stochastic processes is increasingly recognized in community development (Lichter 2000; del Moral 2009).

A popular method to study primary succession is the space for time substitution, called successional chronosequence, where successional sere is constructed by observing plant communities at various locations arranged by the date of disturbance (Cutler et al. 2008; Irl et al. 2019; Sutomo et al. 2011). However, the applicability of chronosequences is restricted because different locations do not share the same history and conditions, so their successional trajectories diverge (Johnson and Miyanishi 2008). Even when site history is controlled, stochastic events alter the successional trajectories (White and Walker 1997).

To evaluate the effects of stochastic events on primary succession and incorporate it into restoration practices, long-term monitoring is required (Prach and Walker 2011). Volcanic eruptions destroy vegetation, thus provide suitable sites for monitoring primary succession. However, only a few studies observe successional processes on a timescale over 20 years after eruptions (e.g., Fridriksson 1982; Karadimou et al. 2018). Mount Usu erupted at distinct locations in 1910 at a foothill called Yosomi and in 1977-78 at the summit. These two sites were covered with forest prior to the eruptions which denuded them, and by now they regained their forest cover. Due to management practices and stochastic events, a mosaic of different forest types developed on the mountain. To observe long-term trends, I compared the successional trajectories 40 and 110 years after the eruptions on Mount Usu in this chapter.

Naturally recovered forests often show higher species richness than plantations, but long-term trends are not observed well (Prach and Walker 2011). On Mount Usu, plantations have been conducted broadly, providing an opportunity to compare the outcomes of the management practices in terms of species diversity and community composition with those of naturally recovered forests. Diversity changes with time passed since disturbance and is

suggested to be highest at intermediate level of disturbances, known as the intermediate disturbance hypothesis (IDH) (Grime 1973). The IDH is usually connected with secondary succession, but it may have implications in cases of primary succession: my hypothesis was that the 1977-78 eruption site was more diverse than the 1910 site, because it was in its early successional stage when plant communities were sensitive to small differences in environment, leading to higher variations in communities than in later successional stages.

## 3.2 Methods

### 3.2.1 Location

The 1910 eruption site was covered with old forest prior to the eruptions (developed after the eruptions of 1822 and 1853; Kadomura, Okada, and Araya 1988) which was completely destroyed due to the ash fall and topographical changes. One side of the area slid into the lake, while another part rose to form Mount Yosomi, a small hill (Katsui et al. 1978). The eruption site was not damaged by the 1977-78 and 2000 eruptions, and the area is covered with a mixture of broad-leaved forest (*Populus suaveolens*, *Acer pictum*, and *Kalopanax septemlobus*), planted *Abies sachalinensis* forests and an old plantation of *A. sachalinensis* in which broadleaved trees are mixed in. The 1910 eruptions site is referred to as Yosomi hereafter.

In contrast to Yosomi, the eruptions, damages, and the subsequent revegetation processes are well studied at the 1977-78 eruptions site. The eruptions occurred at the summit, which was covered with seeded pastures and broad-leaved forests of *Populus suaveolens*, *Betula platyphylla* var. *japonica*, *Ulmus davidiana*, and *Acer pictum* ssp. *mono* prior to the eruptions (Tsuyuzaki 1987). The tephra explosions destroyed the summit except some of the northern and north-eastern areas (Katsui 1981). Due to the thick tephra deposits, for several years the vegetation recovered mostly by vegetative reproduction which spread from the edges of the site. The dominant species were *Fallopia sachalinensis*, *Petasites japonicus*, and *Populus suaveolens* (Kadomura et al. 1988; Tsuyuzaki 1989a).

Pioneer plants started to establish less than five years after the eruptions (Tsuyuzaki 1987), and revegetation happened faster at the caldera rim where rain and snow washed away the volcanic deposits and exposed plant propagules buried in the former topsoil. In the crater basin, the thick tephra slowed down succession by three years relatively to the caldera rim (Tsuyuzaki and Haruki 1996b). Parts of the summit area were subject to aerial seeding and

planting to stabilize the ground surface (Kadomura et al. 1988). At present the caldera rim is covered by a mixture of natural broad-leaved forest (*Populus suaveolens, Acer pictum*), planted broad-leaved forest (*Betula platyphylla, Sorbus commixta, Salix* spp., *Alnus hirsuta*) and planted conifer forest (*Picea glehnii*). Large areas of the crater basin are still in the early successional stages and covered by bare ground or grassland, while a smaller area is covered by an open *P. suaveolens* forest. The 1977-78 eruptions site is called the summit henceforward.

### 3.2.2 Field survey

Satellite and aerial images taken during 1972–2015 (Table 2) were used to identify areas impacted by the 1910 and 1977-78 eruptions. Within the eruption areas, several forest types were identified by supervised classification during image analysis and verified by field observations. These forest types are called at Yosomi as Broadleaf, Abies, and Mixed forests, and at the summit as Closed-broadleaf, Open-broadleaf, Sorbus-Alnus, and Picea forests (Figure 3.1). The Closed- and Open-broadleaf forests regenerated after the eruptions naturally, but light intensity was lower in the former. In each of these forest types multiple random locations were generated (stratified random two-stage sampling), excluding steep areas for safety reasons (identified using the ASTGT digital elevation map, ASTER 2011). Randomization was done using the ArcGIS random point generator function observing a minimum distance of 5 m between the points and from the given forest type edge. For every forest type, five plots were established from these randomly selected points and monitored from 2015 to 2019.

The plots for tree census were 5 m × 5 m in 2015 but were enlarged to 10 m × 10 m for five forest types in 2016 and for the remaining two forest types in 2019 (Open-broadleaf and Picea forests). Tree density did not change between the years, apart when a strong typhoon in 2016 uprooted and broke several trees in certain plots. Four of the Mixed forest plots were not monitored after the typhoon due to damages from fallen trees and heavy machines used to remove the trunks. Plots in the Sorbus-Alnus and Picea forests also suffered tree falls, but monitoring continued in them as only slight damages occurred. To exclude the effects of the typhoon, canopy diversity was calculated by re-constructing the 2016 conditions.

In 2015, two randomly selected quadrats (1 m × 1 m) were used for understorey vegetation (herb layer, less than 2 m in height) survey in every plot, but in the subsequent years the number of quadrats was increased to four. Cover percentage and aboveground shoot

density were recorded for every plant rooted inside the quadrat; the latter was either counted or estimated in an interval scale if counting was not possible (Table 3.1). The shoot density and the midpoint of the interval categories correlated well ($r = 0.93$, $P < 0.001$). Therefore, the midpoints of the intervals were used in the absence of exact density scores. Cover was recorded at 5% intervals. Unidentified plants were photographed and identified in the lab. If species could not be identified, they were treated at genus or family level and included in the diversity analysis.

Plots and quadrats were surveyed once a year during August or September, when understorey herbs were easy to record. To ensure that this early autumn survey is representative for year-around conditions, the herbs were surveyed at an additional time during June or July in 2016 and 2017.

In four plots of the Mixed forests the quadrats were not monitored from 2017 because of the typhoon damage.

### 3.2.3 Biodiversity measurements

Plant species diversity was measured at three levels: canopy, herb layer, and total diversity. Canopy diversity was based on the stem number of woody species with a DBH above 3 cm; herb layer diversity was based on shoot number or cover of plants smaller than 2 m; and total diversity was calculated as the mean of canopy and herb layer diversity scores.

Diversity was evaluated by the true diversity index (Jurasinski and Koch 2011; Moreno and Rodríguez 2011; Tuomisto 2011), also known as Hill numbers (Hill 1973), because true diversity measures the effective species number, which is easier to compare among sites than the Shannon index and Simpson index (Jost 2006). The α-, β- (multiplicative) and γ true diversity indices were calculated for order 0 ($N_0$, species richness), order 1 ($N_1$, all species equally important), and order 2 ($N_2$, sensitive to common species) using the equations of Jost (2006). Order 0 is based on presence-absence, while order 1 and 2 take abundance into account. Order 1 incorporates the relative abundance of all species equally, whereas order 2 emphasizes common species, giving more weight to their relative abundance (less influence of rare species).

### 3.2.4 Statistical analysis

Vegetation surveys in autumn and summer, and diversities evaluated by cover and density were compared by linear models (LM) and Pearson's correlation coefficient ($r$). The dominant

herb layer species were ranked by total shoot density and cover percentage: the scores of each species were added from the four quadrats to calculate plot cover and density. Because a species could have been observed in any of the 5 plots in a forest type and in any of the 5 observation years, the average species score was calculated by summing annual scores and dividing the sum by 25 —except for the Mixed forest, where the sum was divided by 13 (5-5 plots in 2015–2016, and 1 plot in 2017–2019). The differences in species composition between the plots were measured by Bray-Curtis dissimilarity index (Bray and Curtis 1957) and compared by non-metric multidimensional scaling (nMDS) using the vegan package in R (Oksanen et al. 2019). ANOSIM was used to determine the uniqueness of forest groupings with ten thousand permutations. True diversities of order 0-2 were calculated for every plot from their quadrats as γ-diversity, and α-, γ-, and β-diversities were calculated for every forest from their plots annually. Canopy diversities were calculated for only 2016 conditions.

I used generalized linear models (GLM, log-normal distribution) and general linear hypotheses comparison (GLH, Hothorn, Bretz, and Westfall 2008) to compare the canopy diversities, where the explanatory variables were the forest type, and the dependent variables were the ordered diversities at plot level or α-, β-, and γ-diversities at the forest level. For herb layer diversity, linear mixed models (LMM, (Bates et al. 2015; Lüdecke 2021) and GLH were used to compare plot diversities of order 0–2, where year was the random effect, and generalized linear mixed-effects models (GLMM, log-normal distribution) were used to compare α-, β-, and γ-diversities, where the fixed effects were forest type and order of diversity and the random factor was the year of survey. Data from 2015 was excluded from the statistical analysis of the herb layer diversity because smaller area was sampled in that year. Spatial autocorrelation was examined by Moran's *I* (Moran 1950), and the effect of elevation on the different order of diversities was tested with LM. All analyses were conducted in R programming environment (Edwards 2020; Hlavac 2018; Pedersen 2020; R Core Team 2018; Wickham et al. 2019; Wickham and Seidel 2020).

## 3.3 Results

### 3.3.1 Summer and autumn diversities

The summer and autumn plant diversity indices correlated well, with Pearson correlation coefficients ranging from 0.89 to 0.96 for density, and 0.82 to 0.93 for cover, in 2016 and 2017, respectively (Figure 3.2). Although species richness, density, and cover were greater

during the summer surveys than during the autumn ones, the diversities in autumn and summer followed similar patterns. This similarity indicated that the autumn diversity indices described year-round vegetation diversity with high accuracy.

### 3.3.2 Species composition

The dominant species differed within the forest types depending on whether species were ranked by density or cover (Table 3.2), but the rankings of all species correlated with each other (Kendall's tau between 0.80–0.85 for all forest types). Therefore, the dominant species description was based on the density ranking.

At the summit, *Pyrola asarifolia*, *Fallopia sachalinensis*, and *Petasites japonicus* were observed in most forest types. At Yosomi, *Rhus ambigua* and *Sanicula chinensis* established in two or more of the forest types. Species common at both sites were *Asperula odorata* and *Hydrangea petiolaris*. A few species ranked only in certain forests: at the summit, *S. chinensis* and *Ranunculus repens* were recorded in the Closed-broadleaf forest, *Artemisia montana* and *Trifolium repens* in the Open-broadleaf forest, *Celastrus orbiculatus* and *Stellaria media* in the Sorbus-Alnus forest, *R. ambigua* in the Picea forest. At Yosomi, the dominant species of the Mixed forest was different from that of other forests, with *Abies sachalinensis* and three other species being unique to it. Dominant species of the Broadleaf forest were *Onoclea orientalis* and *Acer pictum* saplings, while in the Abies plantation *Hylodesmum podocarpum* and *Phryma leptostachya* occurred most often.

The tree composition of the forests varied between the naturally regenerated forests and plantations (Table 3.3). At the summit, *Salix* ssp. and *Betula* spp. were common in all forests, and *Populus suaveolens* occurred everywhere except for the Sorbus-Alnus forest. The dominant species of the conifer plantation was *Picea glehnii*, but *Populus suaveolens* and *Salix* spp. naturally immigrated from outside the plantation. The Sorbus-Alnus plantation had low immigration and emigration rates, shown by the high number of unique species, such as *Sorbus commixta* and *Alnus* spp. The natural broadleaved forests were rich in *P. suaveolens* and *Acer pictum*.

At Yosomi, the common tree species were *Abies sachalinensis*, *Morus australis*, *P. suaveolens*, and *Alnus hirsuta*. The Broadleaf tree composition resembled the natural forest characteristic of the area around Mount Usu. The Mixed forest had a higher density of immigrating species than the Abies forest, and among the ranked species, *Hydrangea paniculata* and *Swida controversa* were recorded only there. The dominant species of the

broadleaved forests, *Acer* spp. and *Kalopanax septemlobus*, did not occur in high density in other forests. In the Abies forest the planted *A. sachalinensis* was the most dominant, and other species only had low density, such as *Magnolia kobus* and *Betula platyphylla*.

### 3.3.3 Species ordination

The nMDS by density distinguished the forest types and showed distinct groups both on herb (ANOSIM, r = 0.57, $P < 0.001$) and tree compositions (r = 0.88, p < 0.001). The summit forests occupied the right half of the multidimensional space along the first axis, while the Yosomi forests occupied the left half (Figure 3.3a). The herb layer composition overlapped within the Yosomi forest plots, although the Mixed forest plots remained separated from the other forest plots (characteristic species: e.g., *H. paniculata*, *A. sachalinensis*). At the summit, the Picea plots displayed large variations, one of its plots being positioned far away from the others. In this plot the forest floor was covered with needle leaves and little light reached the ground surface, resulting in no understorey herbs (pers. obs.). The Sorbus-Alnus forest plots also displayed distinct herb layer species composition, locating in the upper part of the nMDS space (e.g., *Urtica platyphylla*, *Adoxa moschatellina*, *Circaea mollis*).

The tree species composition showed greater differences than the herb layer composition of the forests and had distinct positions in the nMDS space (Figure 3.3b). The canopy plots of the forest types were almost always closest to their own forest centroid than to other centroids, whereas this was not true for many herb plots. The Yosomi forests clearly separated from each other, while at the summit, the Closed- and Open-broadleaf plots had overlapping tree compositions, but the other forest plots formed unique groups.

Tree composition of the canopy changed little during the five years, except for typhoon damages (Table 3.4). However, the herb layer composition of the forests altered during the years: the scores of summit forests displayed leftward movement, and those of Yosomi forests generally displayed downward movements in the nMDS space apart from the Broadleaf forest (Figure 3.4). The relative position of the forest types did not change within Yosomi and the summit, but as the summit forests were located on the right side in the nMDS space and the Yosomi forests on the left, the young summit forests' scores moved towards the mature Yosomi forest communities. The movement was slow, except between 2015 and 2016, when a large shift occurred in the herb communities, probably as a result of the doubling of the herb survey area between those years. At Yosomi, no large shift was observed between 2015 and 2016, suggesting that increasing the surveyed area had less effect there.

### 3.3.4 Forest diversities

Cover and density based diversities had high correlation (Spearman's $r = 0.85$), so only the density based diversity analysis was presented here. The herb level plot diversities showed different tendencies depending on their order (Figure 3.5). $N_0$, i.e., species richness, tended to increase with time, even after doubling the quadrat area from 2015 to 2016. When abundance of the species was included, i.e., using $N_1$ and $N_2$, the plot diversity displayed little change over the years (the survey year explained 18% variation for $N_0$ and 1% for $N_{1,2}$, Figure 3.6).

The forest level diversities calculated from the five plots showed that the γ-diversities differed depending on which order was used, but that natural broadleaved forests had consistently high diversity scores. The β-diversities were higher at the summit than at Yosomi, with Closed-broadleaf forest having the highest scores for $N_{0,1}$ and Picea forest for $N_2$ (Figure 3.7, Table 3.5). $N_0$ showed that the Mixed and Picea forests had the lowest scores ($t = -5.7$ and $t = -6.3$, GLMM with log-normal distribution, $P < 0.001$) and the Closed-broadleaf forest had the highest scores ($t = 2.5$, $P < 0.05$). As the order increased, the Picea forest showed higher scores and placed among the most diverse forests ($t = 2.8$, $P < 0.01$), while the scores of the Sorbus-Alnus forest remained low ($t = -1.1$, NS).

The canopy level plot diversities showed that the mature Yosomi forests, apart from the Abies plantation, were more diverse than the young summit forests. The forest with the most diverse tree composition and highest species richness was the Broadleaf forest (GLM, $P < 0.001$, Figure 3.8), while the Abies plantation showed the lowest plot diversity ($P < 0.001$, $t = -3.8$ – $-5.0$). Forest level diversities showed that the Broadleaf forest had low β- , but highest γ-diversity, whereas Mixed forest had the highest β-diversity (Figure 3.9). At the summit, both the Closed-broadleaf and the Picea forests had high α-, β-, and γ-diversities, and the Open-broadleaf forest had low diversities.

The herb layer and canopy diversities were not related (Figure 3.10), especially when presence-absence data were used. $N_{0,1}$ was higher for herb layer than for canopy in the case of α- and γ-diversity, but $N_2$ was similar. The canopy showed higher β-diversity than the herb layer at both sites, indicating that the tree composition was more heterogeneous than the herb layer composition. With increasing order of diversity, the Picea plantation changed from the least diverse forest to one of the most diverse forest.

### 3.3.5 Spatial autocorrelation and elevation

Moran's *I* showed, that $N_0$ of herb layer spatially autocorrelated ($I = 0.1$, $P = 0.03$). However, if calculated by density ($N_{1,2}$), autocorrelation did not occur ($P = 0.23$ and 0.66 respectively). If the diversities were calculated by cover, the spatial autocorrelation was significant at $N_{1,2}$ ($P = 0.04$ and $P = 0.05$). When the Yosomi and summit plots were analyzed separately, spatial autocorrelation was present only between cover-based diversities and both cover and density based richness at the summit. Elevation did not influence any order of diversities, depending neither on whether it was calculated by cover or density, nor on whether all plots were analyzed together or separated into Yosomi and summit.

## 3.4 Discussion

### 3.4.1 Differences in canopy and herb layer responses to early successional events

The herb layer was less influenced by the early successional events (i.e., plantation) than the tree species composition, shown by the overlap of herb layer composition between the forests. Canopy composition remained different among the forests while the eruption sites were distinguishable during ordination. Tree establishment in the early successional stages often determines the trajectory of succession (Mudrák, Doležal, and Frouz 2016), and in later stages the canopy and herb layer mutually influences each other's successional trajectories (Gilliam 2007). On Mount Usu, the Sorbus-Alnus forest displayed distinct canopy and herb layer composition, suggesting that the woody species affected the development of the herb layer. Dispersal limitation is known to influence the understorey species composition (Baeten et al. 2015; Graae, Hansen, and Sunde 2004; Verheyen et al. 2003), but the Sorbus-Alnus forest was close to forests surrounding the summit and to the Closed-broadleaf forest. Therefore, its herb layer composition was unlikely to be restricted by seed dispersal, but by competition for resources (Bourgeois, Vanasse, and Poulin 2016). In the other forests, the herb composition was weakly influenced by the canopy composition and diversity (Halpern and Lutz 2013).

Natural succession was slow on the summit where the tephra had been accumulated (Tsuyuzaki and Haruki 1996a), and this delay remained detectable on the canopy cover of Open-broadleaf forest. The Open-broadleaf forest lay farther away from the other forests and had not been connected to seed sources after the eruptions, so the seed dispersion and establishment were limited (Jones and del Moral 2009). Areas with slow revegetation immediately after the disturbance developed the plant cover faster in later stages on Mount St.

Helens, Surtsey, and Usu (del Moral and Magnússon 2014; Tsuyuzaki 2019). However, the succession at the Open-broadleaf forest was slow to start and slow to progress. In the early successional stages, plants often facilitate the establishment, survival, and growth of each other, accelerating revegetation (Cutler et al. 2008). These positive effects were counterbalanced by the harsh conditions, low seed immigration rate, and lack of vegetative reproduction at the Open-broadleaf forest at the beginning of the succession, delaying the development of closed canopy forest.

The Yosomi forests had higher herb layer species richness, but lower $N_{1,2}$ than the summit forests, mostly due to high β-diversities at the summit. This indicated that the forests at the summit had higher inter-plot variations, especially in the case of Picea plantation. However, the canopy diversity showed opposing trend: the Yosomi forests had higher richness and diversity values than the summit forests. Because the herb layer was more diverse than the canopy layer at the summit and vice versa at the Yosomi, the total diversities were not different between the forest types. The opposing relationship between canopy and herb layer diversity at Yosomi and the summit suggests that if the canopy and herb layer followed an IDH like curve by time, they moved at different pace.

### 3.4.2 Active management versus passive restoration

The plantations retained their non-native tree species and restricted the establishment of native trees in them. Active management of post-disturbance areas often decreases native species immigration: the landscape alien *Larix kaempferi* plantation on the volcano Mount Koma impeded the development of natural forests (Kondo and Tsuyuzaki 1999), and trees grew slower on seeded plots than on unseeded ones on Mount St. Helens (Dale and Adams 2003). Although native species started to immigrate into the Picea forest by seed immigration from the surrounding natural forests, the process is slow (Cain et al. 1998; Sorrells and Warren 2011), shown also by the low ratio of broadleaved trees in the older Mixed forest at Yosomi. At Mount St. Helens, it took more than 30 years after the eruptions for most of the original species to re-establish (del Moral and Wood 2012). The present study covered areas 40 and 110 years after the eruptions, and the species composition remained different between the two sites, indicating that re-establishment was still in progress at the summit, 40 years after the eruptions.

Tree plantations often fostered and increased heterogeneity: the mosaic structure of the Picea forest resulted in high β-diversity scores because the quadrats falling between the rows

of trees included more species than quadrats falling below the trees; similarly, the Abies plantation had the highest β-diversity at Yosomi. The heterogeneous nature of the planting resembles thinning, which is an often used management strategy to increase the diversity of understory species (Kitagawa, Ueno, and Masaki 2017). While thinning may result in a decrease of diversity due to the machines used (Nagai and Yoshida 2006), the high β-diversity scores of the plantations suggest that spacious planting design has long-lasting positive impact without additional management.

Active management often delays the establishment of native species (Dale and Adams 2003; Kondo and Tsuyuzaki 1999) whereas non-intervention is a cost-effective and successful restoration approach (Mansourian et al. 2005; Prach and Hobbs 2008) when monitored properly (Gilbert and Anderson 1998). When comparing the coniferous Picea with the broadleaved Sorbus-Alnus plantation, the plot diversity was higher in the Sorbus-Alnus forest, but forest level α-, β-, and γ-diversities were lower. In addition, the common *P. suaveolens* did not establish in the Sorbus-Alnus plantation, as the conditions needed for its establishment are different from that of to survive as an adult (Young et al. 2005). So even though the Sorbus-Alnus forest was successful in the context of recovering cover quickly, it was not successful in the context of promoting high diversity (del Moral, Walker, and Bakker 2007), falling behind naturally recovered forests.

### 3.4.3 Resilience to post-disturbances: the impact of the typhoon

The plantations suffered intensive tree damage both at the summit and at Yosomi, showing that even though plantations had comparable herb diversity to natural forests, they were more sensitive to post-disturbances. Although wind speed is influenced by the terrain (Nakajima et al. 2009), the forests were located close to each other suggesting that wind speed was not the cause of the differences. At the summit, the soil layer was thin and planted trees were not able to reach deep enough to secure themselves: the Sorbus-Alnus forest was planted on landslide prevention dams and sandbags, and the *Picea* spp. were planted so close that their roots inter-vined, one falling tree pulling 6-8 other trees in the row with itself. The frequency of typhoons and other extreme weather events are predicted to increase due to climate change (IPCC 2013). Therefore, restoration activities need to aim not only to reach healthy ecosystems, but also to create resilient ecosystems.

## 3.5 Conclusion

Management activities and stochastic events influenced the development of forest communities, and their effects were larger on the canopy than on the understorey species. While canopy diversities were lower at the summit than at Yosomi, herb layer diversities were higher. The conifer and broadleaved plantations had fewer canopy species than the naturally recovered forests around the plantations, although the β-diversity of the Picea plantation was high due to its mosaicked structure. The herb layer diversity was less influenced by management activities than canopy diversity, but the herb layer composition was different between natural and planted forests. The aim of restoration is complex as it has to cater for the needs of both people and nature (Prach and Walker 2020) and setting goals is difficult in an ever-changing environment (White and Bratton 1980). Native species dispersed to plantations with time, but the process was slow; additional actions are needed to foster the transition of plantations into forests (Bourgeois et al. 2016), and improve their resilience to secondary disturbances.

**Tables and figures**

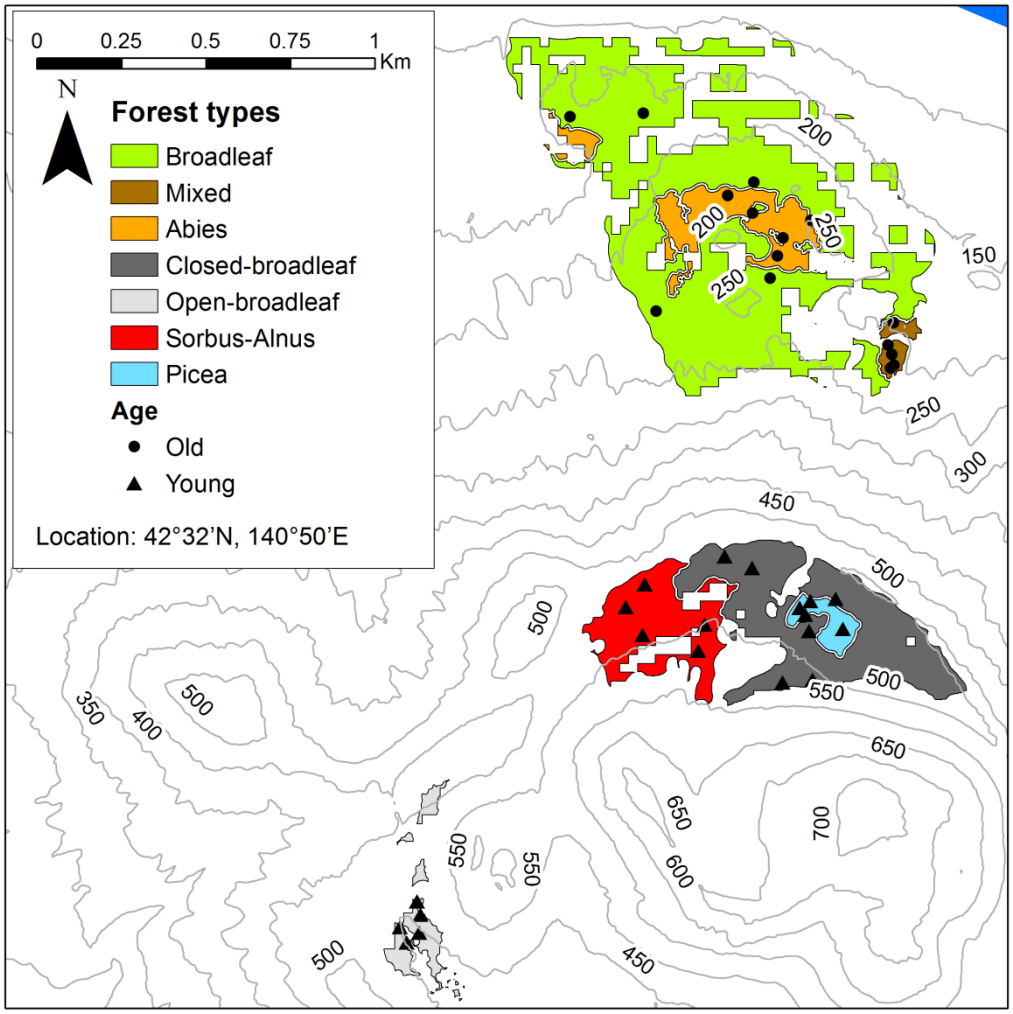


Figure 3.1 The forest types and plots examined during the study. The first three forests in the legend box are at Yosomi (old plots) and the last four are at the summit (young plots).

Table 3.1 Research design on annual monitoring. For all years cover and density were recorded in early autumn, with additional summer surveys in 2016 and 2017. Species cover is recorded at 5 % intervals, while density was either recorded as aboveground shoot number or on an interval scale. "Yes" indicates surveyed, "No" indicates not surveyed.

| | | 2015 | 2016 | 2017 | 2018 | 2019 | Density level intervals |
|---|---|---|---|---|---|---|---|
| Cover | Summer | No | Yes | Yes | No | No | 1-5 |
| | Autumn | Yes | Yes | Yes | Yes | Yes | 6-10 |
| Density | Summer | No | Yes | Yes | No | No | 11-25 |
| | Autumn | No | No | Yes | Yes | Yes | 26-50 |
| Density intervals | Summer | No | No | No | No | No | 51-100 |
| | Autumn | Yes | Yes | Yes | No | Yes | 100 < |

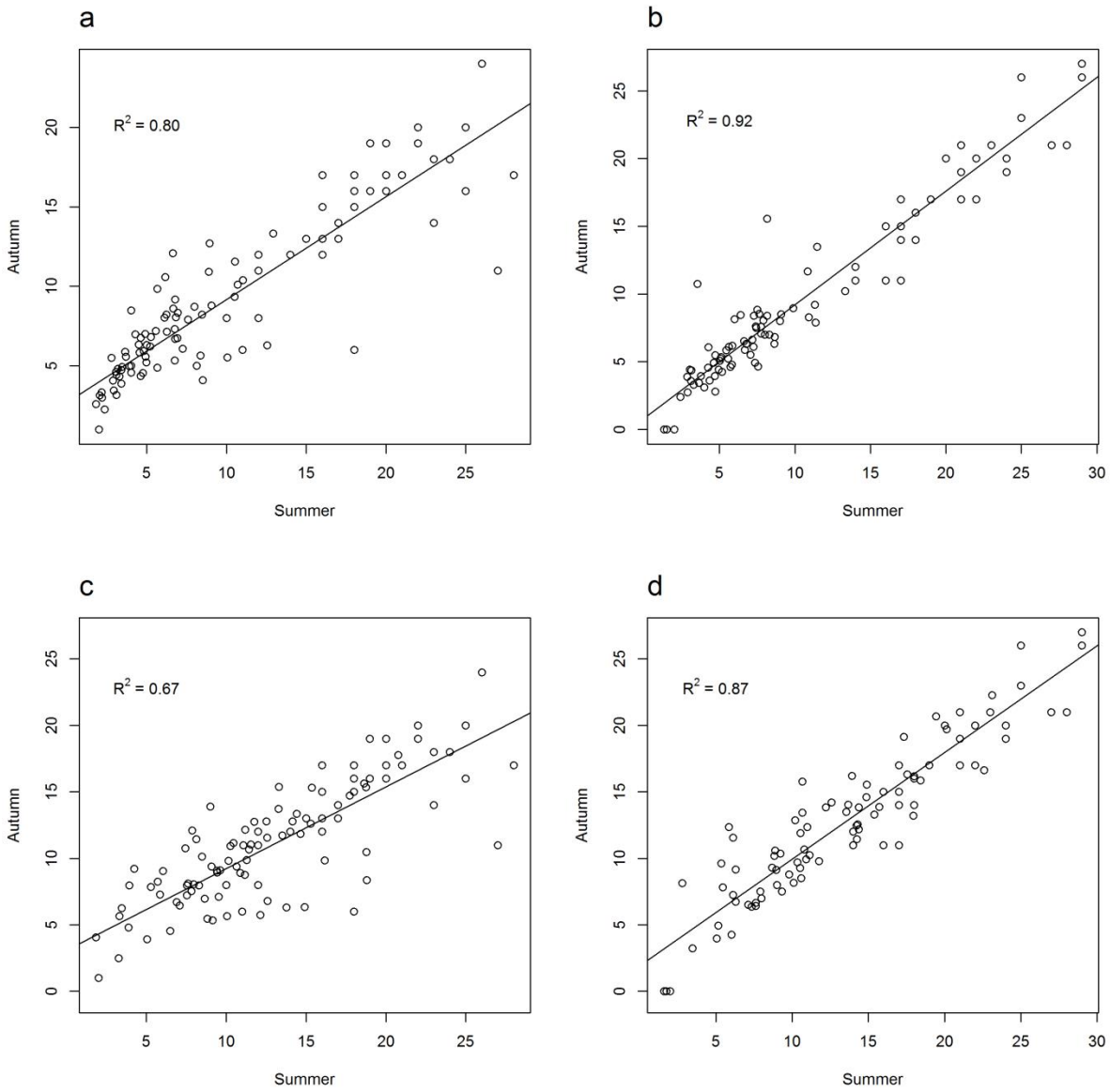


Figure 3.2 Correlations between summer (June-July) and autumn (Aug-Sep) true diversities of order 0, 1, and 2. Plot (a) and (b) show density based true diversities in 2016 and 2017, respectively, while plot (c) and (d) shows cover based diversities. $R^2$ is the coefficient of determination. $P < 0.001$ in all cases.

Table 3.2 Ranking and scores of dominant herb layer species by forest types. The rank is determined by the mean scores from 2015–2019 (shown in parentheses). Density based ranking is marked by n and cover based ranking is marked by %. Only species with a rank of 1-5 are shown.

| | Closed-broadleaf | | Open-broadleaf | | Sorbus-Alnus | | Picea | |
|---|---|---|---|---|---|---|---|---|
| Summit | n | % | n | % | n | % | n | % |
| *Artemisia montana* | | | 2 (41.7) | 1 (49.8) | | | | |
| *Asperula odorata* | 1 (71.5) | 2 (23.2) | 1 (63.8) | 2 (23.8) | 2 (56.2) | 1 (27.4) | | |
| *Celastrus orbiculatus* | | | | | 10 (4.1) | 9 (10.4) | | |
| *Fallopia sachalinensis* | 4 (15.0) | 1 (31.6) | 10 (4.4) | 5 (16.8) | | | 1 (8.5) | 1 (15.8) |
| *Geum macrophyllum* var. *sachalinense* | | | | | 5 (9.4) | 6 (18.0) | | |
| *Hydrangea petiolaris* | | | | | 4 (21.6) | 1 (27.4) | 3 (2.9) | 4 (4.0) |
| *Onoclea orientalis* | | | | | 6 (6.6) | 4 (22.6) | | |
| *Petasites japonicus* | 11 (4.2) | 4 (20.8) | 11 (4.0) | 4 (20.0) | 8 (4.4) | 5 (20.8) | 5 (1.7) | 2 (6.2) |
| *Pilea pumila* | | | | | 1 (62.0) | 3 (23.2) | | |
| *Pyrola asarifolia* | 2 (25.7) | 3 (22.4) | 3 (22.8) | 5 (16.8) | | | 2 (3.3) | 8 (3.0) |
| *Ranunculus repens* | 3 (21.3) | 5 (16.8) | | | | | | |
| *Rhus ambigua* | | | | | | | 11 (1.1) | 5 (3.4) |
| *Sanicula chinensis* | 5 (12.8) | 10 (11.6) | | | | | | |
| *Solidago virgaurea* var. *asiatica* | | | 5 (10.4) | 2 (23.8) | | | 4 (2.7) | 3 (5.0) |
| *Stellaria media* | | | | | 3 (29.8) | 8 (13.8) | | |
| *Trifolium repens* | | | 4 (18.0) | 11 (8.8) | | | | |

| | Broadleaf | | Mixed | | Abies | |
|---|---|---|---|---|---|---|
| Yosomi | n | % | n | % | n | % |
| *Abies sachalinensis* | | | 2 (21.7) | 2 (25.8) | | |
| *Acer pictum* | 6 (8.8) | 3 (25.0) | | | | |
| *Asperula odorata* | 1 (74.3) | 4 (24.4) | 1 (28.9) | 6 (14.6) | 1 (69.1) | 2 (25.2) |
| *Disporum sessile* | 5 (11.5) | 5 (20.8) | | | | |
| *Dryopteris crassirhizoma* | | | 9 (2.5) | 1 (30.0) | | |
| *Hydrangea petiolaris* | | | 3 (14.4) | 3 (23.1) | | |
| *Hylodesmum podocarpum* | | | | | 5 (9.4) | 5 (17.4) |
| *Onoclea orientalis* | 4 (11.9) | 2 (28.4) | | | | |
| *Phryma leptostachya* | | | | | 4 (13.8) | 3 (18.6) |
| *Rhus ambigua* | 2 (17.3) | 1 (31.6) | 4 (12.0) | 4 (19.6) | 2 (19.2) | 1 (42.8) |
| *Sanicula chinensis* | 3 (16.3) | 5 (20.8) | | | 3 (15.7) | 4 (18.0) |
| *Schizophragma hydrangoides* | | | 5 (11.1) | 5 (16.5) | | |

Table 3.3 Ranking and stem number of dominant trees by forest types. Only the first five dominant species are displayed with stem number in parentheses.

| Summit | Closed-broadleaf | Open-broadleaf | Sorbus-Alnus | Picea |
|---|---|---|---|---|
| *Acer pictum* subsp. *mono* | 2 (32) | 5 (4) | | |
| *Alnus hirsuta* | | | 3 (19) | |
| *Alnus viridis* subsp. *maximowiczii* | | | 5 (4) | |
| *Betula ermanii* | | 4 (3) | | 4 (5) |
| *Betula maximowicziana* | 4 (5) | | | |
| *Betula platyphylla* | | 3 (8) | 4 (16) | |
| *Larix kaempferi* | | 5 (2) | | |
| *Picea glehnii* | | | | 1 (133) |
| *Populus suaveolens* | 1 (51) | 1 (41) | | 2 (26) |
| *Salix caprea* | | 5 (2) | | 3 (9) |
| *Salix gracilistyla* | | 5 (2) | | |
| *Salix udensis* | 3 (6) | 2 (13) | 2 (20) | |
| *Sorbus commixta* | | | 1 (22) | |
| *Ulmus davidiana* | 5 (4) | | | |
| *Viburnum opulus* var. *clavescens* | | | | 5 (3) |

| Yosomi | Broadleaf | Mixed | Abies |
|---|---|---|---|
| *Abies sachalinensis* | | 1 (28) | 1 (62) |
| *Acer pictum* subsp. *mayrii* | 1 (18) | | |
| *Acer pictum* subsp. *mono* | 5 (7) | | |
| *Alnus hirsuta* | | 5 (3) | 2 (3) |
| *Betula platyphylla* | | | 3 (2) |
| *Hydrangea paniculata* | | 2 (11) | |
| *Kalopanax septemlobus* | 2 (8) | | |
| *Magnolia kobus* | | | 3 (2) |
| *Morus australis* | 2 (8) | 3 (4) | |
| *Populus suaveolens* | 2 (8) | | 3 (2) |
| *Swida controversa* | | 3 (4) | |

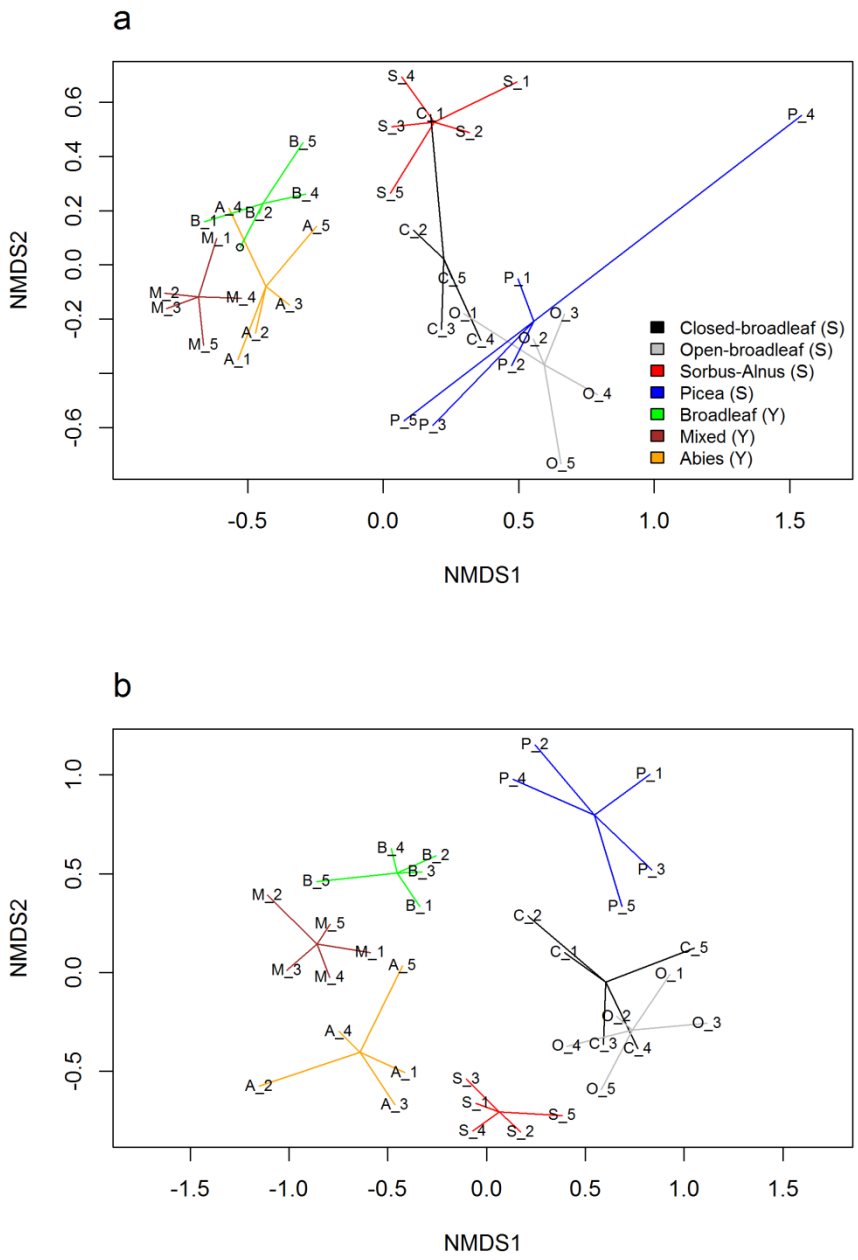


Figure 3.3 Non-metric multidimensional scaling of plots based on species composition. (a) herb layer scores by density, and (b) canopy layer scores by stem number. Forests are abbreviated to their first letters and numbers mark the different plots. Summit forests are indicated by (S) and Yosomi forests by (Y).

Table 3.4 Typhoon damage in the forests. Percentage of trees broken, fallen, or tilted are shown.

| Summit | | Yosomi | |
|---|---|---|---|
| Closed-broadleaf | 16% | Broadleaf | 9% |
| Open-broadleaf | 5% | Mixed | 59% |
| Sorbus-Alnus | 23% | Abies | 0% |
| Picea | 3% | | |

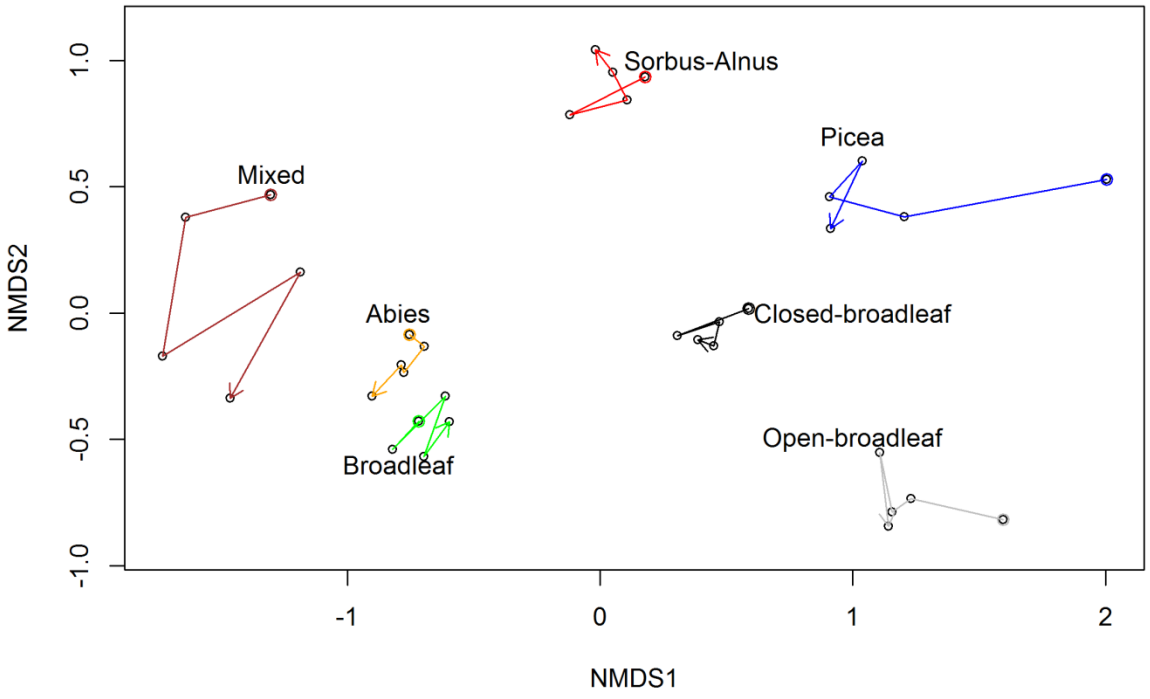


Figure 3.4 Annual changes of forests' scores in the nMDS space by herb layer density. The start of the arrow represents 2015 and the arrow-head shows 2019.

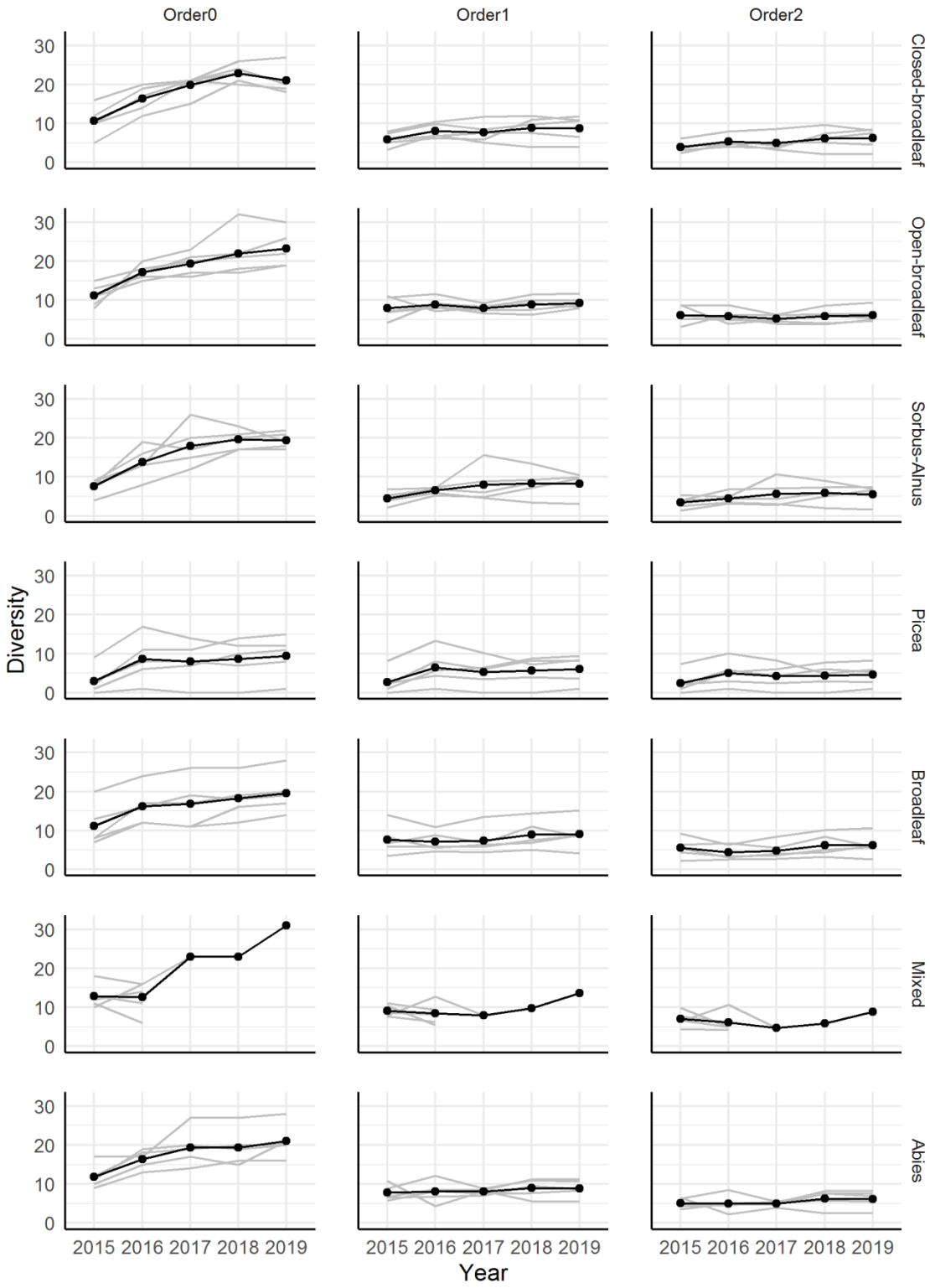


Figure 3.5 Annual changes in the plot diversities of the forests by diversity orders. The upper four rows show the forests at the summit, and lower three rows show the forests at Yosomi. Grey lines are individual plots and black lines are their mean. From 2017, only one plot was surveyed in the Mixed forests, due to the typhoon damages. The indices are calculated using the density of the herb layer shoots.

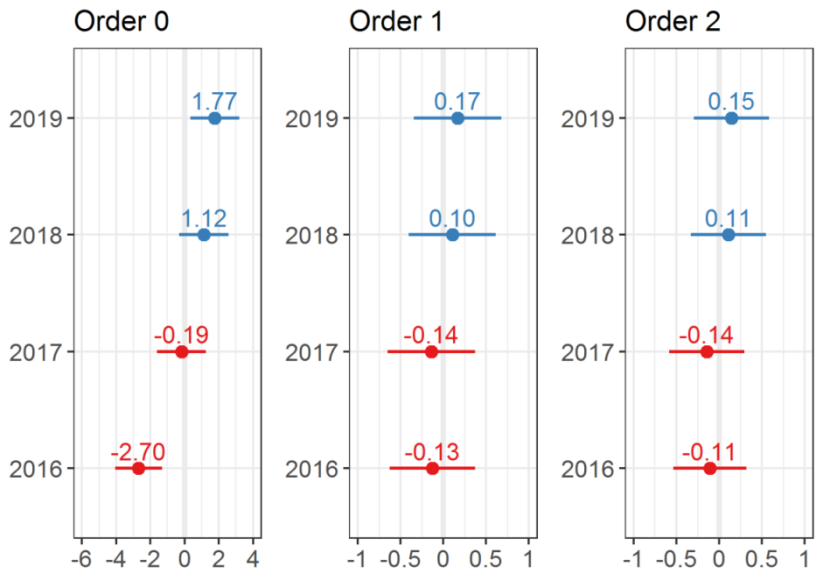


Figure 3.6 The effect of time on the plot diversity of the herb layer. The *y* axis shows time (year) and the *x* axis shows the variation from the overall model estimate. The graph is based on LMM model where year of survey was the random effect and forest type was the fixed effect.

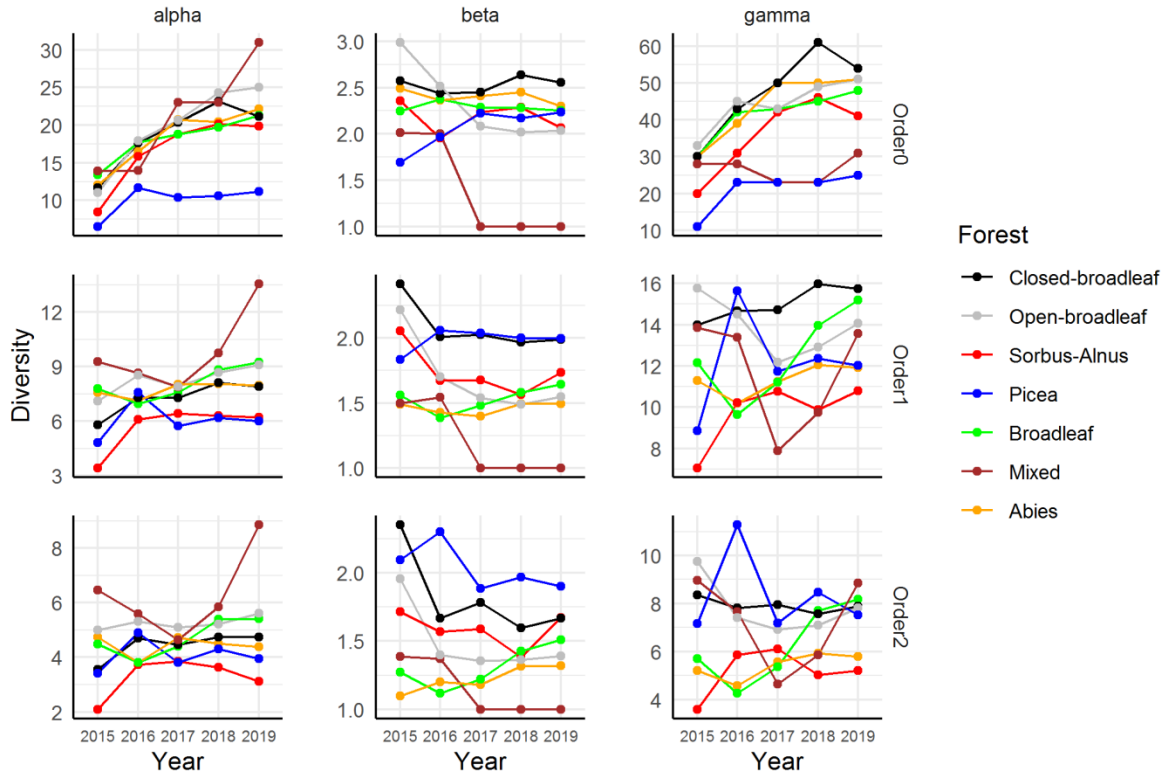


Figure 3.7 Herb layer diversity in forests evaluated by density of shoots. β-diversity of the Mixed forest after 2017 is 1 because of typhoon damages in four plots. The first four forests are at the summit.

Table 3.5 Statistical summary of forest level herb layer diversity. Mean is shown with standard deviation in parentheses, and the first three forests are at Yosomi. Statistical significance was calculated by GLMM models (log-normal distribution) using year of survey as random effect and forest type as fixed effect. Letters mark significant difference at $P$ <0.05. *: $P < 0.05$, **: $P < 0.01$, and ***: $P < 0.001$.

| Order 0 | Alpha | | | Beta | | | Gamma | | |
|---|---|---|---|---|---|---|---|---|---|
| Broadleaf | 19.4 | (1.5)*** | d | 2.3 | (0.1)*** | a | 44.5 | (2.6)*** | ab |
| Mixed | 22.7 | (7)*** | a | 1.3 | (0.5)*** | b | 26.2 | (3.9)*** | c |
| Abies | 20 | (2.4) | cd | 2.4 | (0.1) | a | 47.5 | (5.7) | ab |
| Closed-broadleaf | 20.6 | (2.3)*** | bc | 2.5 | (0.1) | a | 52 | (7.5)* | a |
| Open-broadleaf | 22 | (3.3)*** | ab | 2.2 | (0.2) | a | 47 | (3.7) | ab |
| Sorbus-Alnus | 18.6 | (2)* | d | 2.1 | (0.2) | a | 40 | (6.4) | b |
| Picea | 11 | (0.6)*** | e | 2.1 | (0.1) | a | 23.5 | (1.0)*** | c |
| Order 1 | | | | | | | | | |
| Broadleaf | 8.1 | (1.1)*** | b | 1.5 | (0.1)*** | b | 12.5 | (2.5)*** | ab |
| Mixed | 10 | (2.5)*** | a | 1.1 | (0.3)*** | c | 11.1 | (2.8) | b |
| Abies | 7.8 | (0.5) | bc | 1.5 | (0.05) | b | 11.3 | (0.9) | b |
| Closed-broadleaf | 7.7 | (0.4) | bc | 2 | (0.02)*** | a | 15.3 | (0.7)** | a |
| Open-broadleaf | 8.6 | (0.5) | ab | 1.6 | (0.1) | b | 13.4 | (1.1) | ab |
| Sorbus-Alnus | 6.3 | (0.1)*** | c | 1.7 | (0.1) | b | 10.4 | (0.4)* | b |
| Picea | 6.4 | (0.8)** | c | 2 | (0.03)*** | a | 12.9 | (1.8) | ab |
| Order 2 | | | | | | | | | |
| Broadleaf | 4.8 | (0.8)*** | bc | 1.3 | (0.2)*** | ce | 6.4 | (1.9)*** | ab |
| Mixed | 6.2 | (1.8)*** | a | 1.1 | (0.2)** | e | 6.7 | (1.9) | ab |
| Abies | 4.4 | (0.4) | bc | 1.3 | (0.1) | de | 5.5 | (0.6) | b |
| Closed-broadleaf | 4.7 | (0.1) | bc | 1.7 | (0.1)*** | b | 7.8 | (0.2) | ab |
| Open-broadleaf | 5.3 | (0.2) | ab | 1.4 | (0.02) | cd | 7.3 | (0.4) | ab |
| Sorbus-Alnus | 3.6 | (0.3)** | c | 1.6 | (0.1)** | bc | 5.5 | (0.5) | b |
| Picea | 4.2 | (0.5) | bc | 2 | (0.2)*** | a | 8.6 | (1.9)** | a |

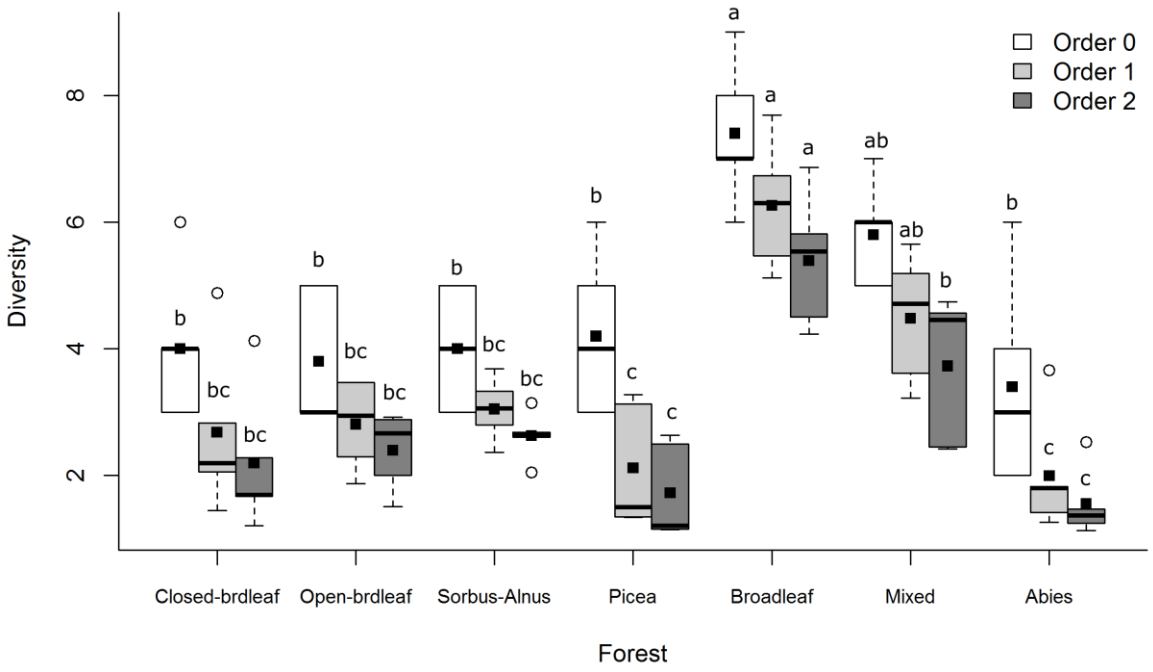


Figure 3.8 Canopy plot diversities based on 2016 conditions. The first four forests are on the summit and the others are on Yosomi. Significant differences are determined by GLM (log-normal distribution) at $P < 0.05$.

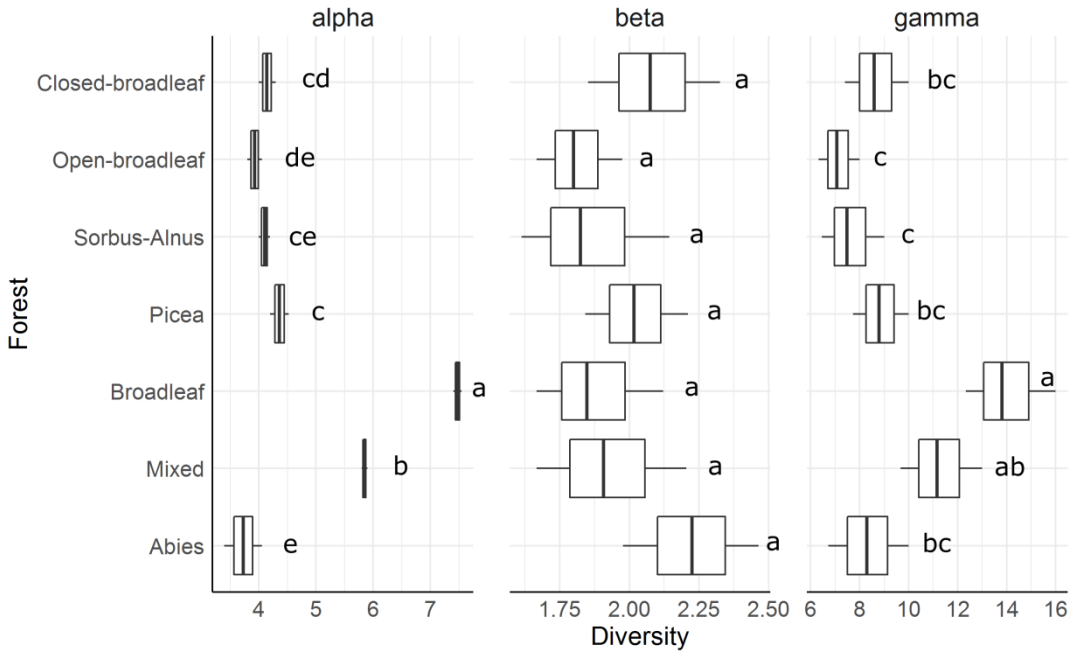


Figure 3.9 Forest level canopy diversities.The first four forests are at the summit, the others are at Yosomi. Significant differences are determined by GLM (log-normal distribution) at $P < 0.05$.

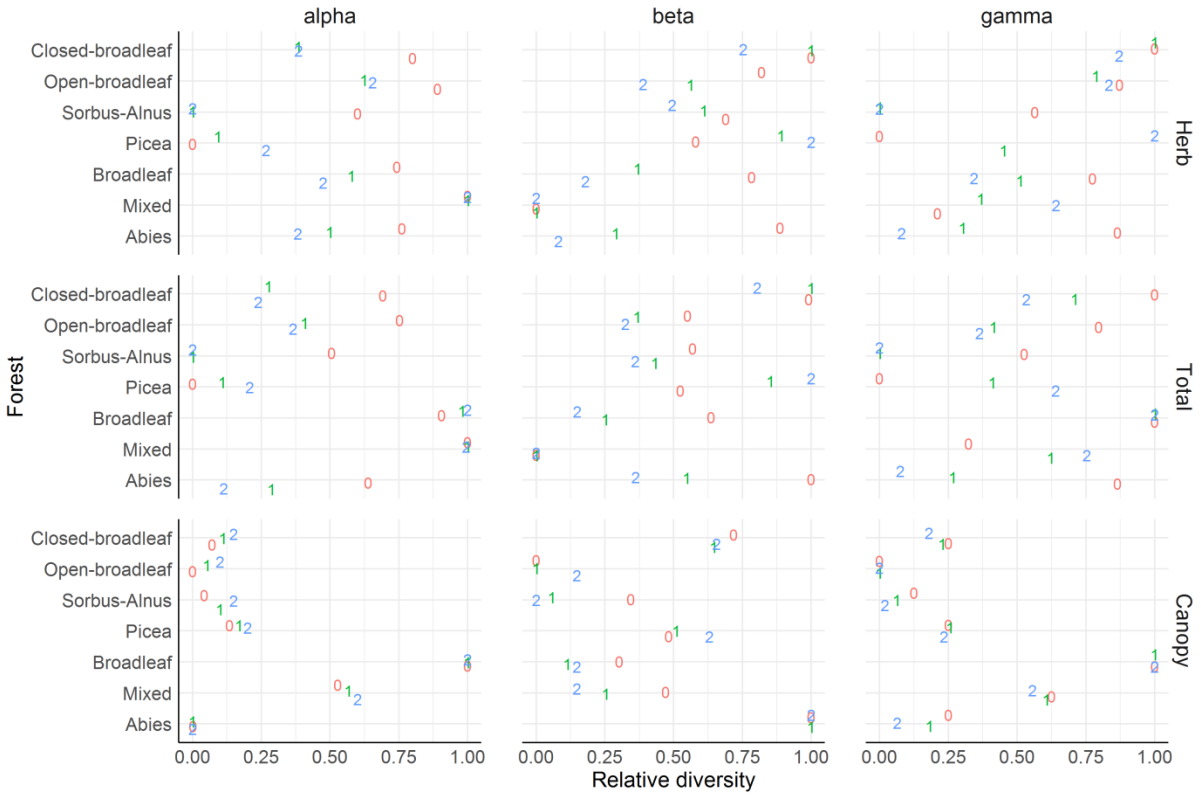


Figure 3.10 Herb layer, total, and canopy true diversities. The numbers represent order 0 (species richness), order 1, and order 2. The scores were scaled so that the highest score became 1 and the lowest score became 0 in the facets. The first four forests are on the summit.

# Chapter 4 Light, soil conditions, and seedbank of different forest types 40 and 110 years after the eruptions


## Abstract

Abiotic factors, such as light, temperature, and nutrient availability in soil, affect the speed and trajectory of succession. After established plants improve the harsh conditions, soil development patterns became spatially heterogeneous. To examine differences in soil nutrient content, temperature, and light between various forests at the 1910 and 1977-78 eruption sites of Mount Usu (hereafter, Yosomi and summit), soil samples were collected, and temperature and light were recorded in the forests. Soil sampling was performed annually between 2015 and 2017, and water content, pH, electrical conductivity, nitrogen-, phosphor-, and silica content of the soil were measured. The seedbank of the soil samples was examined by seed germination in a greenhouse and an incubator. Light and temperature were recorded from 2016 to 2017. Cluster analysis and nMDS of the soil properties showed that chemical properties did not differ among the forests, apart from the Sorbus-Alnus plantation, which formed its own group. *Alnus* spp. are nitrogen-fixers, and they established in large number in the Sorbus-Alnus forest; thus, they affected the chemical properties and nutrient content. The Sorbus-Alnus forest also had the highest seedbank density (1430 seed/$m^2$), while the light and temperature were similar among the forests. The seedbank density and percentage similarity of the seedbank to the standing vegetation was higher in the summit forests than in the Yosomi forests and was largest in the plantations. Temperature did not differ between the forests in Yosomi and the summit, but light intensity was higher in the summit forests. The plantations had low light density, which likely aided the establishment and survival of seedbank species, increasing the percentage similarity. Therefore, light and successional age affected more the seedbank and vegetation similarities than temperature and soil chemical composition.

## 4.1 Introduction

During primary succession, the environment is harsh; therefore, facilitation and environmental amelioration are important to develop the site habitability for the subsequent species (del Moral et al. 2007). Tephra produced by volcanic eruptions often covers the soil, so the seedbank becomes unavailable and immigrated seeds cannot establish due to the lack of nutrients (Hulshof and Spasojevic 2020). Therefore, vegetation recovers slowly on tephra in general, but quickly on exposed topsoil on Mount Usu, where the seedbank is present (Tsuyuzaki 1995). In areas covered by tephra, seed immigration by wind dispersal is the major pathway towards vegetation recovery (Fuller and del Moral 2003). However, the lack of nutrients in the volcanic ejecta, especially the low nitrogen concentrations, restricts early vegetation development (Bishop et al. 2010).

In early successional stages, the effects of soil properties are stronger than in late successional stages (van Breugel et al. 2019; Chang et al. 2019). Inter-species facilitation prevails competition in the harsh habitats during early stages (Kamijo et al. 2002; Uesaka and Tsuyuzaki 2005); for example, nitrogen-fixing plants, such as *Alnus* spp., facilitate plant establishment by increasing the soil nitrogen (N) content after the eruption on Mount St. Helens, USA (Titus 2009). The net impact of facilitation and competition depends on the species, their life cycles, and successional stages (van der Putten et al. 2013; Titus and Bishop 2014). Occasionally, species present in the vegetation patches inhibit their own seedling recruitment (Kardol et al. 2007; van der Putten et al. 2013), so the species composition is different from the seedbank in the soil (Hopfensperger 2007).

The seedbank and soil properties in the former topsoil are surveyed after the 1977-78 eruptions at the summit of Mount Usu (Tsuyuzaki 1989b, 2010a; Tsuyuzaki and Goto 2001), but the seedbank and soil properties of the volcanic ejecta have not been surveyed at the summit and Yosomi. Soil conditions change during succession due to litter accumulation and other factors, such as weathering, affecting seedbank and species composition of the understorey layer (Galván-Tejada et al. 2014). Although seeds of the cold temperate region do not show marked adaptation to volcanic eruptions, such as darkness, smoke, and heat in the volcanic deposits (Tsuyuzaki and Miyoshi 2009), the composition of seedbank affects resilience and future successional trajectories (Prach and Walker 2020). Therefore, investigating and understanding changes in the seedbank composition over long periods help

to focus restoration efforts and detect alien species (Meiners et al. 2015; Perrow and Davy 2002).

While facilitation is one of the major interactions among plants during early successional stages, competition for light is more dominant in later stages (Cutler et al. 2008). Light competition affects understorey communities in forests, as shrubs and trees provide protection from extreme environmental conditions (Titus 2009; Uesaka and Tsuyuzaki 2005). This chapter aimed to examine the soil properties, seedbank, temperature, and light at the Yosomi foothill and summit area of Mount Usu (1910 and 1977-78 eruption sites, respectively) to see whether the diversity relations of the forests—explored in the previous chapter—are accompanied by distinct environmental characteristics.

## 4.2 Methods

### 4.2.1 Soil samples

The study sites and forest plots examined are described in Chapter 3, section 3.2.1. During 2015–2017, two 100 $cm^3$ soil samples were collected from every plot for nutrient analysis and for germination experiments. In 2015, one of the soil samples was collected from 0–10 cm depth (topsoil) in each plot, and the other one was from 15–25 cm depth (deep-soil). As seed germination was low from the deep-soil samples in 2015, two topsoil samples were collected from each plot in 2016 and 2017. Soil samples were stored in an incubator below 10°C until use, and kept there for more than 6 weeks before germination experiments (Tsuyuzaki and Miyoshi 2009). Since four plots of the Mixed forest at the 1910 eruption site were destroyed by the typhoon in the late summer of 2016, no samples were collected from them in 2017.

To avoid underestimation and bias from a single seed germination method (Mesgaran et al. 2007), two seed germination methods were applied. One of the two soil samples collected from each plot was germinated in greenhouse under natural light conditions (12–14 ml water/day); the another one was sieved (2 mm > 1 mm > 500 μm in hole size) under running water (Mesgaran et al. 2007), and the residues left on the 1 mm and 500 μm sieves were incubated on wet filter paper (Whatman No. 1) under a cycle of 25°C/15°C–12h light/12h dark conditions. To confirm the efficiency of greenhouse germination, the soil samples from 2016 were re-collected after no more seedlings emerged and were wet-sieved and incubated as described above. Germination rate was calculated by dividing the number of soil samples where at least one seedling was observed by the total number of soil samples.

The seedlings were identified to species or higher level genus, with grouping graminoids together. Mortality before identification was measured by dividing the number of withered seedlings by the number of total seedlings.

Before the germination experiments started, I took three sets of 5 g soil from every sample for soil analysis and measured the following characteristics: gravimetric water content, pH, electrical conductivity (EC), nitrogen content ($NH_4$, $NO_2$, $NO_3$, TNi–total dissolved inorganic N calculated as their sum, and TNo–total dissolved organic N calculated as TN - TNi), phosphor content ($PO_4$, TP–total phosphor, and TPi–total dissolved phosphor) and silica content ($SiO_2$). Total nitrogen (TN) and total phosphor (TP) were not measured in 2017. One set of the 5 g samples was dried at 37°C for more than 48 hours for gravimetric water content measurement calculated as

$$\left(\frac{M_{\text{wet}} - M_{\text{dry}}}{M_{\text{dry}}}\right) \times 100,$$

where $M_{\text{wet}}$ and $M_{\text{dry}}$ are the weights of soil before and after drying, respectively (Smith and Mullins 1991). The second set of 5 g samples was diluted with 50 ml distilled water and shaken for more than 1 hour for measuring pH and EC (Lutron WA-2017SD recorder). In 2017, pH was also measured in situ during the soil collection (Custom, PH-6011A-OM pH meter). The third set was diluted with 50 ml 2M KCl (Keeney and Nelson 1983), shook for more than 1 hour, and filtered for nutrient analysis (QuAATro TNTP Multi water analyzer, Bran Luebbe Co., Tokyo). The samples collected in 2015 were percolated by a filter paper (Whatman No. 2), while the samples collected in 2016 and 2017 were additionally filtered by a cellulose acetate membrane (ADVANTEC Membrane Filter, pore size 0.45 μm). Until measurement, the samples were stored in an incubator below 10°C and were diluted by distilled water to either 10 or 20 times concentration before measurement.

### 4.2.2 Temperature and light intensity of plots

From 2015 September 05 to 2017 September 04, temperature (°C) and light intensity (lux) was measured at 1 hour intervals by six data loggers (HOBO Pendant Data Logger, Onset). The loggers were placed in one of the plots of each forest type at Yosomi, and in one of the plots of the Picea, Open- and Closed- broadleaf forest at the summit. The loggers recorded the maximum, minimum, and daily mean temperature and light intensity from 24 hours cycles.

The data from 2016 was used for the statistical analyses. The position of the Mixed forest logger was changed once due to the typhoon in 2016.

### 4.2.3 Statistical analysis

Differences in the chemical properties of the two topsoil samples per plot in 2016 and 2017 were examined annually by generalized linear model (GLM), where the independent variable was the sample ID per plot and the dependent variables were the soil variables measured. The two topsoil samples did not differ in their chemical characteristics (GLM, $P = 0.07–0.99$), so the measurements from the two samples were averaged for each plot. The pH measured in situ in 2017 did not differ from the pH measured in the laboratory (Kendall's tau = 0.77); therefore, pH measured in the laboratory were used for statistical analysis. The measurement ranges of nutrients differed between the years because of the machine calibration; therefore, the soil samples were analysed year by year.

Outliers and measurement errors (e.g., sub-zero levels after machine calibration) were deleted from the dataset. The variables were scaled by dividing them with their standard deviation. The forest plots were grouped by agglomerative cluster analysis (complete-linkage method, Sneath and Sokal 1973) with Manhattan distance dissimilarity matrix made by the chemical soil properties and also ordinated by nMDS.

The seed germination rates between the topsoil–deep-soil samples and between greenhouse–incubator methods were compared by $\chi^2$-test, while the germination rate of the forest types in 2015 was compared by Kruskal-Wallis test. The deep-soil and topsoil seed densities were compared by Wilcoxon test because of their non-normal distribution (Shapiro test, $P < 0.001$). The seed densities between the forest types were compared by generalized linear mixed model (GLMM) by Poisson distribution with log link, where the forest type was the fixed effect and the sampling year was the random effect. The number and species of seedlings emerged during the greenhouse and incubator germination experiments were pooled to compare the seedbank between the forest types and between the eruption sites.

Species diversity of the seedbank was examined by comparing the effective species number gained from order 0–2 of true diversities (Jost 2006). Order 0 marks the effective species richness, order 1 marks the effective species number when all species have equal importance, and order 2 when common species are given more weight. Similarities of species composition for each plot between the topsoil seedbank and aboveground herb layer composition was obtained by Sørensen similarity index ($2 \times w/(2 \times w + a + b)$, where $w$ was

the number of species occurring both in the seedbank and standing vegetation (Chapter 3) and *a* and *b* are the number of species present only in the seedbank or standing vegetation, respectively). The percentage similarity of the forest types was compared by GLM (Poisson distribution with log link) summarizing data from 2015 to 2017, while seed diversity was compared by LM. Graminoids were not included in the similarity and diversity analysis, because they were excluded from the herb layer surveys.

Because the temperature showed bimodal distribution, Kruskal-Wallis test and pairwise Wilcoxon test were used to compare the forest types, while light intensity was examined by GLM with log-normal distribution, where forest type was the independent variable and light intensity was the dependent variable. All analyses were undertaken in R programming environment (Burchett et al. 2017; Hlavac 2018; Oksanen et al. 2019; R Core Team 2018; Wickham et al. 2019).

## 4.3 Results

### 4.3.1 Soil analysis

The Yosomi and summit plots displayed mixed clustering by their soil properties (Figure 4.1), indicating that the soil characteristics did not differ greatly between the forests (Table 4.1). Nevertheless, a few distinct groups were shown by the cluster analysis: the Sorbus-Alnus and Mixed forest plots mostly formed their own clusters.

The nMDS space enclosed by the forest plots also overlapped among the forests, although the Open-broadleaf and Sorbus-Alnus forest were relatively separated in 2016 and 2017. The Open-broadleaf forest was aligned with changes in the pH level, while the Sorbus-Alnus forest aligned with the TNi content (especially nitrate) and EC. These two forests and chemical variables occupied the opposite side of the nMDS space.

### 4.3.2 Seed germination

In total, 390 seedlings emerged during the germination experiments (lasting between 106–149 days depending on seedling emergence) and 262 of them were identified at species or higher level (Appendix 1). The number of taxa was 49.

The seed germination rates in 2015 were 34% in the deep-soil and 74% in the topsoil ($\chi^2$-test, $P < 0.01$), independent of the forest types (Kruskal-test, $P = 0.9$). In total, 44 % of the seedlings died before identification. Most species occurred in the topsoil samples with the

exceptions of *Oenothera biennis* and *Rumex obtusifolius*, which were found only in deep-soil in 2015. Therefore, the deep-soil had little contribution to the seedbank and was not included in the following analysis.

In the greenhouse, the seed germination rates were 74%, 71%, and 77% in 2015, 2016, and 2017, respectively (Table 4.2). During the re-examination of the 2016 soil samples in incubators, nine new seedlings emerged with a corresponding 23% germination rate. The germination rate in the greenhouse in 2016 was significantly higher than that of the re-tested samples ($\chi^2$-test, $P < 0.001$), indicating that the greenhouse treatment induced seed germination with only a small number of dormant seeds remaining. The nine additional seedlings were included in the analyses. The seedling mortality before identification was lowest in 2016 with 20%, while in 2015 and 2017 it was 44% and 37%.

The germination rate in the incubator was 60% in 2016 and 69% in 2017 (Table 4.2), less than the germination rate in the greenhouse, and the number of emerged seedlings was also lower than in the greenhouse (111 against 279). The lower germination rate and seedling number might be the result of loss of seeds during sieving, although efforts to incubate residues from the 250 μm sieve saw the emergence of only two seedlings. Most seeds were captured on the 0.5 mm sieve, and the most numerous group was the graminoids among the seedlings, similar to the greenhouse samples. The ratio of unidentified species was 12% and 42% in 2016 and 2017, respectively.

### 4.3.3 Seedbank of the eruption sites and forest types

The mean seed densities in the forests at the summit ranged between 1016–1900/$m^2$, while the seed densities ranged between 833–1200/$m^2$ in the forests at Yosomi (Table 4.3). The highest and lowest seed density occurred in the plantations: the Sorbus-Alnus forest had the largest seedbank (GLMM, $P < 0.001$), and the Mixed and Abies forests had the lowest ($P < 0.001$).

The percentage similarity between the seedbank and standing vegetation was low across all forest types. The summit forests showed slightly higher similarity, with the Picea forest displaying the highest scores (GLM, $P < 0.05$, Figure 4.2) and the Abies forest displaying the lowest. The seed diversity followed the same pattern: the summit forests had higher α- and β-diversities than the Yosomi forests (Figure 4.3). The plantations displayed the highest diversities, the Sorbus-Alnus being the first followed by the Picea forest. In contrast, the planted forests at Yosomi did not display significantly higher diversities. Departing from the trend observed in aboveground vegetation in Chapter 3, β-diversity of the seedbanks was

higher at Yosomi. The seedlings of graminoids appeared in large numbers in every forest type, whereas woody species were generally absent (Appendix 1). Summit forests had greater proportions of graminoids, with the Picea forest having the largest number of graminoids in its seedbank. The seeds of most species displayed a site preference for either the summit or Yosomi forests, but there were some common species at the two sites, such as *Aralia cordata*, *Pilea* spp., or *Viola grypoceras*, which occurred widely.

#### 4.3.4 Temperature and light fluctuations

The broadleaved forests at the summit showed higher light intensity than the forests at Yosomi (GLM, $t$ = 5.7 to 12.5, $P < 0.001$, Table 4.4), while the plantations showed low light intensity, with the Picea plantation being the darkest (GLM, $t$ = - 6.5, $P < 0.001$). The forest with the highest light intensity was the Open-broadleaf forest at the summit ($t$ = 12.5, Figure 4.4). The Mixed forest plantation showed a peak in light intensity after August 2016, because the canopy was damaged by the typhoon, but after the logger was re-located, the light intensity returned to levels observed before the typhoon. The Open-broadleaf forest also had a peak in October 2016, although no perceptible differences were noticed in its surroundings.

The summit plots had lower temperature than the Yosomi plots (Figure 4.4, Table 4.4). However, the Open-broadleaf forest showed no significant differences compared to the Yosomi forests (Wilcoxon-test, $P$ = 0.5 to 0.7) due to its open canopy which let more sunshine through. The lowest temperature was recorded in the Picea forest at the summit ($T_{avg}$ = 5.61°C, Wilcoxon test, $P < 0.01$), and the highest one was recorded from the Mixed forest at Yosomi ($T_{avg}$ = 7.65°C).

## 4.4 Discussion

#### 4.4.1 Soil properties

The chemical properties were in range of those measured at Mount Fuji and Mount St. Helens (Yoshitake et al. 2016; Yurkewycz et al. 2014), and compared to the measurements in 1986 on Mount Usu, the soil pH was higher (Haruki and Tsuyuzaki 2001). The soil characteristics were not different between the forest types, except the characteristics of the Sorbus-Alnus forest at the summit, which formed its own cluster and also separated in the nMDS space from the other forests. The Sorbus-Alnus forest had a high abundance of *Alnus* trees (Chapter 3), and *Alnus* species are nitrogen fixers and facilitate the establishment of late successional

species (Kamijo et al. 2002; Titus 2009). During early successional stages, nitrogen limits plant development and underground competition for resources, and this limitation may be more severe than aboveground competition (Haruki and Tsuyuzaki 2001). In areas where the *Alnus* trees established, the nitrogen level of the soil increased, thus the nutrient content of the soil was improved in in the Sorbus-Alnus forest.

Even though the soil conditions were not different between the forest types except for the Sorbus-Alnus forest, the plant composition and diversity of the forests on Mount Usu showed a wide range (Chapter 3). Thus, the plant diversity was neither influenced nor was it affected by the nutrient content of the soil. The effects of soil conditions on plant diversity are weaker than the effects of time and climate on the volcanic Sanary (Canary islands, north-western side of African continent, Irl et al. 2019). Correspondingly, soil development exerts only weak control over succession on coastal dunes, where competition and regeneration determine the successional processes (Lichter 2000). Further factors also influence primary succession, like the presence or absence of mycorrhiza (Kwon and Tsuyuzaki 2016; Meiners et al. 2015); but as the effect of mycorrhiza is secondary compared to that of the topsoil when restoring denuded areas (Jasper 2007), it was not examined here.

### 4.4.2 Seedbank

The seedbank density and diversity were higher in the forests at the summit damaged by the 1977-78 eruptions than in the forests at Yosomi damaged by the 1910 eruptions, indicating that the seedbank density and diversity decreased with successional age. Declining seedbank density is often observed during secondary succession with increasing successional age (Hyatt and Casper 2000). However, as the seedbank density in the former topsoil 10 years after the eruptions was higher at the summit than the density measured in this chapter (Tsuyuzaki 1989b), the declining trend might change in the future. The recovery of seedbank in temperate forests which developed on abandoned agriculture lands has not yet finished even after 150 years of secondary succession (Plue et al. 2010). Therefore, the seedbank density and diversity seemed to move towards climax conditions on Mount Usu, independent of the soil properties.

The Sorbus-Alnus forest had the highest seed density in the seedbank and together with the other summit forests, the percentage similarity between the seedbank and herb layer species composition was higher compared to the forests at Yosomi. The similarity of seedbank species with standing vegetation is generally low in well-developed forests

(Hopfensperger 2007), and decreases with increasing forest age in Belgium where the climate is similar (Bossuyt, Heyn, and Hermy 2002). There are several hypotheses why the percentage similarity is low in forest habitats, for example late successional species may experience increased seed predation, or seeds in the persistent seedbank may not tolerate shade (Hopfensperger 2007). I observed the highest similarity scores in the Picea forest which was also the darkest forest. This result contradicts the shade intolerance hypothesis. In addition, the Open-broadleaf forest, where the light intensity was highest, did not show increased similarity between its seedbank and standing vegetation. Although the similarity scores were highest in these two forests, the share of graminoids in the seedbank differed largely. Graminoids were common in the Picea seedbank but were not observed during the herb layer surveys (Chapter 3), whereas graminoids were rare in the seedbank of Open-broadleaf but established in the plots. The similarity between the seedbank and standing vegetation decreases with increasing succession in subalpine meadows and grasslands (Ma, Du, and Zhou 2009; Török et al. 2018), so while lack of light could be one of the factors that inhibited the establishment of graminoids in the Picea forest, successional age was an important factor as well.

On the species composition, *Rumex obtusifolius* was the most dominant species in the seedbank of the former topsoil for three decades after the 1977-78 eruptions at the summit, a remnant of the meadows prior to the eruptions (Tsuyuzaki 2010b). The present study did not record any *R. obtusifolius* seedlings, suggesting that the seedbank either differs widely across different locations or that the seeds of *R. obtusifolius* did not immigrate to the forests.

### 4.4.3 Light and temperature

The average temperatures did not differ among the forest types, but decreased with elevation, thus the summit forests had lower temperatures. High elevation slows down succession, partly due to the harsh environments and short growing season (Nakashizuka et al. 1993; Tsuyuzaki 2019). Because the forests at the summit seemed to ameliorate the soil and harsh conditions, the herb layer diversity of the summit forests was not affected by the temperature (Chapter 3).

In addition, low temperatures were supplemented by high light intensity at the summit. The Open-broadleaf forest at the summit had the highest light intensity, and the Closed-broadleaf forest reached higher intensity than the Broadleaf forest at Yosomi. The plantations were the darkest forest types both at the summit and at Yosomi, and the understorey of the Abies and Picea forests were sparse compared to the broadleaved forests. Competition for

light controls the seedling establishment (Hopfensperger 2007), but increased shade aids survival (Bourgeois et al. 2016). As the soil characteristics did not differ greatly among the surveyed forests, successional age and shade, as a result of management history, should affect vegetation development more than cold temperature or soil characteristics.

### 4.5 Conclusion

The soil conditions were similar between the young and mature forests, but the planting of *Alnus* trees changed soil development for long-term. The plantation forests were darker than the natural forests, which seemed to increase the similarity between the seedbank and standing vegetation. The seedbank density and diversity were higher in the young forests, especially under *Alnus* trees. The soil nutrients limit species establishment during succession (Hulshof and Spasojevic 2020), but microclimate and time since disturbance have larger impact (Irl et al. 2019). As several young and mature forest plots were clustered in the same nMDS groups, the presence of nitrogen-fixing plants and light intensity in the forests had larger influence on plant diversity than soil characteristics.

## Tables and Figures

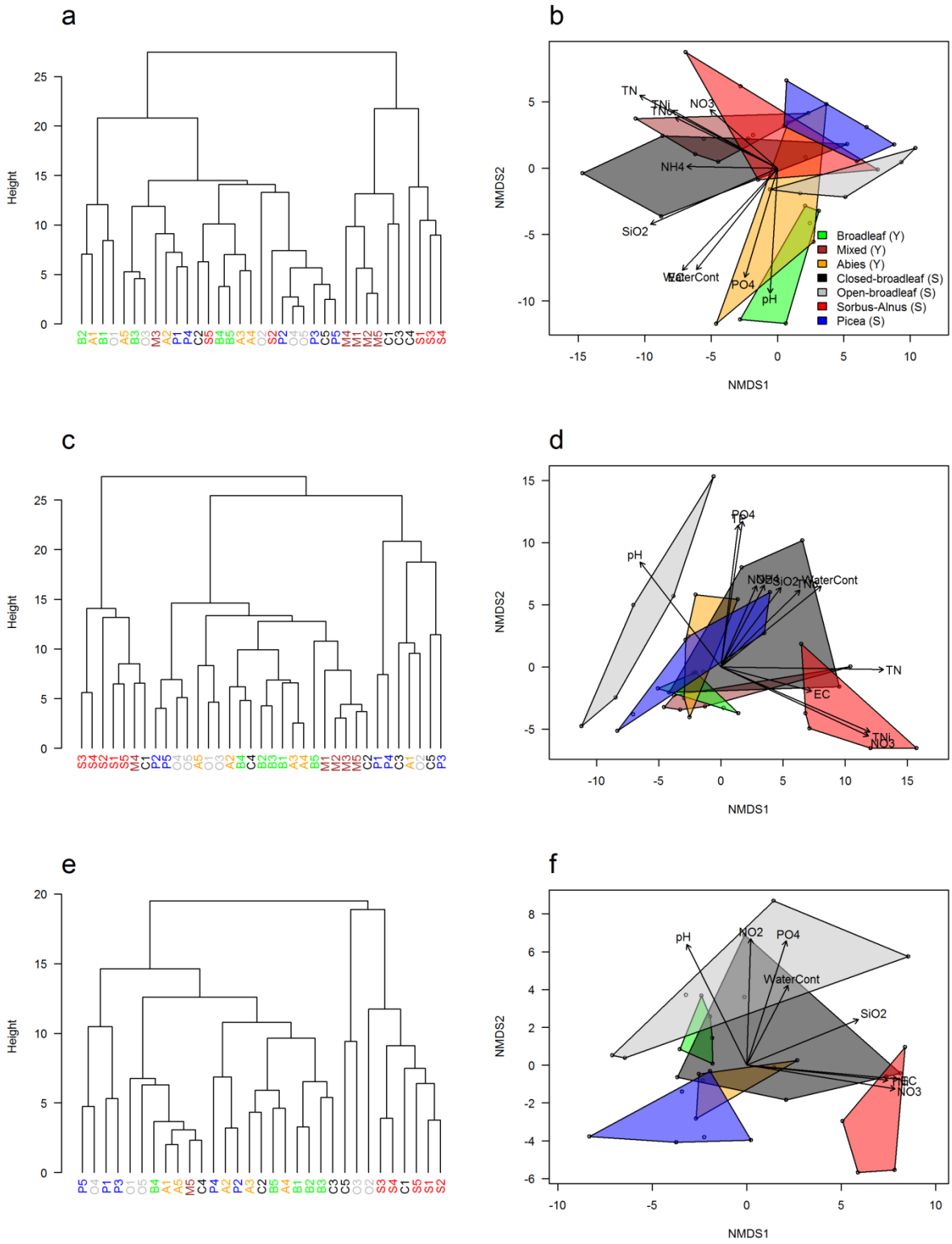


Figure 4.1 Dendrograms and nMDS scores of plots based on soil chemistry, with environmental factors overlaid. The (a, b), (c, d), and (e, f) figures show 2015, 2016, and 2017 conditions respectively. Abbreviations are: B – Broadleaf, M – Mixed, A – Abies, C – Closed-broadleaf, O – Open-broadleaf, S – Sorbus-Alnus, P – Picea forests.

Table 4.1 Soil characteristics of the forests. Means are shown with standard deviations in parentheses. The unit of nutrients is μg/g.

| | | Broadleaf | | Mixed | | Abies | | Closed-broadleaf | | Open-broadleaf | | Sorbus-Alnus | | Picea | |
|---|---|---|---|---|---|---|---|---|---|---|---|---|---|---|---|
| | 2015 | 63.2 | (7.7) | 39.4 | (2.7) | 45.8 | (7.5) | 57.7 | (14.7) | 21.4 | (5.0) | 43.5 | (7.7) | 18.4 | (1.8) |
| Water % | 2016 | 53.5 | (4.5) | 44.8 | (5.9) | 52.3 | (4.7) | 63.9 | (13.4) | 36.2 | (9.6) | 51.7 | (6.0) | 45.7 | (9.5) |
| | 2017 | 61.6 | (4.9) | – | – | 53.9 | (7.2) | 74.3 | (13.3) | 42.7 | (11.0) | 50.7 | (7.1) | 42.1 | (9.4) |
| | 2015 | 7.2 | (0.1) | 6.6 | (0.1) | 6.5 | (0.2) | 6.6 | (0.1) | 6.7 | (0.1) | 5.9 | (0.2) | 6.0 | (0.2) |
| pH | 2016 | 6.3 | (0.1) | 6.6 | (0.1) | 6.3 | (0.1) | 6.6 | (0.1) | 6.9 | (0.1) | 5.6 | (0.1) | 5.8 | (0.1) |
| | 2017 | 6.8 | (0.1) | – | – | 6.5 | (0.1) | 6.9 | (0.1) | 7.3 | (0.1) | 5.8 | (0.1) | 6.1 | (0.1) |
| | 2015 | 46.3 | (8.3) | 34.0 | (6.6) | 38.3 | (7.7) | 32.4 | (6.2) | 29.4 | (12.8) | 28.4 | (7.4) | 25.4 | (6.2) |
| EC | 2016 | 17.8 | (1.8) | 32.3 | (5.7) | 15.1 | (1.0) | 21.7 | (3.4) | 12.7 | (1.6) | 27.6 | (4.6) | 15.7 | (2.1) |
| | 2017 | 18.6 | (1.7) | – | – | 23.6 | (3.6) | 37.8 | (7.2) | 31.3 | (8.3) | 44.5 | (5.0) | 21.7 | (4.1) |
| | 2015 | 123.1 | (15.5) | 326.2 | (36.0) | 165.7 | (10.7) | 365.7 | (73.0) | 248.6 | (150.7) | 411.6 | (107.4) | 147.5 | (36.9) |
| TN | 2016 | 239.8 | (23.3) | 286.1 | (35.4) | 250.7 | (22.0) | 384.7 | (62.9) | 179.4 | (17.7) | 646.3 | (94.2) | 402.0 | (86.6) |
| | 2017 | – | – | – | – | – | – | – | – | – | – | – | – | – | – |
| | 2015 | 50.1 | (6.6) | 208.2 | (16.4) | 99.3 | (16.1) | 181.7 | (46.4) | 43.9 | (10.9) | 77.5 | (17.9) | 117.6 | (37.0) |
| TNo | 2016 | 134.2 | (6.7) | 161.4 | (15.7) | 147.6 | (16.7) | 195.4 | (24.9) | 116.8 | (13.7) | 173.2 | (13.2) | 350.1 | (84.0) |
| | 2017 | – | – | – | – | – | – | – | – | – | – | – | – | – | – |
| | 2015 | 73.0 | (17.3) | 118.0 | (20.8) | 66.4 | (19.4) | 184.1 | (58.5) | 204.7 | (145.0) | 334.1 | (114.8) | 29.9 | (2.8) |
| TNi | 2016 | 105.6 | (20.1) | 124.7 | (28.1) | 103.2 | (8.6) | 189.3 | (60.1) | 62.6 | (4.6) | 473.1 | (88.2) | 51.9 | (3.4) |
| | 2017 | 93.5 | (9.1) | – | – | 129.4 | (25.6) | 194.7 | (49.8) | 146.9 | (54.7) | 325.2 | (34.3) | 164.5 | (61.8) |
| | 2015 | 27.8 | (1.9) | 129.5 | (25.2) | 30.9 | (8.8) | 88.7 | (21.2) | 60.7 | (33.9) | 28.2 | (4.7) | 27.1 | (4.0) |
| $NH_4$ | 2016 | 50.3 | (6.2) | 48.9 | (4.3) | 48.1 | (8.6) | 109.1 | (52.4) | 47.7 | (5.6) | 50.9 | (2.7) | 34.1 | (4.6) |
| | 2017 | 82.5 | (5.7) | – | – | 66.4 | (4.4) | 86.8 | (12.2) | 91.6 | (13.9) | 69.1 | (5.6) | 197.5 | (79.4) |
| | 2015 | 7.8 | (0.3) | 5.0 | (1.0) | 7.9 | (0.9) | 8.4 | (1.0) | 8.2 | (0.4) | 7.8 | (0.3) | 7.4 | (0.8) |
| $NO_2$ | 2016 | 20.8 | (0.7) | 23.6 | (0.3) | 23.5 | (0.6) | 24.3 | (0.7) | 24.3 | (1.1) | 22.7 | (0.4) | 19.3 | (0.5) |
| | 2017 | 9.1 | (0.5) | – | – | 7.9 | (0.3) | 8.2 | (0.2) | 10.3 | (0.5) | 7.5 | (1.1) | 5.4 | (0.4) |
| | 2015 | 217.2 | (74.1) | 70.6 | (11.7) | 177.3 | (96.7) | 498.5 | (247.9) | 686.7 | (647.8) | 1371.7 | (513.6) | 29.4 | (1.7) |
| $NO_3$ | 2016 | 266.6 | (90.4) | 352.0 | (123.9) | 259.6 | (37.0) | 430.3 | (190.9) | 80.5 | (8.0) | 1888.6 | (382.9) | 86.8 | (2.6) |
| | 2017 | 117.9 | (29.5) | – | – | 333.9 | (106.2) | 552.6 | (229.9) | 321.5 | (223.8) | 1192.2 | (146.5) | 42.1 | (3.2) |
| | 2015 | 5.9 | (1.7) | 4.3 | (0.5) | 6.3 | (2.2) | 11.9 | (4.7) | 25.3 | (21.1) | 8.4 | (1.2) | 5.2 | (1.2) |
| TP | 2016 | 10.2 | (0.8) | 9.7 | (0.8) | 12.8 | (1.3) | 19.7 | (4.8) | 17.5 | (2.9) | 12.8 | (1.3) | 22.6 | (6.6) |
| | 2017 | – | – | – | – | – | – | – | – | – | – | – | – | – | – |
| | 2015 | 14.1 | (6.6) | 1.0 | (0.3) | 5.9 | (4.2) | 16.6 | (12.2) | 67.5 | (61.7) | 4.6 | (2.2) | 3.9 | (2.6) |
| $PO_4$ | 2016 | 26.6 | (3.0) | 25.0 | (2.7) | 34.8 | (5.9) | 54.7 | (16.1) | 40.8 | (8.0) | 29.5 | (4.1) | 59.7 | (26.3) |
| | 2017 | 38.4 | (15.2) | – | – | 26.5 | (10.7) | 72.2 | (22.5) | 144.2 | (60.0) | 34.4 | (8.1) | 21.6 | (6.5) |
| | 2015 | 432.5 | (67.4) | 487.3 | (44.0) | 441.4 | (101.4) | 451.2 | (71.9) | 209.8 | (49.0) | 362.8 | (78.9) | 260.9 | (46.5) |
| $SiO_2$ | 2016 | 361.1 | (47.1) | 236.0 | (23.8) | 488.4 | (47.6) | 393.5 | (59.3) | 361.4 | (59.5) | 402.3 | (37.7) | 550.6 | (161.6) |
| | 2017 | 351.3 | (24.4) | – | – | 307.5 | (16.6) | 370.8 | (37.6) | 358.8 | (89.0) | 423.3 | (36.9) | 327.9 | (58.1) |

Table 4.2 Characteristics of the seed germination experiments.

| Greenhouse | Germination rate | Number of seedlings | Identified seedlings | Species |
|---|---|---|---|---|
| 2015 | 74% | 120 | 67 (56%) | 17 |
| 2016 | 71% | 83 | 66 (80%) | 17 |
| 2017 | 77% | 76 | 48 (63%) | 22 |
| All years | 74% | 279 | 181 (65%) | 40 |

| Incubator | Germination rate | Number of seedlings | Identified seedlings | Species |
|---|---|---|---|---|
| 2016 (Greenhouse) | 23% | 9 | 7 (78%) | 5 |
| 2016 | 60% | 49 | 43 (88%) | 11 |
| 2017 | 69% | 53 | 31 (58%) | 13 |
| All years | 89% | 111 | 81 (73%) | 19 |

Table 4.3 Seed density in the seedbank of each forest. Means are shown with standard deviation in parentheses, calculated from germination experiments in the greenhouse and incubator. Significance is calculated by GLMM (Poisson-log) and $P < 0.001$ unless otherwise marked. Letters indicate difference at $P < 0.05$.

| Site | Forest | 2015 | | 2016 | | 2017 | | Average | | |
|---|---|---|---|---|---|---|---|---|---|---|
| Yosomi | Broadleaf | 2000 | (1323) | 850 | (742) | 750 | (468) | 1200 | (1032) | c |
| | Mixed | 1700 | (1037) | 750 | (500) | 500 | (224) | 988 | (925) | e |
| | Abies | 1300 | (1440) | 550 | (411) | 650 | (548) | 833 | (920) | e |
| Summit | Closed-broadleaf | 900 | (1025) | 550 | (570) | 1600 | (1825) | 1017 | (1245) | d |
| | Open-broadleaf | 1400 | (1949) | 1450 | (1081) | 850 | (720) | 1233** | (1283) | c |
| | Sorbus-Alnus | 2800 | (3457) | 1600 | (1925) | 1300 | (1242) | 1900 | (2316) | a |
| | Picea | 1900 | (1517) | 1300 | (991) | 1200 | (371) | 1467 | (1039) | b |

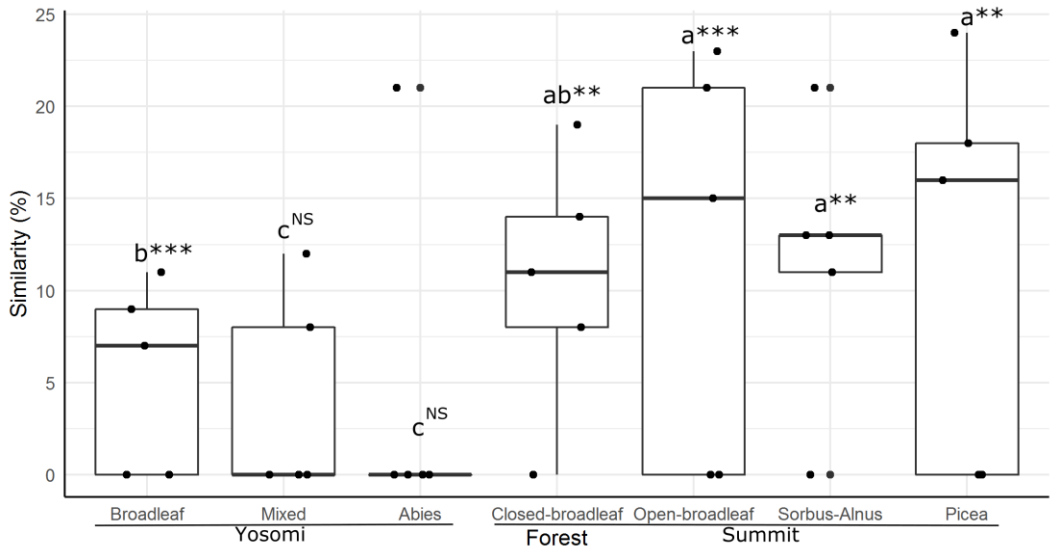


Figure 4.2 Percentage similarities between the seedbank and herb layer species. Dots show individual plot scores, and differences are examined by GLM using Poisson distribution with log link. Letters indicate significance differences at $P < 0.05$.

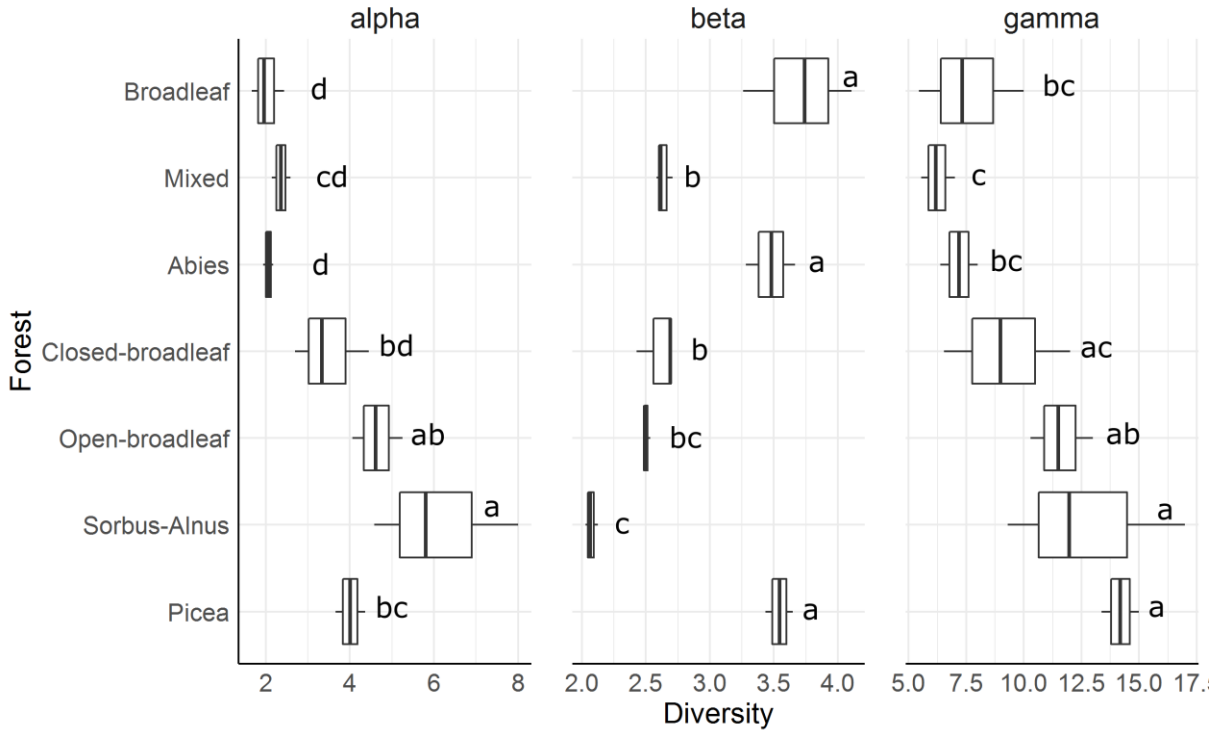


Figure 4.3 Seedbank species diversity. The first three forests are at Yosomi, the others are at the summit. Significant differences are determined by LM at $P < 0.05$.

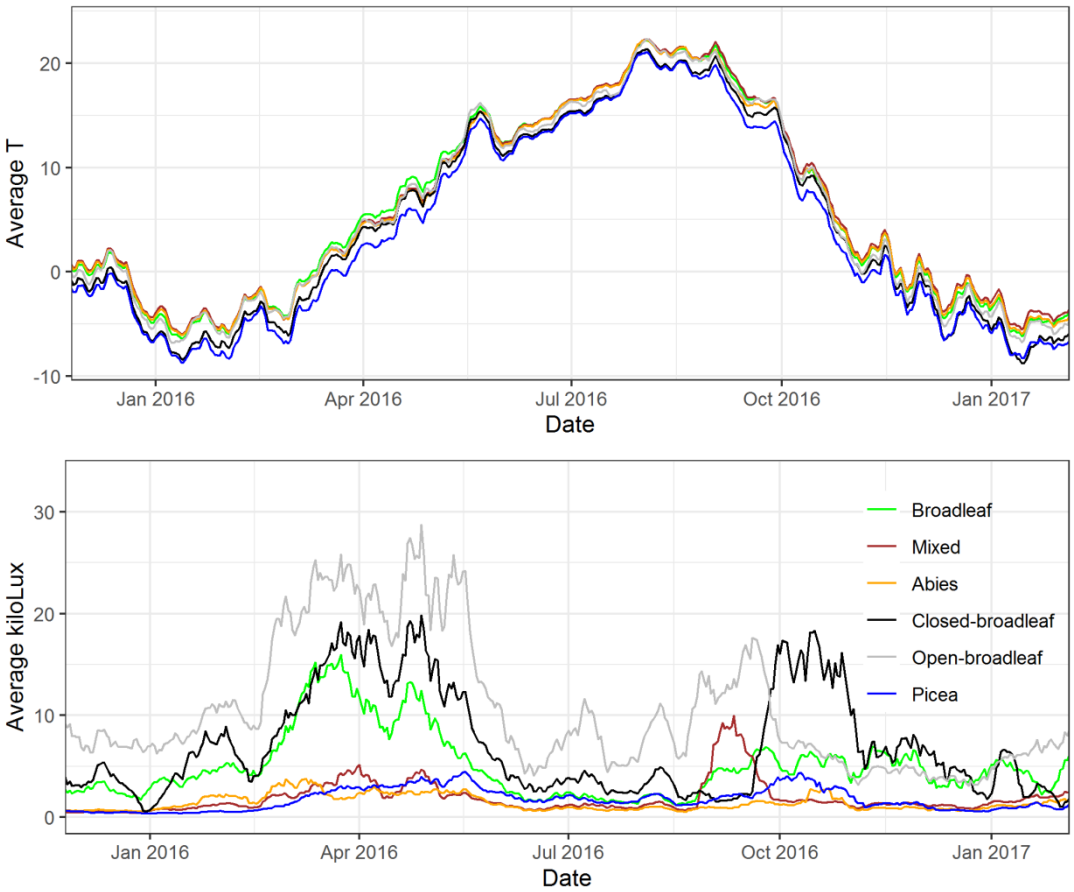


Figure 4.4 Ten days moving average of temperature and light intensity in the forests. The first three forests in the legend are at Yosomi, the last three are at the summit.

Table 4.4 Temperature and light intensity in the forests in 2016. Mean is shown with standard deviation in parentheses. Significance values are obtained by Wilcoxon test in the case of temperature and from GLM (log-normal distribution) in the case of light intensity ($P < 0.001$). Letters indicate difference at $P < 0.05$.

| Site | Forest | Temperature (°C) | | | Light intensity (kLux) | | |
|---|---|---|---|---|---|---|---|
| Yosomi | Broadleaf | 7.6 | (9.3) | a | 5.4 | (4.6) | c |
| | Mixed | 7.7 | (9.2) | a | 2.03 | (2.6) | d |
| | Abies | 7.4 | (9.2) | a | 1.5 | (1.3) | d |
| Summit | Closed-broadleaf | 6.4 | (9.6) | b$^{NS}$ | 7.79 | (7.64) | b |
| | Open-broadleaf | 7.2 | (9.4) | a | 11.26 | (9.43) | a |
| | Picea | 5.6 | (9.6) | b* | 1.92 | (1.44) | d |

# General discussion

To design appropriate management regimes and to restore disturbed habitats, an understanding of large scale succession is necessary. Although succession has been studied by field observations after 1977-78 eruptions at the summit on Mount Usu (Tsuyuzaki 1987, 2019) and lately after the 2000 eruptions at Konpira (Obase et al. 2008; Otaki et al. 2016), the research areas have been limited. This study combined remote sensing with field surveys and examined changes in the vegetation development and diversities of various forest types at large scale. By combining remote and field surveys, the study bridged the gap between spatial scales and detected local and regional factors.

Chapter 1 proposed a new method, called imagery chronosequence, to determine vegetation patch dynamics after eruptions differing in scale. Although remote sensing is applied to analyse revegetation on a few volcanoes, including Mount St. Helens (De Rose et al. 2011; De Schutter et al. 2015; Lawrence and Ripple 2000), those analyses do not clarify vegetation patch dynamics because they concentrate on pixel by pixel changes. The imagery chronosequence modelled patch dynamics by clustering pixels and detected changes by combining different image sources. The results showed that touching patches had lower mortality rate and grew faster than isolated patches, especially at the small disturbance site, due probably to the facilitation among plants and amelioration. The large scale disturbance slowed patch development, and the patch formation and size were important factors in revegetation. These indicated that individual patch size was more important than the total habitat area, contrary to the habitat amount hypothesis (Fahrig 2013). At the summit, previous active management practices, i.e., plantations, were concentrated on contiguous small areas (Chapters 2–3); therefore, their effects remained local in the wake of the large scale disturbance. The patch dynamics observed by imagery chronosequence indicate that planting woody species in patches over a larger area would improve the succession rate and increase β-diversity by the development of patchy vegetation patterns (Kitagawa et al. 2017).

As the resolutions of remote sensors increase spatially and temporarily (Kark, Levin, and Phinn 2008; Wulder et al. 2004), creating imagery chronosequences becomes convenient. However, the sensor resolution needs to suit the species studied (Paganini et al. 2016; Skidmore et al. 2015). Chapter 2 determined that the suitable resolution for estimating the diversity of the temperate forests on Mount Usu is 3.2 m, irrespective of whether canopy or

total diversities are examined. Although *H'* and *D* are popular to measure diversity (Oldeland et al. 2010; Wang and Gamon 2019), *J'* and $N_{1,2}$ correlated stronger with the spectral diversities in the forests on Mount Usu. If spectral diversities and imagery chronosequences are combined, patch dynamics could be linked to patch diversity, making it possible to follow past changes in diversity or even species composition (Clark et al. 2005; Underwood et al. 2003). In addition, the combination of these two methods will help to monitor current conditions after management activities and to evaluate and modify restoration efforts if necessary (Adams et al. 2019; Perrow and Davy 2002).

To accurately detect species diversity at large scale, field measurements need to support remote sensing (Feilhauer et al. 2014; Wang, Gamon, Schweiger, et al. 2018); Chapter 3 and 4 fulfilled this role by concentrating on field observations. Chapter 3 showed that the canopy diversity was higher on the Yosomi forests than on the summit forests, while the herb layer diversity was lower. These differences were not detected by the spectral indicators; thus, the field studies will help to develop and improve spectral indicators to estimate species compositional variances.

Chapter 3 showed that plantations and naturally recovered forests had different species composition and diversities, indicating that management histories affected the succession for 70 years. The impacts of management activities on species recruitment have been shown to last 15 and 33 years on Mount St. Helens (Dale and Adams 2003; Fischer et al. 2019); Chapter 3 suggests that the effects linger longer. The impact is more characterized if woody species are involved (Kondo and Tsuyuzaki 1999) than if only seeding of herbaceous species takes place (Uchida 2017). On Mount Usu, the woody plantations displayed lower α- and γ-diversities, and also differed in their herb layer species composition compared to the natural forests, especially, when N-fixing *Alnus* spp. established.

Site amelioration is necessary for the establishment and survival of late successional species (Hulshof and Spasojevic 2020). Chapter 4 concluded that the soil chemistry and temperature did not greatly affect revegetation on Mount Usu. However, shading and successional age influenced the seedbank of the forests: younger forests and dark plantations had denser and more diverse seedbank. In addition, the seedbank showed higher similarity to standing vegetation in these forests. Remote sensing estimates canopy and surface temperature at large scales (Huang et al. 2020; Yi et al. 2020), but does not detect most abiotic factors well, such as soil chemistry or seedbank. Both management practices and stochastic events influence soil and seedbank characteristics, affecting successional

trajectories (Karadimou et al. 2018; Prach and Walker 2020; Walker and del Moral 2003). On Mount Usu, stochastic events were less important than management practices; the different history of forest management and successional age affected shading and N-content (Bossuyt et al. 2002), resulting in more diverse seedbanks in the young plantations at the summit.

Active management practices, such as plantations, increase ground surface stability, but intervene with species recruitment and slow the establishment of subsequent species (Dale and Adams 2003; Prach and Hobbs 2008; Young et al. 2005). The various plantations had distinct species composition on Mount Usu, but with increasing age the species composition changed toward that of naturally recovered forests. The immigration of native species into the plantations indicates that management practices had larger impact on the successional trajectory than stochastic effects. Global comparison of volcanic disturbances indicates that alien species are rare to dominate during primary succession (Prach and Walker 2020). However, to prevent the emergence of undesirable communities, monitoring is necessary (Bourgeois et al. 2016; Perrow and Davy 2002). For example, seeded herbaceous species disappear after native species establish on the Sakurajima volcano, Japan (Uchida 2017), but the plantation of alien larch have long-lasting impact on the succession after eruptions on Mount Koma, Japan (Kondo and Tsuyuzaki 1999). The present study supported that canopy species composition and diversity was more influenced by management history and stochastic events than herb layer composition and diversity. Additionally, the canopy species diversity was higher at the well-developed Yosomi forests than at the young summit forests, while the opposite pattern was observed for the herb layer diversity.

Assuming that diversity follows a hump-shaped curve in response to time as proposed by the IDH (Grime 1973), the canopy diversity was in the increasing section of the curve at Yosomi, while the herb layer diversity has been past the peak and declined. Hump-shaped diversity patterns are also observed along the disturbance gradient (Chang et al. 2019), but finer temporal scale is needed to confirm this pattern after eruptions. The present findings are also limited to forest ecosystems, whereas grasslands and shrubs are present on Mount Usu and determine later successional stages.

Successional processes and mechanisms are comparable across geographical distances (Tsuyuzaki and del Moral 1995), even though volcanic succession is divergent (Prach and Walker 2020). In spite of the distinct species composition observed at plantations, this active management facilitated fast revegetation and prevented surface erosion, both of which are important aspects to protect human settlements close to disturbed areas (Sakurai 2019).

However, the plantations did not compensate the slow succession rate caused by the large disturbance often associated with volcanic eruptions. With the advent of remote sensing and imagery chronosequence developed here, the success of management activities can be monitored effectively and identify areas where field surveys or further interventions are needed.

## Acknowledgements

Many people supported me during my research at Hokkaido University. Foremost, I thank my supervisor, Prof. Shiro Tsuyuzaki, for providing advice and comments throughout my studies. He taught me a great deal about the vegetation of Mount Usu while patiently identifying the plants on my amateur pictures from field surveys.

My gratitude goes to Dr. TaeOh Kwon, who first introduced me to Mount Usu, and Prof. Takashi Dempo at the Toyako research station who secured me a bicycle for daily commuting to my research site, and for picking me up and dropping me off at the bus station during my field trips. I thank the Ministry of the Environment, Hokkaido District Bureau for permitting me to carry out my research, especially to Yuki Nakayama who helped me with the application process. I would have encountered much more difficulties without the help of Yuko Ito and Natsuko Yukino, who helped me find my way among the Japanese documents and university system. I am grateful to the Ministry of Sports and Education for providing me with the scholarship to carry out my research.

My time at Hokudai would have been less exciting without the early support of my laboratory and division mates: Muklish Jamal Musa Holle, Bayarsaikhan Demidkhorloo, Doddy Juli Irawan, Harisoa Rakotonoely, Junichi Fujinuma, Yuki Mizunaga, Akari Shibata, and without the cheers during the final months of the students of Prof. Ram Avtar. I also gained valuable support in times of crisis from my friends I got to know through Nitobe College: Prof. Kaori Kuribayashi-Shigetomi, Michal Mazur, and Qianran Wang.

I am grateful to my personal friends in Sapporo, too numerous to name them all, for bearing me during the good and bad times.

Finally, I thank my family for their steady support and love during my studies. Their unwavering trust made me feel that everything is possible.

# References


Adams, Bryce T., Stephen N. Matthews, Matthew P. Peters, Anantha Prasad, and Louis R. Iverson. 2019. 'Mapping Floristic Gradients of Forest Composition Using an Ordination-Regression Approach with Landsat OLI and Terrain Data in the Central Hardwoods Region'. *Forest Ecology and Management* 434:87–98. doi: 10.1016/j.foreco.2018.12.018.

ASTER. 2011. 'Advanced Spaceborne Thermal Emission and Reflection Radiometer (ASTER) Global Digital Elevation Model (GDEM),Version 2; ASTER GDEM Is a Product of METI and NASA'.

Baeten, Lander, T. Jonathan Davies, Kris Verheyen, Hans Van Calster, and Mark Vellend. 2015. 'Disentangling Dispersal from Phylogeny in the Colonization Capacity of Forest Understorey Plants'. *Journal of Ecology* 103(1):175–83. doi: 10.1111/1365-2745.12333.

Bates, Douglas, Martin Mächler, Ben Bolker, and Steve Walker. 2015. 'Fitting Linear Mixed-Effects Models Using Lme4'. *Journal of Statistical Software, Articles* 67(1):1–48. doi: 10.18637/jss.v067.i01.

Berdugo, Miguel, Santiago Soliveres, Sonia Kéfi, and Fernando T. Maestre. 2019. 'The Interplay between Facilitation and Habitat Type Drives Spatial Vegetation Patterns in Global Drylands'. *Ecography* 42(4):755–67. doi: 10.1111/ecog.03795.

Bishop, John G., Niamh B. O'Hara, Jonathan H. Titus, Jennifer L. Apple, Richard A. Gill, and Louise Wynn. 2010. 'N-P Co-Limitation of Primary Production and Response of Arthropods to N and P in Early Primary Succession on Mount St. Helens Volcano'. *PLOS ONE* 5(10):e13598. doi: 10.1371/journal.pone.0013598.

Bossuyt, B., M. Heyn, and M. Hermy. 2002. 'Seed Bank and Vegetation Composition of Forest Stands of Varying Age in Central Belgium: Consequences for Regeneration of Ancient Forest Vegetation'. *Plant Ecology* 162(1):33–48. doi: 10.1023/A:1020391430072.

Botta-Dukát, Zoltán. 2005. 'Rao's Quadratic Entropy as a Measure of Functional Diversity Based on Multiple Traits'. *Journal of Vegetation Science* 16(5):533–40. doi: 10.1111/j.1654-1103.2005.tb02393.x.

Bourgeois, Bérenger, Anne Vanasse, and Monique Poulin. 2016. 'Effects of Competition, Shade and Soil Conditions on the Recolonization of Three Forest Herbs in Tree-Planted Riparian Zones'. *Applied Vegetation Science* 19(4):679–88. doi: 10.1111/avsc.12246.

Bray, J. Roger, and John Curtis. 1957. 'An Ordination of the Upland Forest Communities of Southern Wisconsin'. *Ecol. Monogr* 27:325–49.

van Breugel, Michiel, Dylan Craven, Hao Ran Lai, Mario Baillon, Benjamin L. Turner, and Jefferson S. Hall. 2019. 'Soil Nutrients and Dispersal Limitation Shape Compositional Variation in Secondary Tropical Forests across Multiple Scales'. *Journal of Ecology* 107(2):566–81. doi: 10.1111/1365-2745.13126.

Brooker, Rob W., and Terry V. Callaghan. 1998. 'The Balance between Positive and Negative Plant Interactions and Its Relationship to Environmental Gradients: A Model'. *Oikos* 81(1):196. doi: 10.2307/3546481.

Brooker, Rob W., Fernando T. Maestre, Ragan M. Callaway, Christopher L. Lortie, Lohengrin A. Cavieres, Georges Kunstler, Pierre Liancourt, Katja Tielbörger, Justin M. J. Travis, Fabien Anthelme, Cristina Armas, Lluis Coll, Emmanuel Corcket, Sylvain Delzon, Estelle Forey, Zaal Kikvidze, Johan Olofsson, Francisco Pugnaire, Constanza L. Quiroz, Patrick Saccone, Katja Schiffers, Merav Seifan, Blaize Touzard, and Richard Michalet. 2008. 'Facilitation in Plant Communities: The Past, the Present, and the Future'. *Journal of Ecology* 96(1):18–34. doi: 10.1111/j.1365-2745.2007.01295.x.

Buma, B., S. M. Bisbing, G. Wiles, and A. L. Bidlack. 2019. '100 Yr of Primary Succession Highlights Stochasticity and Competition Driving Community Establishment and Stability'. *Ecology* 100(12):e02885. doi: 10.1002/ecy.2885.

Burchett, Woodrow W., Amanda R. Ellis, Solomon W. Harrar, and Arne C. Bathke. 2017. 'Nonparametric Inference for Multivariate Data: The *R* Package **Npmv**'. *Journal of Statistical Software* 76(4). doi: 10.18637/jss.v076.i04.

Cain, Michael L., Hans Damman, and Angela Muir. 1998. 'Seed Dispersal and the Holocene Migration of Woodland Herbs'. *Ecological Monographs* 68(3):325–47. doi: 10.1890/0012-9615(1998)068[0325:SDATHM]2.0.CO;2.

Camathias, Linda, Ariel Bergamini, Meinrad Küchler, Silvia Stofer, and Andri Baltensweiler. 2013. 'High-Resolution Remote Sensing Data Improves Models of Species Richness'. *Applied Vegetation Science* 16(4):539–51. doi: 10.1111/avsc.12028.

Carlson, Kimberly M., Gregory P. Asner, R. Flint Hughes, Rebecca Ostertag, and Roberta E. Martin. 2007. 'Hyperspectral Remote Sensing of Canopy Biodiversity in Hawaiian Lowland Rainforests'. *Ecosystems* 10(4):536–49. doi: 10.1007/s10021-007-9041-z.

Cayuela, Luis, José María Rey Benayas, Ana Justel, and Javier Salas-Rey. 2006. 'Modelling Tree Diversity in a Highly Fragmented Tropical Montane Landscape'. *Global Ecology and Biogeography* 15(6):602–13. doi: https://doi.org/10.1111/j.1466-8238.2006.00255.x.

Chang, Cynthia C., Charles B. Halpern, Joseph A. Antos, Meghan L. Avolio, Abir Biswas, James E. Cook, Roger del Moral, Dylan G. Fischer, Andrés Holz, Robert J. Pabst, Mark E. Swanson, and Donald B. Zobel. 2019. 'Testing Conceptual Models of Early Plant Succession across a Disturbance Gradient'. *Journal of Ecology* 107(2):517–30. doi: 10.1111/1365-2745.13120.

Chapin, David M., and L. C. Bliss. 1989. 'Seedling Growth, Physiology, and Survivorship in a Subalpine, Volcanic Environment'. *Ecology* 70(5):1325–34. doi: 10.2307/1938192.

Chavez, Pat S. 1988. 'An Improved Dark-Object Subtraction Technique for Atmospheric Scattering Correction of Multispectral Data'. *Remote Sensing of Environment* 24(3):459–79. doi: 10.1016/0034-4257(88)90019-3.

Cipriotti, Pablo A., and Martín R. Aguiar. 2015. 'Is the Balance between Competition and Facilitation a Driver of the Patch Dynamics in Arid Vegetation Mosaics?' *Oikos* 124(2):139–49. doi: 10.1111/oik.01758.

Clark, Matthew L., Dar A. Roberts, and David B. Clark. 2005. 'Hyperspectral Discrimination of Tropical Rain Forest Tree Species at Leaf to Crown Scales'. *Remote Sensing of Environment* 96(3):375–98. doi: 10.1016/j.rse.2005.03.009.

Clarke, K. R. 1993. 'Non-Parametric Multivariate Analyses of Changes in Community Structure'. *Australian Journal of Ecology* 18(1):117–43. doi: 10.1111/j.1442-9993.1993.tb00438.x.

Clements, Frederic E. (Frederic Edward). 1916. *Plant Succession; an Analysis of the Development of Vegetation*. Vol. no.242 (1916). Washington,: Carnegie Institution of Washington,.

Cohen, Jacob. 1960. 'A Coefficient of Agreement for Nominal Scales'. *Education and Psychological Measurement* 20(1):37–46.

Cutler, N. A., L. R. Belyea, and A. J. Dugmore. 2008. 'The Spatiotemporal Dynamics of a Primary Succession'. *Journal of Ecology* 96(2):231–46. doi: 10.1111/j.1365-2745.2007.01344.x.

Dale, Virginia H., and Wendy M. Adams. 2003. 'Plant Reestablishment 15 Years after the Debris Avalanche at Mount St. Helens, Washington'. *Science of The Total Environment* 313(1–3):101–13. doi: 10.1016/S0048-9697(03)00332-2.

De Rose, Ronald Charles, Takashi Oguchi, Wataru Morishima, and Mario Collado. 2011. 'Land Cover Change on Mt. Pinatubo, the Philippines, Monitored Using ASTER VNIR'. *International Journal of Remote Sensing* 32(24):9279–9305. doi: 10.1080/01431161.2011.554452.

De Schutter, Ann, Matthieu Kervyn, Frank Canters, Sonja A. Bosshard-Stadlin, Majura A. M. Songo, and Hannes B. Mattsson. 2015. 'Ash Fall Impact on Vegetation: A Remote Sensing Approach of the Oldoinyo Lengai 2007–08 Eruption'. *Journal of Applied Volcanology* 4(1):15. doi: 10.1186/s13617-015-0032-z.

Dogan, Hakan Mete, and Musa Dogan. 2006. 'A New Approach to Diversity Indices – Modeling and Mapping Plant Biodiversity of Nallihan (A3-Ankara/Turkey) Forest Ecosystem in Frame of Geographic Information Systems'. *Biodiversity & Conservation* 15(3):855–78. doi: 10.1007/s10531-004-2937-4.

Dudley, Kenneth L., Philip E. Dennison, Keely L. Roth, Dar A. Roberts, and Austin R. Coates. 2015. 'A Multi-Temporal Spectral Library Approach for Mapping Vegetation Species across Spatial and Temporal Phenological Gradients'. *Special Issue on the Hyperspectral Infrared Imager (HyspIRI)* 167:121–34. doi: 10.1016/j.rse.2015.05.004.

Edwards, Stefan McKinnon. 2020. *Lemon: Freshing Up Your 'ggplot2' Plots*.

Efford, Jt, Bd Clarkson, and Rj Bylsma. 2014. 'Persistent Effects of a Tephra Eruption (AD 1655) on Treeline Composition and Structure, Mt Taranaki, New Zealand'. *New Zealand Journal of Botany* 52(2):245–61. doi: 10.1080/0028825X.2014.886599.

Endo, Megumi, Yasuo Yamamura, Atsushi Tanaka, Takashi Nakano, and Taisuke Yasuda. 2008. 'Nurse-Plant Effects of a Dwarf Shrub on the Establishment of Tree Seedlings in a Volcanic Desert on Mt. Fuji, Central Japan'. *Arctic, Antarctic, and Alpine Research* 40(2):335–42. doi: 10.1657/1523-0430(07-013)[ENDO]2.0.CO;2.

Fahrig, Lenore. 2013. 'Rethinking Patch Size and Isolation Effects: The Habitat Amount Hypothesis'. *Journal of Biogeography* 40(9):1649–63. doi: 10.1111/jbi.12130.

Feilhauer, Hannes, Carola Dahlke, Daniel Doktor, Angela Lausch, Sebastian Schmidtlein, Gundula Schulz, and Stefanie Stenzel. 2014. 'Mapping the Local Variability of Natura 2000 Habitats with Remote Sensing'. *Applied Vegetation Science* 17(4):765–79. doi: https://doi.org/10.1111/avsc.12115.

Feilhauer, Hannes, and Sebastian Schmidtlein. 2009. 'Mapping Continuous Fields of Forest Alpha and Beta Diversity'. *Applied Vegetation Science* 12(4):429–39. doi: https://doi.org/10.1111/j.1654-109X.2009.01037.x.

Feilhauer, Hannes, Frank Thonfeld, Ulrike Faude, Kate S. He, Duccio Rocchini, and Sebastian Schmidtlein. 2013. 'Assessing Floristic Composition with Multispectral Sensors—A Comparison Based on Monotemporal and Multiseasonal Field Spectra'. *International Journal of Applied Earth Observation and Geoinformation* 21:218–29. doi: 10.1016/j.jag.2012.09.002.

Fischer, Dylan G., Joseph A. Antos, Abir Biswas, and Donald B. Zobel. 2019. 'Understorey Succession after Burial by Tephra from Mount St. Helens'. *Journal of Ecology* 107(2):531–44. doi: 10.1111/1365-2745.13052.

Foody, Giles M., and Mark E. J. Cutler. 2003. 'Tree Biodiversity in Protected and Logged Bornean Tropical Rain Forests and Its Measurement by Satellite Remote Sensing'. *Journal of Biogeography* 30(7):1053–66. doi: 10.1046/j.1365-2699.2003.00887.x.

Fridriksson, Sturla. 1982. 'Life Develops on Surtsey'. *Endeavour* 6(3):100–107. doi: 10.1016/0160-9327(82)90041-2.

Fuller, R. N., and Roger del Moral. 2003. 'The Role of Refugia and Dispersal in Primary Succession on Mount St. Helens, Washington'. *Journal of Vegetation Science* 14(5):637–44. doi: 10.1111/j.1654-1103.2003.tb02195.x.

Galván-Tejada, Nadeshda Cosette, Víctor Peña-Ramírez, Lucy Mora-Palomino, and Christina Siebe. 2014. 'Soil P Fractions in a Volcanic Soil Chronosequence of Central Mexico and Their Relationship to Foliar P in Pine Trees'. *Journal of Plant Nutrition and Soil Science* 177(5):792–802. doi: 10.1002/jpln.201300653.

Gilbert, O. L., and Penny Anderson. 1998. *Habitat Creation and Repair*. New York: Oxford University Press.

Gillespie, Alan R., Anne B. Kahle, and Richard E. Walker. 1986. 'Color Enhancement of Highly Correlated Images. I. Decorrelation and HSI Contrast Stretches'. *Remote Sensing of Environment* 20(3):209–35. doi: 10.1016/0034-4257(86)90044-1.

Gillespie, Thomas W. 2005. 'Predicting Woody-Plant Species Richness in Tropical Dry Forests: A Case Study from South Florida, USA'. *Ecological Applications* 15(1):27–37. doi: 10.1890/03-5304.

Gilliam, Frank S. 2007. 'The Ecological Significance of the Herbaceous Layer in Temperate Forest Ecosystems'. *BioScience* 57(10):845–58. doi: 10.1641/B571007.

Gitelson, Anatoly A., Yoram J. Kaufman, Robert Stark, and Don Rundquist. 2002. 'Novel Algorithms for Remote Estimation of Vegetation Fraction'. *Remote Sensing of Environment* 80(1):76–87. doi: 10.1016/S0034-4257(01)00289-9.

Gleason, H. A. 1926. 'The Individualistic Concept of the Plant Association'. *Bulletin of the Torrey Botanical Club* 53(1):7–26. doi: 10.2307/2479933.

Gould, William. 2000. ‘Remote Sensing of Vegetation, Plant Species Richness, and Regional Biodiversitzy Hotspots’. *Ecological Applications* 10(6):1861–70. doi: 10.1890/1051-0761(2000)010[1861:RSOVPS]2.0.CO;2.

Graae, Bente Jessen, T. Hansen, and P. B. Sunde. 2004. ‘The Importance of Recruitment Limitation in Forest Plant Species Colonization: A Seed Sowing Experiment’. *Flora - Morphology, Distribution, Functional Ecology of Plants* 199(3):263–70. doi: 10.1078/0367-2530-00154.

Grime, J. P. 1973. ‘Competitive Exclusion in Herbaceous Vegetation’. *Nature* 242(5396):344–47. doi: 10.1038/242344a0.

Hakkenberg, C. R., K. Zhu, R. K. Peet, and C. Song. 2018. ‘Mapping Multi-Scale Vascular Plant Richness in a Forest Landscape with Integrated LiDAR and Hyperspectral Remote-Sensing’. *Ecology* 99(2):474–87. doi: 10.1002/ecy.2109.

Hall, Karin, Triin Reitalu, Martin T. Sykes, and Honor C. Prentice. 2012. ‘Spectral Heterogeneity of QuickBird Satellite Data Is Related to Fine-Scale Plant Species Spatial Turnover in Semi-Natural Grasslands’. *Applied Vegetation Science* 15(1):145–57. doi: 10.1111/j.1654-109X.2011.01143.x.

Halpern, Charles B., and James A. Lutz. 2013. ‘Canopy Closure Exerts Weak Controls on Understory Dynamics: A 30-Year Study of Overstory–Understory Interactions’. *Ecological Monographs* 83(2):221–37. doi: 10.1890/12-1696.1.

Haruki, Masahiro, and Shiro Tsuyuzaki. 2001. ‘Woody Plant Establishment during the Early Stages of Volcanic Succession on Mount Usu, Northern Japan’. *Ecological Research* 16(3):451–57. doi: 10.1046/j.1440-1703.2001.00407.x.

Hill, M. O. 1973. ‘Diversity and Evenness: A Unifying Notation and Its Consequences’. *Ecology* 54(2):427. doi: 10.2307/1934352.

Hlavac, Marek. 2018. *Stargazer: Well-Formatted Regression and Summary Statistics Tables*. R package version 5.2.2. Bratislava, Slovakia: Central European Labour Studies Institute (CELSI).

Hopfensperger, Kristine N. 2007. ‘A Review of Similarity between Seed Bank and Standing Vegetation across Ecosystems’. *Oikos* 116(9):1438–48. doi: 10.1111/j.0030-1299.2007.15818.x.

Hothorn, Torsten, Frank Bretz, and Peter Westfall. 2008. ‘Simultaneous Inference in General Parametric Models’. 50(3):346–63.

Huang, Ran, Jian-xi Huang, Chao Zhang, Hong-yuan Ma, Wen Zhuo, Ying-yi Chen, De-hai Zhu, Qingling Wu, and Lamin R. Mansaray. 2020. ‘Soil Temperature Estimation at Different Depths, Using Remotely-Sensed Data’. *Journal of Integrative Agriculture* 19(1):277–90. doi: 10.1016/S2095-3119(19)62657-2.

Huemmrich, K. F., J. A. Gamon, C. E. Tweedie, P. K. E. Campbell, D. R. Landis, and E. M. Middleton. 2013. ‘Arctic Tundra Vegetation Functional Types Based on Photosynthetic Physiology and Optical Properties’. *IEEE Journal of Selected Topics in Applied Earth Observations and Remote Sensing* 6(2):265–75. doi: 10.1109/JSTARS.2013.2253446.

Hulshof, Catherine M., and Marko J. Spasojevic. 2020. ‘The Edaphic Control of Plant Diversity’. *Global Ecology and Biogeography* 29(10):1634–50. doi: 10.1111/geb.13151.

Hyatt, Laura A., and Brenda B. Casper. 2000. 'Seed Bank Formation during Early Secondary Succession in a Temperate Deciduous Forest'. *Journal of Ecology* 88(3):516–27. doi: 10.1046/j.1365-2745.2000.00465.x.

IPCC. 2013. *Climate Change 2013: The Physical Science Basis. Contribution of Working Group I to the Fifth Assessment Report of the Intergovernmental Panel on Climate Change*. edited by Stocker, T.F., D. Qin, G.-K. Plattner, M. Tignor, S.K. Allen, J. Boschung, A. Nauels, Y. Xia, V. Bex, and P.M. Midgley. Cambridge, United Kingdom and New York, NY, USA: Cambridge University Press.

Irl, Severin D. H., Andreas H. Schweiger, Samuel Hoffmann, Carl Beierkuhnlein, Hanna Hartmann, Thomas Pickel, and Anke Jentsch. 2019. 'Spatiotemporal Dynamics of Plant Diversity and Endemism during Primary Succession on an Oceanic-Volcanic Island'. *Journal of Vegetation Science* 30(4):587–98. doi: 10.1111/jvs.12765.

Iwatsuki, Kunio. 1993. *Flora of Japan*. Vols 1–4. Kodansha.

Jasper, David A. 2007. 'Beneficial Soil Microorganisms of the Jarrah Forest and Their Recovery in Bauxite Mine Restoration in Southwestern Australia'. *Restoration Ecology* 15(s4):S74–84. doi: 10.1111/j.1526-100X.2007.00295.x.

JMA. 2019. 'Date Meteorological Station'. *Japan Meteorological Agency*. Retrieved 27 September 2019 (https://www.data.jma.go.jp/obd/stats/etrn/view/annually_a.php?prec_no=21&block_no=0132&year=&month=&day=&view=).

Johansen, Bernt, and Hans Tømmervik. 2014. 'The Relationship between Phytomass, NDVI and Vegetation Communities on Svalbard'. *International Journal of Applied Earth Observation and Geoinformation* 27:20–30. doi: https://doi.org/10.1016/j.jag.2013.07.001.

Johnson, Edward A., and Kiyoko Miyanishi. 2008. 'Testing the Assumptions of Chronosequences in Succession'. *Ecology Letters* 11(5):419–31. doi: 10.1111/j.1461-0248.2008.01173.x.

Jones, Chad C., and Roger del Moral. 2009. 'Dispersal and Establishment Both Limit Colonization during Primary Succession on a Glacier Foreland'. *Plant Ecology* 204(2):217–30. doi: 10.1007/s11258-009-9586-3.

Jost, Lou. 2006. 'Entropy and Diversity'. *Oikos* 113(2):363–75.

Jurasinski, Gerald, and Marian Koch. 2011. 'Commentary: Do We Have a Consistent Terminology for Species Diversity? We Are on the Way'. *Oecologia* 167(4):893–902. doi: 10.1007/s00442-011-2126-6.

Jurasinski, Gerald, and with contributions from Vroni Retzer. 2012. *Simba: A Collection of Functions for Similarity Analysis of Vegetation Data*.

Kadomura, Hiroshi, Hiromu Okada, and Tohru Araya. 1988. *1977-82 Volcanism and Environmental Hazards of Usu Volcano*. Japan: Hokkaido University Press.

Kamijo, Takashi, Kanehiro Kitayama, Aya Sugawara, Shinya Urushimichi, and Kanako Sasai. 2002. 'Primary Succession of the Warm-Temperate Broad-Leaved Forest on a Volcanic Island, Miyake-Jima, Japan'. *Folia Geobotanica* 37(1):71–91. doi: 10.1007/BF02803192.

Karadimou, E., A. S. Kallimanis, I. Tsiripidis, T. Raus, E. Bergmeier, and P. Dimopoulos. 2018. 'Functional Diversity Changes over 100 Yr of Primary Succession on a Volcanic Island: Insights into Assembly Processes'. *Ecosphere* 9(9):e02374. doi: 10.1002/ecs2.2374.

Kardol, Paul, Nelleke J. Cornips, Monique M. L. van Kempen, J. M. Tanja Bakx-Schotman, and Wim H. van der Putten. 2007. 'Microbe-Mediated Plant-Soil Feedback Causes Historical Contingency Effects in Plant Community Assembly'. *Ecological Monographs* 77(2):147–62. doi: 10.1890/06-0502.

Kark, S., N. Levin, and S. Phinn. 2008. 'Global Environmental Priorities: Making Sense of Remote Sensing. Reply to TREE Letter: Satellites Miss Environmental Priorities by Loarie et al. (2007).' *Trends in Ecology & Evolution* 23 4:181–82; author reply 183-4.

Katsui, Yoshio. 1981. *Field Excursion Guide to Usu and Tarumai Volcanoes and Noboribetsu Spa*. Volcanological Society of Japan.

Katsui, Yoshio, Y. Ōba, K. Onuma, T. Suzuki, Y. Kondo, T. Watanabe, K. Niida, T. Uda, S. Hagiwara, T. Nagao, and others. 1978. 'Preliminary Report of the 1977 Eruption of Usu Volcano'. *J. Fac. Sci. Hokkaido University* 18(3):385–408.

Katsui, Yoshio, Izumi Yokoyama, and Masayo Murozumi. 1981. 'Usu Volcano'. in *Field excursion guide to Usu and Tarumai volcanoes and Noboribetsu spa*. Japan: Volcanological Society of Japan.

Keeney, D. R., and D. W. Nelson. 1983. 'Nitrogen—Inorganic Forms'. Pp. 643–98 in *Methods of Soil Analysis*. John Wiley & Sons, Ltd.

Kerr, Jeremy T., and Marsha Ostrovsky. 2003. 'From Space to Species: Ecological Applications for Remote Sensing'. *Trends in Ecology & Evolution* 18(6):299–305. doi: 10.1016/S0169-5347(03)00071-5.

Kitagawa, Ryo, Mitsuru Ueno, and Takashi Masaki. 2017. 'Thinning Affects Understorey Tree Community Assembly in Monoculture Plantations by Facilitating Stochastic Immigration from the Landscape'. *Applied Vegetation Science* 20(4):673–82. doi: 10.1111/avsc.12327.

Kondo, Toshihiro, and Shiro Tsuyuzaki. 1999. 'Natural Regeneration Patterns of the Introduced Larch, Larix Kaempferi (Pinaceae), on the Volcano Mount Koma, Northern Japan'. *Diversity and Distributions* 5(5):223–33. doi: 10.1046/j.1472-4642.1999.00056.x.

Korb, Julie E., W. W. Covington, and Peter Z. Fulé. 2003. 'Sampling Techniques Influence Understory Plant Trajectories After Restoration: An Example from Ponderosa Pine Restoration'. *Restoration Ecology* 11(4):504–15. doi: 10.1046/j.1526-100X.2003.rec0170.x.

Krause, Keith. 2003. 'Radiance Conversion of QuickBird Data'.

Kwon, TaeOh, and Shiro Tsuyuzaki. 2016. 'Differences in Nitrogen Redistribution between Early and Late Plant Colonizers through Ectomycorrhizal Fungi on the Volcano Mount Koma'. *Ecological Research* 31(4):557–67. doi: 10.1007/s11284-016-1364-9.

Laliberté, Etienne, Anna K. Schweiger, and Pierre Legendre. 2020. 'Partitioning Plant Spectral Diversity into Alpha and Beta Components'. *Ecology Letters* 23(2):370–80. doi: 10.1111/ele.13429.

Lassau, Scott A., Gerasimos Cassis, Paul K. J. Flemons, Lance Wilkie, and Dieter F. Hochuli. 2005. 'Using High-Resolution Multi-Spectral Imagery to Estimate Habitat Complexity in Open-Canopy Forests: Can We Predict Ant Community Patterns?' *Ecography* 28(4):495–504. doi: 10.1111/j.0906-7590.2005.04116.x.

Lawrence, Rick L., and William J. Ripple. 1998. 'Comparisons among Vegetation Indices and Bandwise Regression in a Highly Disturbed, Heterogeneous Landscape: Mount St. Helens, Washington'. *Remote Sensing of Environment* 64(1):91–102.

Lawrence, Rick L., and William J. Ripple. 2000. 'Fifteen Years of Revegetation of Mount St. Helens: A Landscape-Scale Analysis'. *Ecology* 81(10):2742–52. doi: 10.1890/0012-9658(2000)081[2742:FYOROM]2.0.CO;2.

Legendre, Pierre. 1993. 'Spatial Autocorrelation: Trouble or New Paradigm?' *Ecology* 74(6):1659–73. doi: 10.2307/1939924.

Legendre, Pierre, and Louis Legendre. 2012. *Numerical Ecology*. 3rd English ed. Amsterdam ; Tokyo: Elsevier.

Levin, Noam, Avi Shmida, Oded Levanoni, Hagit Tamari, and Salit Kark. 2007. 'Predicting Mountain Plant Richness and Rarity from Space Using Satellite-Derived Vegetation Indices'. *Diversity and Distributions* 13(6):692–703. doi: 10.1111/j.1472-4642.2007.00372.x.

Lichter, John. 2000. 'Colonization Constraints during Primary Succession on Coastal Lake Michigan Sand Dunes: Colonization Constraints during Primary Succession'. *Journal of Ecology* 88(5):825–39. doi: 10.1046/j.1365-2745.2000.00503.x.

Loarie, Scott, Lucas Joppa, and Stuart Pimm. 2008. 'Satellites Miss Environmental Priorities'. *Trends in Ecology & Evolution* 22:630–32. doi: 10.1016/j.tree.2007.08.018.

Lüdecke, Daniel. 2021. *SjPlot: Data Visualization for Statistics in Social Science*.

Ma, Miaojun, Guozhen Du, and Xianhui Zhou. 2009. 'Role of the Soil Seed Bank during Succession in a Subalpine Meadow on the Tibetan Plateau'. *Arctic, Antarctic, and Alpine Research* 41(4):469–77. doi: 10.1657/1938-4246-41.4.999.

Madonsela, Sabelo, Moses Azong Cho, Abel Ramoelo, and Onisimo Mutanga. 2017. 'Remote Sensing of Species Diversity Using Landsat 8 Spectral Variables'. *ISPRS Journal of Photogrammetry and Remote Sensing* 133:116–27. doi: 10.1016/j.isprsjprs.2017.10.008.

Makoto, K., and Scott D. Wilson. 2016. 'New Multicentury Evidence for Dispersal Limitation during Primary Succession'. *The American Naturalist* 187(6):804–11. doi: 10.1086/686199.

Mansourian, Stephanie, Daniel Vallauri, and Nigel Dudley. 2005. *Forest Restoration in Landscapes : Beyond Planting Trees*. New York, N.Y.: Springer.

Mantel, Nathan. 1967. 'The Detection of Disease Clustering and a Generalized Regression Approach'. *Cancer Research* 27(2 Part 1):209.

Marignani, Michela, Eva Del Vico, and Simona Maccherini. 2007. 'Spatial Scale and Sampling Size Affect the Concordance between Remotely Sensed Information and Plant Community Discrimination in Restoration Monitoring'. *Biodiversity and Conservation* 16(13):3851–61. doi: 10.1007/s10531-007-9184-4.

Marler, Thomas E., and Roger del Moral. 2011. 'Primary Succession along an Elevation Gradient 15 Years after the Eruption of Mount Pinatubo, Luzon, Philippines'. *Pacific Science* 65(2):157–73. doi: 10.2984/65.2.157.

Marler, Thomas E., and Roger del Moral. 2013. 'Primary Succession in Mount Pinatubo: Habitat Availability and Ordination Analysis'. *Communicative & Integrative Biology* 6(6):e25924. doi: 10.4161/cib.25924.

Meiners, Scott J., Marc W. Cadotte, Jason D. Fridley, Steward T. A. Pickett, and Lawrence R. Walker. 2015. 'Is Successional Research Nearing Its Climax? New Approaches for Understanding Dynamic Communities'. *Functional Ecology* 29(2):154–64. doi: 10.1111/1365-2435.12391.

Mesgaran, M. B., H. R. Mashhadi, E. Zand, and H. M. Alizadeh. 2007. 'Comparison of Three Methodologies for Efficient Seed Extraction in Studies of Soil Weed Seedbanks'. *Weed Research* 47(6):472–78. doi: 10.1111/j.1365-3180.2007.00592.x.

Miller, Thomas Lumley based on Fortran code by Alan. 2020. *Leaps: Regression Subset Selection*.

Miller, Todd F., David J. Mladenoff, and Murray K. Clayton. 2002. 'Old-Growth Northern Hardwood Forests: Spatial Autocorrelation and Patterns of Understory Vegetation'. *Ecological Monographs* 72(4):487–503. doi: 10.1890/0012-9615(2002)072[0487:OGNHFS]2.0.CO;2.

del Moral, Roger. 2007. 'Limits to Convergence of Vegetation during Early Primary Succession'. *Journal of Vegetation Science* 18(4):479–88. doi: 10.1111/j.1654-1103.2007.tb02562.x.

del Moral, Roger. 2009. 'Increasing Deterministic Control of Primary Succession on Mount St. Helens, Washington'. *Journal of Vegetation Science* 20(6):1145–54. doi: 10.1111/j.1654-1103.2009.01113.x.

del Moral, Roger. 2010. 'The Importance of Long-Term Studies of Ecosystem Reassembly after the Eruption of the Kasatochi Island Volcano'. *Arctic, Antarctic, and Alpine Research* 42(3):335–41. doi: 10.1657/1938-4246-42.3.335.

del Moral, Roger, and Andrew J. Eckert. 2005. 'Colonization of Volcanic Deserts from Productive Patches'. *American Journal of Botany* 92(1):27–36. doi: 10.3732/ajb.92.1.27.

del Moral, Roger, and B. Magnússon. 2014. 'Surtsey and Mount St. Helens: A Comparison of Early Succession Rates'. *Biogeosciences* 11(7):2099–2111. doi: 10.5194/bg-11-2099-2014.

del Moral, Roger, Jason M. Saura, and Jennifer N. Emenegger. 2010. 'Primary Succession Trajectories on a Barren Plain, Mount St. Helens, Washington: Primary Succession Trajectories'. *Journal of Vegetation Science* 21(5):857–67. doi: 10.1111/j.1654-1103.2010.01189.x.

del Moral, Roger, Jonathan H. Titus, and Arlene M. Cook. 1995. 'Early Primary Succession on Mount St. Helens, Washington, USA'. *Journal of Vegetation Science* 6:107–20. doi: 10.2307/3236262.

del Moral, Roger, Lawrence R. Walker, and Jan P. Bakker. 2007. 'Insights Gained from Succession for the Restoration of Landscape Structure and Function'. Pp. 19–44 in

*Linking Restoration and Ecological Succession*, edited by L. R. Walker, J. Walker, and R. J. Hobbs. New York, NY: Springer New York.

del Moral, Roger, and David M. Wood. 2012. 'Vegetation Development on Permanently Established Grids, Mount St. Helens (1986–2010)'. *Ecology* 93(9):2125–2125. doi: 10.1890/12-0344.1.

Moran, P. A. P. 1950. 'Notes on Continuous Stochastic Phenomena'. *Biometrika* 37(1/2):17–23. doi: 10.2307/2332142.

Moreno, Claudia E., and Pilar Rodríguez. 2011. 'Commentary: Do We Have a Consistent Terminology for Species Diversity? Back to Basics and toward a Unifying Framework'. *Oecologia* 167(4):889–92. doi: 10.1007/s00442-011-2125-7.

Mudrák, Ondřej, Jiří Doležal, and Jan Frouz. 2016. 'Initial Species Composition Predicts the Progress in the Spontaneous Succession on Post-Mining Sites'. *Ecological Engineering* 95:665–70. doi: 10.1016/j.ecoleng.2016.07.002.

Nagai, Mio, and Toshiya Yoshida. 2006. 'Variation in Understory Structure and Plant Species Diversity Influenced by Silvicultural Treatments among 21- to 26-Year-Old Picea Glehnii Plantations'. *Journal of Forest Research* 11(1):1–10. doi: 10.1007/s10310-005-0176-5.

Nagendra, Harini, Duccio Rocchini, R. Ghate, B. Sharma, and S. Pareeth. 2010. 'Assessing Plant Diversity in a Dry Tropical Forest: Comparing the Utility of Landsat and Ikonos Satellite Images'. 2(2):478–96. doi: https://doi.org/10.3390/rs2020478.

Nakajima, Tohru, Jung-soo Lee, Takaaki Kawaguchi, Satoshi Tatsuhara, and Norihiko Shiraishi. 2009. 'Risk Assessment of Wind Disturbance in Japanese Mountain Forests'. *Écoscience* 16(1):58–65. doi: 10.2980/16-1-3179.

Nakashizuka, T., S. Iida, W. Suzuki, and T. Tanimoto. 1993. 'Seed Dispersal and Vegetation Development on a Debris Avalanche on the Ontake Volcano, Central Japan'. *Journal of Vegetation Science* 4(4):537–42. doi: 10.2307/3236081.

Oba, Y. 1966. 'Geology and Petrology of Usu Volcano, Hokkaido, Japan'. 13:185–236.

Obase, Keisuke, Yutaka Tamai, Takashi Yajima, and Toshizumi Miyamoto. 2008. 'Mycorrhizal Colonization Status of Plant Species Established in an Exposed Area Following the 2000 Eruption of Mt. Usu, Hokkaido, Japan'. *Landscape and Ecological Engineering* 4(1):57–61. doi: 10.1007/s11355-008-0035-6.

Okitsu, Susumu. 2003. 'Forest Vegetation of Northern Japan and the Southern Kurils'. Pp. 231–61 in *Forest Vegetation of Northeast Asia*, edited by J. Kolbek, M. Šrůtek, and E. O. Box. Dordrecht: Springer Netherlands.

Oksanen, Jari, F. Guillaume Blanchet, Michael Friendly, Roeland Kindt, Pierre Legendre, Dan McGlinn, Peter R. Minchin, R. B. O'Hara, Gavin L. Simpson, Peter Solymos, M. Henry H. Stevens, Eduard Szoecs, and Helene Wagner. 2019. *Vegan: Community Ecology Package*.

Oldeland, Jens, Dirk Wesuls, Duccio Rocchini, Michael Schmidt, and Norbert Jürgens. 2010. 'Does Using Species Abundance Data Improve Estimates of Species Diversity from Remotely Sensed Spectral Heterogeneity?' *Ecological Indicators* 10(2):390–96. doi: 10.1016/j.ecolind.2009.07.012.

Otaki, Michiru, Fumiko Takeuchi, and Shiro Tsuyuzaki. 2016. ‘Changes in Microbial Community Composition in the Leaf Litter of Successional Communities after Volcanic Eruptions of Mount Usu, Northern Japan’. *Journal of Mountain Science* 13(9):1652–62. doi: 10.1007/s11629-016-3835-4.

Paganini, Marc, Allison K. Leidner, Gary Geller, Woody Turner, and Martin Wegmann. 2016. ‘The Role of Space Agencies in Remotely Sensed Essential Biodiversity Variables’ edited by H. Nagendra and C. Atzberger. *Remote Sensing in Ecology and Conservation* 2(3):132–40. doi: 10.1002/rse2.29.

Palmer, Michael W., Peter G. Earls, Bruce W. Hoagland, Peter S. White, and Thomas Wohlgemuth. 2002. ‘Quantitative Tools for Perfecting Species Lists’. *Environmetrics* 13(2):121–37. doi: 10.1002/env.516.

Parviainen, Miia, Miska Luoto, and Risto K. Heikkinen. 2009. ‘The Role of Local and Landscape Level Measures of Greenness in Modelling Boreal Plant Species Richness’. *Ecological Modelling* 220(20):2690–2701. doi: https://doi.org/10.1016/j.ecolmodel.2009.07.017.

Pedersen, Thomas Lin. 2020. *Patchwork: The Composer of Plots*.

Peng, Shaolin, Ting Zhou, Liyin Liang, and Wentao Ren. 2012. ‘Landscape Pattern Dynamics and Mechanisms during Vegetation Restoration: A Multiscale, Hierarchical Patch Dynamics Approach’. *Restoration Ecology* 20(1):95–102. doi: 10.1111/j.1526-100X.2010.00741.x.

Perrow, Martin R., and A. J. Davy. 2002. *Principles of Restoration*. Vol. v. 1. Cambridge, UK: Cambridge University Press.

Pickett, S. T. A., and Peter S. White. 1985. *The Ecology of Natural Disturbance and Patch Dynamics*. Orlando, Fla. ; Tokyo: Academic Press.

Plue, Jan, Kris Verheyen, Hans Van Calster, Damien Marage, Ken Thompson, Rein Kalamees, Malgorzata Jankowska-Blaszczuk, Beatrijs Bossuyt, and Martin Hermy. 2010. ‘Seed Banks of Temperate Deciduous Forests during Secondary Succession’. *Journal of Vegetation Science* 21(5):965–78.

Prach, Karel, and Richard J. Hobbs. 2008. ‘Spontaneous Succession versus Technical Reclamation in the Restoration of Disturbed Sites’. *Restoration Ecology* 16(3):363–66. doi: 10.1111/j.1526-100X.2008.00412.x.

Prach, Karel, and Lawrence R. Walker. 2011. ‘Four Opportunities for Studies of Ecological Succession’. *Trends in Ecology & Evolution* 26(3):119–23. doi: 10.1016/j.tree.2010.12.007.

Prach, Karel, and Lawrence R. Walker. 2020. *Comparative Plant Succession among Terrestrial Biomes of the World*. Cambridge University Press.

van der Putten, Wim H., Richard D. Bardgett, James D. Bever, T. Martijn Bezemer, Brenda B. Casper, Tadashi Fukami, Paul Kardol, John N. Klironomos, Andrew Kulmatiski, Jennifer A. Schweitzer, Katherine N. Suding, Tess F. J. Van de Voorde, and David A. Wardle. 2013. ‘Plant–Soil Feedbacks: The Past, the Present and Future Challenges’. *Journal of Ecology* 101(2):265–76. doi: 10.1111/1365-2745.12054.

R Core Team. 2018. *R: A Language and Environment for Statistical Computing*. Vienna, Austria: R Foundation for Statistical Computing.

Räsänen, Aleksi, and Tarmo Virtanen. 2019. 'Data and Resolution Requirements in Mapping Vegetation in Spatially Heterogeneous Landscapes'. *Remote Sensing of Environment* 230:111207. doi: 10.1016/j.rse.2019.05.026.

Rasmussen, Jesper, Georgios Ntakos, Jon Nielsen, Jesper Svensgaard, Robert N. Poulsen, and Svend Christensen. 2016. 'Are Vegetation Indices Derived from Consumer-Grade Cameras Mounted on UAVs Sufficiently Reliable for Assessing Experimental Plots?' *European Journal of Agronomy* 74:75–92. doi: 10.1016/j.eja.2015.11.026.

Rocchini, Duccio. 2007. 'Effects of Spatial and Spectral Resolution in Estimating Ecosystem α-Diversity by Satellite Imagery'. *Remote Sensing of Environment* 111(4):423–34. doi: 10.1016/j.rse.2007.03.018.

Rocchini, Duccio, Niko Balkenhol, Gregory A. Carter, Giles M. Foody, Thomas W. Gillespie, Kate S. He, Salit Kark, Noam Levin, Kelly Lucas, Miska Luoto, Harini Nagendra, Jens Oldeland, Carlo Ricotta, Jane Southworth, and Markus Neteler. 2010. 'Remotely Sensed Spectral Heterogeneity as a Proxy of Species Diversity: Recent Advances and Open Challenges'. *Ecological Informatics* 5(5):318–29. doi: 10.1016/j.ecoinf.2010.06.001.

Rocchini, Duccio, Sandra Luque, Nathalie Pettorelli, Lucy Bastin, Daniel Doktor, Nicolò Faedi, Hannes Feilhauer, Jean-Baptiste Féret, Giles M. Foody, Yoni Gavish, Sergio Godinho, William E. Kunin, Angela Lausch, Pedro J. Leitão, Matteo Marcantonio, Markus Neteler, Carlo Ricotta, Sebastian Schmidtlein, Petteri Vihervaara, Martin Wegmann, and Harini Nagendra. 2018. 'Measuring β-Diversity by Remote Sensing: A Challenge for Biodiversity Monitoring'. *Methods in Ecology and Evolution* 9(8):1787–98. doi: https://doi.org/10.1111/2041-210X.12941.

Rocchini, Duccio, Carlo Ricotta, and A. Chiarucci. 2007. 'Using Satellite Imagery to Assess Plant Species Richness: The Role of Multispectral Systems'. *Applied Vegetation Science* 10(3):325–31. doi: 10.1111/j.1654-109X.2007.tb00431.x.

Rouse, J. W., R. H. Haas, J. A. Schell, and D. W. Deering. 1974. 'Monitoring Vegetation Systems in the Great Plains with ERTS'. Pp. 48–62 in *Proceedings of Third Earth Resources Technology Satellite-1 Symposium*. Vol. 1. Washington, DC, USA.

Sakurai, Ryo. 2019. *Human Dimensions of Wildlife Management in Japan: From Asia to the World*. Singapore: Springer.

Schmidtlein, Sebastian, and Fabian Ewald Fassnacht. 2017. 'The Spectral Variability Hypothesis Does Not Hold across Landscapes'. *Remote Sensing of Environment* 192:114–25. doi: 10.1016/j.rse.2017.01.036.

Skidmore, A. K., Nathakie Pettorelli, Nicholas Coops, Gary Geller, Matthew Hansen, Richard Lucas, Caspar Muncher, Brian O'Connor, Marc Paganini, Henrique Pereira, Michael Schaepman, Woody Turner, Tiejun Wang, and M. Wegman. 2015. 'Environmental Science : Agree on Biodiversity Metrics to Track from Space'. *Nature* 523(7561):403–5. doi: 10.1038/523403a.

Smith, Keith A., and Chris E. Mullins. 1991. *Soil Analysis : Physical Methods*. New York: M. Dekker.

Sneath, P. H. A., and R. R. Sokal. 1973. *Numerical Taxonomy*. San Fransisco: Freeman.

Sorrells, Jesse, and Robert J. Warren. 2011. 'Ant-Dispersed Herb Colonization Lags behind Forest Re-Establishment'. *The Journal of the Torrey Botanical Society* 138(1):77–84. doi: 10.3159/10-RA-037.1.

Stickler, Claudia M., and Jane Southworth. 2008. 'Application of Multi-Scale Spatial and Spectral Analysis for Predicting Primate Occurrence and Habitat Associations in Kibale National Park, Uganda'. *Remote Sensing of Environment* 112(5):2170–86. doi: https://doi.org/10.1016/j.rse.2007.10.013.

Sutomo, S., R. J. Hobbs, and V. Cramer. 2011. 'Plant Community Establishment on the Volcanic Deposits Following the 2006 Nuées Ardentes (Pyroclastic Flows) of Mount Merapi: Diversity and Floristic Variation'. *Biodiversitas* 12:86–91.

Taylor, Martin. 2009. 'IKONOS Planetary Reflectance and Mean Solar Exoatmospheric Irradiance'. 3.

Thenkabail, Prasad S., Jefferson Hall, Tiffany Lin, Mark S. Ashton, David Harris, and Eden A. Enclona. 2003. 'Detecting Floristic Structure and Pattern across Topographic and Moisture Gradients in a Mixed Species Central African Forest Using IKONOS and Landsat-7 ETM+ Images'. *International Journal of Applied Earth Observation and Geoinformation* 4(3):255–70. doi: 10.1016/S0303-2434(03)00006-0.

Tirado, Reyes, Francisco I. Pugnaire, and Ove Eriksson. 2005. 'Community Structure and Positive Interactions in Constraining Environments'. *Oikos* 111(3):437–44.

Titus, Jonathan H. 2009. 'Nitrogen-Fixers Alnus and Lupinus Influence Soil Characteristics but Not Colonization by Later Successional Species in Primary Succession on Mount St. Helens'. *Plant Ecology* 203(2):289–301. doi: 10.1007/s11258-008-9549-0.

Titus, Jonathan H., and John G. Bishop. 2014. 'Propagule Limitation and Competition with Nitrogen Fixers Limit Conifer Colonization during Primary Succession'. *Journal of Vegetation Science* 25(4):990–1003. doi: 10.1111/jvs.12155.

Török, Péter, András Kelemen, Orsolya Valkó, Tamás Miglécz, Katalin Tóth, Edina Tóth, Judit Sonkoly, Réka Kiss, Anikó Csecserits, Tamás Rédei, Balázs Deák, Péter Szűcs, Nóra Varga, and Béla Tóthmérész. 2018. 'Succession in Soil Seed Banks and Its Implications for Restoration of Calcareous Sand Grasslands'. *Restoration Ecology* 26(S2):S134–40. doi: 10.1111/rec.12611.

Torresani, Michele, Duccio Rocchini, Ruth Sonnenschein, Marc Zebisch, Matteo Marcantonio, Carlo Ricotta, and Giustino Tonon. 2019. 'Estimating Tree Species Diversity from Space in an Alpine Conifer Forest: The Rao's Q Diversity Index Meets the Spectral Variation Hypothesis'. *Ecological Informatics* 52:26–34. doi: https://doi.org/10.1016/j.ecoinf.2019.04.001.

Tsuyuzaki, Shiro. 1987. 'Origin of Plants Recovering on the Volcano Usu, Northern Japan, since the Eruptions of 1977 and 1978'. *Vegetatio* 73(1):53–58.

Tsuyuzaki, Shiro. 1989a. 'Analysis of Revegetation Dynamics on the Volcano Usu, Northern Japan, Deforested by 1977-78 Eruptions'. *American Journal of Botany* 76(10):1468–77. doi: 10.1002/j.1537-2197.1989.tb15128.x.

Tsuyuzaki, Shiro. 1989b. 'Contribution of Buried Seeds to Revegetation after Eruptions of the Volcano Usu, Northern Japan'. *The Botanical Magazine = Shokubutsu-Gaku-Zasshi* 102(4):511–20. doi: 10.1007/BF02488433.

Tsuyuzaki, Shiro. 1995. ‘Vegetation Recovery Patterns in Early Volcanic Succession’. *Journal of Plant Research* 108(2):241–48.

Tsuyuzaki, Shiro. 2009. ‘Causes of Plant Community Divergence in the Early Stages of Volcanic Succession’. *Journal of Vegetation Science* 20(5):959–69.

Tsuyuzaki, Shiro. 2010a. ‘Seed Survival for Three Decades under Thick Tephra’. *Seed Science Research* 20(03):201–7. doi: 10.1017/S0960258510000139.

Tsuyuzaki, Shiro. 2010b. ‘Seed Survival for Three Decades under Thick Tephra’. *Seed Science Research* 20(3):201–7. doi: 10.1017/S0960258510000139.

Tsuyuzaki, Shiro. 2019. ‘Vegetation Changes from 1984 to 2008 on Mount Usu, Northern Japan, after the 1977–1978 Eruptions’. *Ecological Research*. doi: 10.1111/1440-1703.12045.

Tsuyuzaki, Shiro, and Masaki Goto. 2001. ‘Persistence of Seed Bank under Thick Volcanic Deposits Twenty Years after Eruptions of Mount Usu, Hokkaido Island, Japan’. *American Journal of Botany* 88(10):1813–17.

Tsuyuzaki, Shiro, and Masahiro Haruki. 1996a. ‘Tree Regeneration Patterns on Mount Usu, Northern Japan, since the 1977–78 Eruptions’. *Vegetatio* 126(2):191–98.

Tsuyuzaki, Shiro, and Masahiro Haruki. 1996b. ‘Tree Regeneration Patterns on Mount Usu, Northern Japan, since the 1977–78 Eruptions’. *Vegetatio* 126(2):191–98.

Tsuyuzaki, Shiro, and C. Miyoshi. 2009. ‘Effects of Smoke, Heat, Darkness and Cold Stratification on Seed Germination of 40 Species in a Cool Temperate Zone in Northern Japan’. *Plant Biology* 11(3):369–78. doi: 10.1111/j.1438-8677.2008.00136.x.

Tsuyuzaki, Shiro, and Roger del Moral. 1995. ‘Species Attributes in Early Primary Succession on Volcanoes’. *Journal of Vegetation Science* 517–22.

Tuomisto, Hanna. 2010. ‘A Consistent Terminology for Quantifying Species Diversity? Yes, It Does Exist’. *Oecologia* 164(4):853–60. doi: 10.1007/s00442-010-1812-0.

Tuomisto, Hanna. 2011. ‘Commentary: Do We Have a Consistent Terminology for Species Diversity? Yes, If We Choose to Use It’. *Oecologia* 167(4):903–11. doi: 10.1007/s00442-011-2128-4.

Turner, Woody, Sacha Spector, Ned Gardiner, Matthew Fladeland, Eleanor Sterling, and Marc Steininger. 2003. ‘Remote Sensing for Biodiversity Science and Conservation’. *Trends in Ecology & Evolution* 18(6):306–14. doi: 10.1016/S0169-5347(03)00070-3.

Uchida, T. 2017. ‘Evaluating the Dynamics of Alien Species (Poaceae) Used for Erosion Control on Sakurajima Volcano’. *International Journal of Geomate*.

Uesaka, Shohei, and Shiro Tsuyuzaki. 2005. ‘Differential Establishment and Survival of Species in Deciduous and Evergreen Shrub Patches and on Bare Ground, Mt. Koma, Hokkaido, Japan’. *Plant Ecology* 175(2):165–77. doi: 10.1007/s11258-005-4839-2.

Underwood, Emma, Susan Ustin, and Deanne DiPietro. 2003. ‘Mapping Nonnative Plants Using Hyperspectral Imagery’. *Remote Sensing of Environment* 86(2):150–61. doi: https://doi.org/10.1016/S0034-4257(03)00096-8.

Verheyen, Kris, Glenn R. Guntenspergen, Bernard Biesbrouck, and Martin Hermy. 2003. ‘An Integrated Analysis of the Effects of Past Land Use on Forest Herb Colonization at the

Landscape Scale'. *Journal of Ecology* 91(5):731–42. doi: 10.1046/j.1365-2745.2003.00807.x.

Viedma, Olga, Iván Torres, Beatriz Pérez, and José M. Moreno. 2012. 'Modeling Plant Species Richness Using Reflectance and Texture Data Derived from QuickBird in a Recently Burned Area of Central Spain'. *Remote Sensing of Environment* 119:208–21. doi: 10.1016/j.rse.2011.12.024.

Walker, Lawrence R., and Roger del Moral. 2003. *Primary Succession and Ecosystem Rehabilitation*. Cambridge: Cambridge University Press.

Wang, Ran, and John A. Gamon. 2019. 'Remote Sensing of Terrestrial Plant Biodiversity'. *Remote Sensing of Environment* 231:111218. doi: 10.1016/j.rse.2019.111218.

Wang, Ran, John A. Gamon, Jeannine Cavender-Bares, Philip A. Townsend, and Arthur I. Zygielbaum. 2018. 'The Spatial Sensitivity of the Spectral Diversity–Biodiversity Relationship: An Experimental Test in a Prairie Grassland'. *Ecological Applications* 28(2):541–56. doi: 10.1002/eap.1669.

Wang, Ran, John A. Gamon, Anna K. Schweiger, Jeannine Cavender-Bares, Philip A. Townsend, Arthur I. Zygielbaum, and Shan Kothari. 2018. 'Influence of Species Richness, Evenness, and Composition on Optical Diversity: A Simulation Study'. *Remote Sensing of Environment* 211:218–28. doi: 10.1016/j.rse.2018.04.010.

Warren, Steven, Martin Alt, Keith Olson, Severin Irl, Manuel Steinbauer, and Anke Jentsch. 2014. 'The Relationship between the Spectral Diversity of Satellite Imagery, Habitat Heterogeneity, and Plant Species Richness'. *Ecological Informatics* 24. doi: 10.1016/j.ecoinf.2014.08.006.

White, Mark A., Meredith W. Cornett, and Peter T. Wolter. 2017. 'Two Scales Are Better than One: Monitoring Multiple-Use Northern Temperate Forests'. *Forest Ecology and Management* 384:44–53. doi: 10.1016/j.foreco.2016.10.032.

White, Peter S., and S. P. Bratton. 1980. 'After Preservation: Philisophical and Practical Problems of Change'. *Biological Conservation* 18:241–55.

White, Peter S., and Joan L. Walker. 1997. 'Approximating Nature's Variation: Selecting and Using Reference Information in Restoration Ecology'. *Restoration Ecology* 5(4):338–49. doi: 10.1046/j.1526-100X.1997.00547.x.

Whittaker, R. H. 1960. 'Vegetation of the Siskiyou Mountains, Oregon and California'. *Ecological Monographs* 30(3):279–338. doi: 10.2307/1943563.

Wickham, Hadley, Mara Averick, Jennifer Bryan, Winston Chang, Lucy D'Agostino McGowan, Romain François, Garrett Grolemund, Alex Hayes, Lionel Henry, Jim Hester, Max Kuhn, Thomas Lin Pedersen, Evan Miller, Stephan Milton Bache, Kirill Müller, Jeroen Ooms, David Robinson, Dana Paige Seidel, Vitalie Spinu, Kohske Takahashi, Davis Vaughan, Claus Wilke, Kara Woo, and Hiroaki Yutani. 2019. 'Welcome to the Tidyverse'. *Journal of Open Source Software* 4(43):1686. doi: 10.21105/joss.01686.

Wickham, Hadley, and Dana Seidel. 2020. *Scales: Scale Functions for Visualization*.

Wilmshurst, Janet M., and Matt S. McGlone. 1996. 'Forest Disturbance in the Central North Island, New Zealand, Following the 1850 BP Taupo Eruption'. *The Holocene* 6(4):399–411. doi: 10.1177/095968369600600402.

Woodcock, Curtis E., and Alan H. Strahler. 1987. 'The Factor of Scale in Remote Sensing'. *Remote Sensing of Environment* 21(3):311–32. doi: 10.1016/0034-4257(87)90015-0.

Wulder, Michael A., Ronald J. Hall, Nicholas C. Coops, and Steven E. Franklin. 2004. 'High Spatial Resolution Remotely Sensed Data for Ecosystem Characterization'. *BioScience* 54(6):511–21. doi: 10.1641/0006-3568(2004)054[0511:HSRRSD]2.0.CO;2.

Yi, Koong, Jake W. Smith, Andrew D. Jablonski, Elizabeth A. Tatham, Todd M. Scanlon, Manuel T. Lerdau, Kimberly A. Novick, and Xi Yang. 2020. 'High Heterogeneity in Canopy Temperature Among Co-Occurring Tree Species in a Temperate Forest'. *Journal of Geophysical Research: Biogeosciences* 125(12):e2020JG005892. doi: 10.1029/2020JG005892.

Yoshitake, S., M. Fujiyoshi, T. Masuzawa, and H. Koizumi. 2016. 'Substrate Limitation to Soil Microbial Communities in a Subalpine Volcanic Desert on Mount Fuji, Japan'. *European Journal of Soil Biology* 73:34–45. doi: 10.1016/j.ejsobi.2016.01.002.

Young, T. P., D. A. Petersen, and J. J. Clary. 2005. 'The Ecology of Restoration: Historical Links, Emerging Issues and Unexplored Realms'. *Ecology Letters* 8(6):662–73. doi: 10.1111/j.1461-0248.2005.00764.x.

Yurkewycz, Raymond P., John G. Bishop, Charles M. Crisafulli, John A. Harrison, and Richard A. Gill. 2014. 'Gopher Mounds Decrease Nutrient Cycling Rates and Increase Adjacent Vegetation in Volcanic Primary Succession'. *Oecologia* 176(4):1135–50. doi: 10.1007/s00442-014-3075-7.

Zhang, Yu, Han Y. H. Chen, and Anthony R. Taylor. 2016. 'Aboveground Biomass of Understorey Vegetation Has a Negligible or Negative Association with Overstorey Tree Species Diversity in Natural Forests'. *Global Ecology and Biogeography* 25(2):141–50. doi: 10.1111/geb.12392.

Zobel, Donald B., and Joseph A. Antos. 2017. 'Community Reorganization in Forest Understories Buried by Volcanic Tephra'. *Ecosphere* 8(12):e02045. doi: 10.1002/ecs2.2045.

Zomer, R. J., A. Trabucco, and S. L. Ustin. 2009. 'Building Spectral Libraries for Wetlands Land Cover Classification and Hyperspectral Remote Sensing'. *Journal of Environmental Management* 90(7):2170–77. doi: https://doi.org/10.1016/j.jenvman.2007.06.028.

# Appendix

Appendix 1 The numbers and species of seeds germinated from the topsoil samples collected from the seven forest types on Yosomi and summit. The table shows the total from all years and incubation method (2500 $cm^3$ soil collected, apart from the Mixed forest, where 1700 $cm^3$ was collected).

| | Yosomi | | | Summit | | | | |
|---|---|---|---|---|---|---|---|---|
| Species | Broadleaf | Mixed | Abies | Closed-Br. | Open-Br. | Sorbus-Alnus | Picea | Total |
| *Actinidia arguta* | 1 | 0 | 0 | 0 | 0 | 0 | 1 | **2** |
| *Amaranthus* spp. | 0 | 0 | 0 | 0 | 1 | 0 | 0 | **1** |
| *Anaphalis margaritacea* | 0 | 0 | 0 | 0 | 3 | 0 | 1 | **4** |
| *Angelica ursina* | 0 | 0 | 0 | 1 | 0 | 0 | 0 | **1** |
| *Aralia cordata* | 0 | 1 | 2 | 3 | 0 | 1 | 1 | **8** |
| *Artemisia montana* | 1 | 0 | 0 | 0 | 1 | 6 | 1 | **9** |
| *Asperula odorata* | 0 | 0 | 0 | 0 | 2 | 0 | 0 | **2** |
| *Aster* spp. | 0 | 0 | 0 | 0 | 0 | 1 | 0 | **1** |
| *Aster ageratoides* | 0 | 0 | 0 | 0 | 0 | 0 | 1 | **1** |
| *Betula maximowicziana* | 2 | 0 | 3 | 0 | 0 | 0 | 0 | **5** |
| *Cardiocrinum cordatum* | 2 | 0 | 1 | 1 | 0 | 0 | 0 | **4** |
| *Chenopodium* ssp. | 0 | 0 | 0 | 0 | 0 | 1 | 0 | **1** |
| *Chenopodium album* | 0 | 3 | 0 | 1 | 0 | 0 | 0 | **4** |
| *Clinopodium micranthum* | 0 | 0 | 0 | 1 | 0 | 0 | 0 | **1** |
| *Epilobium montanum* | 0 | 0 | 0 | 0 | 2 | 1 | 0 | **3** |
| *Erigeron annuus* | 0 | 0 | 0 | 0 | 1 | 0 | 1 | **2** |
| *Erigeron canadensis* | 0 | 0 | 1 | 0 | 0 | 0 | 0 | **1** |
| *Erigeron sumatrensis* | 0 | 0 | 0 | 0 | 3 | 0 | 1 | **4** |
| *Fallopia sachalinensis* | 0 | 0 | 0 | 1 | 4 | 0 | 0 | **5** |
| *Geum macrophyllum* | 0 | 0 | 0 | 0 | 0 | 1 | 0 | **1** |
| Graminoids | 5 | 5 | 9 | 13 | 22 | 24 | 30 | **108** |
| *Hydrangea petiolaris* | 0 | 1 | 1 | 1 | 0 | 1 | 0 | **4** |
| *Hypericum erectum* | 0 | 0 | 0 | 1 | 0 | 0 | 0 | **1** |
| *Ixeris dentata* | 0 | 0 | 0 | 0 | 0 | 1 | 0 | **1** |
| *Lotus corniculatus* | 0 | 0 | 0 | 0 | 0 | 0 | 1 | **1** |
| *Medicago lupulina* | 0 | 0 | 0 | 0 | 0 | 1 | 0 | **1** |
| *Moehringia lateriflora* | 0 | 0 | 0 | 0 | 0 | 3 | 0 | **3** |
| *Oenothera biennis* | 0 | 0 | 0 | 0 | 0 | 0 | 2 | **2** |
| *Patrinia villosa* | 0 | 0 | 1 | 0 | 1 | 0 | 2 | **4** |

| | | | | | | | | |
|---|---|---|---|---|---|---|---|---|
| *Petasites japonicus* | 0 | 0 | 0 | 0 | 0 | 0 | 1 | **1** |
| *Picris hieracioides* | 0 | 0 | 0 | 0 | 2 | 1 | 2 | **5** |
| *Pilea hamaoi* | 4 | 2 | 1 | 0 | 0 | 0 | 0 | **7** |
| *Pilea pumila* | 1 | 0 | 0 | 0 | 1 | 8 | 0 | **10** |
| *Plantago asiatica* | 0 | 0 | 0 | 0 | 2 | 0 | 0 | **2** |
| Polygonaceae | 0 | 0 | 0 | 0 | 0 | 0 | 1 | **1** |
| *Polygonum aviculare* | 0 | 1 | 0 | 0 | 0 | 0 | 0 | **1** |
| *Polygonum sachalinense* | 0 | 0 | 0 | 0 | 0 | 2 | 0 | **2** |
| *Ranunculus repens* | 0 | 0 | 0 | 2 | 0 | 0 | 0 | **2** |
| *Rorippa indica* | 0 | 1 | 0 | 1 | 0 | 0 | 0 | **2** |
| *Solidago virgaurea* | 0 | 0 | 0 | 2 | 1 | 0 | 1 | **4** |
| *Sorbus commixta* | 1 | 0 | 0 | 0 | 0 | 0 | 0 | **1** |
| *Stellaria aquatica* | 0 | 0 | 0 | 0 | 0 | 6 | 0 | **6** |
| *Stellaria media* | 0 | 0 | 0 | 0 | 0 | 1 | 0 | **1** |
| *Syringa japonica* | 1 | 0 | 0 | 0 | 0 | 0 | 0 | **1** |
| *Trifolium pratense* | 0 | 0 | 0 | 0 | 0 | 2 | 2 | **4** |
| *Ulmus davidiana* | 2 | 0 | 0 | 0 | 0 | 0 | 0 | **2** |
| *Viola grypoceras* | 8 | 3 | 1 | 7 | 0 | 6 | 0 | **25** |
| **Total** | **28** | **17** | **20** | **35** | **46** | **67** | **49** | **262** |